PALAEOENVIRONMENTAL RELATIONSHIPS OF MID-CENOZOIC CARBONATE AND VOLCANIC ROCKS, KAKANUI

A thesis submitted in partial fulfilment of the requirements for the Degree

of Master of Science in Geology

in the University of Canterbury

by M. J. Boyland

University of Canterbury

2017

Contents

Acknowledgements

I thank my supervisors, Catherine Reid and Ben Kennedy, for all of their ideas, explanations, critiques, and patience. You were terrific to work with, and I'm thankful for all the time you put in to help with this project.

Funding for fieldwork and external lab analysis was kindly provided by the Mason Trust, Department of Geological Sciences.

I am grateful for the assistance of the University of Canterbury technicians. You were very helpful, and made the lab work much easier. Particular thanks go to Rob Spiers, for his work making thin sections and mounting minerals, to Stephen Brown, for running XRF on the many samples I gave him, to Chris Grimshaw, for his help with foraminiferal preparation and thin section photography, and to Ian Schipper from Victoria University of Wellington for help with microprobe analysis.

Thanks go to Jim Cole, who proof-read my thesis, and offered advice. These suggestions were very helpful as I worked on the final version. Thanks also go to everyone who took the time to meet with me and offer their expertise, including Kari Bassett, Alex Nichols and James White. Your different perspectives helped me to appreciate the multiple aspects of this research. I am also grateful for the input and enthusiasm of James Cowlyn, who accompanied me and Ben Kennedy on one of the initial trips, and Eric Hiatt, who I assisted on a field trip to the study area. You were both a great help, and a pleasure to work with.

Finally, thanks go to my friends and family. For being proud of me, for supporting me, and all too often, for being patient with me when I had to spend time on my thesis instead of with you.

Abstract

The rocks of the Eocene to Oligocene Waitaki region formed in a complex depositional environment, under the influence of changing sea levels, submarine volcanism, and carbonate production. This area was part of a marine basin, which developed while New Zealand was mostly submerged, and the main sediment sources were carbonate deposits, and volcanic material produced in a monogenetic volcanic field. The build-up of volcanic material and the formation of seamounts created a shallow zone offshore. The geology within this former volcanic field is characterised by inner – mid shelf fauna, while deeper-water assemblages occur closer to the palaeoshoreline. This investigation employs a multi-disciplinary approach, in order to understand the nature, timing and importance of the various factors which have influenced deposition within this unusual setting.

The study area of Kakanui is surrounded by good exposures of volcanic and carbonate rocks, formed within a changing depositional environment. In particular, the Kakanui River Section deposits show a number of lithological changes, which were driven by a number of interrelated factors. Sea level was relatively high at the base of the section, but fell by 20 - 30 m near to the top. This resulted in the development of an unconformity, and a shift to coarser grainsizes and shallower-water bioclasts. Volcanism also greatly influenced Kakanui River Section deposits. Nearby volcanoes provided a sudden influx of sediment, followed by a return to carbonate accumulation after the edifices degraded too much.

Geochemical fingerprinting of volcanic deposits around Kakanui revealed that a number of distinct sources were present. Older eruptions had a more felsic composition, but younger eruptions showed more enrichment in compatible elements. This shift is attributed to changing source magma geochemistry, combined with the influence of a new magma body.

This investigation used a combination of field mapping, microfossil investigation and geochemical analysis. These techniques complemented each other, and helped to build a more complete understanding of the palaeoenvironment at Kakanui.

1. Introduction

New Zealand's Waitaki region contains rocks deposited in an Eocene-Miocene marine basin. This basin formed during New Zealand's mid-Cenozoic inundation, when much of the current land area was underwater, and terrestrial sediment supply was too low to form large siliciclastic deposits. This sediment deficit allowed calcareous rocks to accumulate, resulting in the thick limestone deposits which characterise the region (Forsyth, 2001). During this period, part of the Waitaki area was affected by a phase of Cenozoic intraplate volcanism (Hoernle et al., 2006), which produced seamounts, and tens of cubic kilometres of erupted material. This material built up to create shallow, solid bases which were colonised by marine organisms, changing the types of limestones produced.

This thesis investigates the well-exposed, lithologically diverse outcrops around the coastal Waitaki town of Kakanui. These rocks reflect a changing environment, which has been influenced by volcanism, carbonate sedimentation, and sea level changes. It is anticipated that sediment facies analysis, combined with geochemical and microfossil investigation, will provide insight into the evolution of this unique depositional environment. Furthermore, studies of volcanic provenance should help to constrain the timing and location of various local eruptions, with implications for the evolution of the volcanic field as a whole.

1.1 Background information

The Waitaki Region has been intermittently affected by volcanism, most notably from an Eocene to Oligocene monogenetic volcanic field (Coombs et al., 1986). Monogenetic volcanic fields are km-scale zones which contain multiple volcanic edifices fed from the same magma source. These edifices typically lack crustal magma chambers, and are instead formed from direct pulses of magma generated in the mantle in a continuous melting process. This process can be complicated, and may involve the melting of different components over time (Németh et al., 2003). Because of this, the volcanoes in a monogenetic field can still show a distinct geochemical range (McGee & Smith, 2016).

Monogenetic volcanoes form in a single, short eruptive period, and then become inactive. They are usually smaller than polygenetic volcanoes, which can erupt multiple times and build up large complex deposits. The small magmatic pulses which generate monogenetic volcanoes are

too infrequent to maintain a continuous thermal pathway; instead the original conduit seals between eruptions, and the next pulse must take a new pathway to the surface. Because of this intermittent activity, a field may be active for much longer than a composite volcano with comparable magmatic output (Németh, 2010). There are several present day examples of monogenetic volcanic fields, including the Auckland Volcanic Field, in New Zealand's North Island, which has been active for around 0.25 Ma. Eruptions in this field are infrequent enough (an average of one every 3500 years) that the city of Auckland has been built within it (Molloy et al., 2009).

Although in theory monogenetic volcanoes only erupt once, there is a possibility, or even a tendency for multiple monogenetic volcanoes to erupt in a closely spaced area, creating a composite deposit which is effectively polygenetic (Keating et al., 2008; Diez et al., 2009; Valentine and Hirano, 2010; Brenna et al., 2010). This clustering phenomena has been observed within several monogenetic fields, e.g. Rangitoto Island, Auckland Volcanic Field (Shane et al., 2013) La Palma, Canary Islands (e.g. White and Schmincke, 1999; Klügel et al., 2000), the Chatham Islands (Németh et al., 2013), and within the study area at Waitaki (Maicher, 2003; Moorhouse, 2015). Le Corvec et al., (2013) analysed the spatial distribution of volcanoes in 37 monogenetic volcanic fields, and concluded that most showed clustering, which they attributed to lithospheric influences, such as the ambient stress field, or pre-existing crustal structures.

Waitaki volcanism was mainly Surtseyan (Coombs et al., 1986); a style which occurs in shallow marine or lacustrine settings. It is named for the characteristic island volcano Surtsey in the Westmann Islands south of Iceland (Walker, 1973). Surtseyan eruptions involve basaltic magma interacting with water, leading to violently explosive phreatomagmatic activity. These eruptions can produce ballistics, tephra jets, and occasional lava flows (Kokelaar, 1983). Where the vents are subaqueous, the surrounding water strongly influences the deposits produced; the confining pressure limits the height and increases the particle density of eruption columns, and can suppress the formation of vesicles in volcanic clasts (McBirney, 1963; Fisher and Schmincke, 1984; Cas et al., 1989). Water can carry much denser particles than air, and subaqueous volcanism is associated with a number of different types of sediment gravity flows, such as high- and low-concentration turbidity currents, grainflows and debris flows. These may be initiated by pyroclastic activity, or simply by sedimentary processes. The multiple sediment transport methods produce a variety of deposit types, some of which can be difficult to distinguish (Németh et al., 2003; White, 2000).

The Waitaki region contains limestones which formed in an unusual carbonate factory. A typical cool-water carbonate ramp grows progressively deeper with distance from the shore, and this is reflected in the progression of sedimentary facies and biofacies; from shallow, high energy coastal conditions to deep, low energy abyssal conditions (Burchett & Wright, 1992). However, the Waitaki area had a more complex distribution of shallow and deep marine environments during the mid-Cenozoic, due to the influence of volcanism. The offshore carbonate factory was associated with volcanic highs, and was very different from the typical cool-water carbonate ramp model (Thompson et al., 2014).

This study investigates several fossil species, most notably foraminifera. Foraminifera are single-celled, typically marine organisms which live in sediment, or float in the water column. They are usually less than a millimetre in size, although some species with symbiotic zooxanthallae may reach several centimetres (Goldstein, 1999). Foraminifera produce an external shell, or, test; typically from calcium carbonate, or from agglutinated sediment. The composition, overall structure, chamber arrangement and ornamentation of this test can define the order, family, genus and species of foraminifera. Because their fossils are so readily identifiable, widely distributed and easily preserved, they are particularly useful for marine palaeontology (Haynes, 1981).

Foraminifera are considered the most important fossil group in New Zealand for uppermost Cretaceous to Recent biostratigraphic and palaeoenvironmental interpretation (Cooper et al., 2004). Foraminiferal occurrence can be used to correlate rocks of similar ages, and many of New Zealand's geological stages are based on the first appearance datum (FAD) or last appearance datum (LAD) of a particular foraminiferal species. Additionally, types and abundances can provide clues to the palaeoenvironment in which a foraminiferal assemblage lived. There are many factors, such as depth, salinity, turbidity, light penetration, and substrate type, which favour particular foraminiferal assemblages (Corliss, 1985). A good understanding of where and when a species lived can provide a great deal of information about a rock unit in which it has been found.

Foraminifera are easily entrained as grains, and may be transported into different environments than those they lived in. Transport processes can also segregate foraminifera based on size or specific gravity, resulting in a sorted deposit which doesn't match the life assemblage (Murray 2006; Hayward et al. 2010). Whether foraminifera are in situ or not can be difficult to determine,

as their tests are small and robust enough to resist mechanical abrasion, so care must be taken in using them for interpretation.

Glauconite is a common authogenic mineral in the Waitaki region. It is a hydrated iron-rich micaceous clay mineral, which forms ideally in an environment with decaying organic matter and low sedimentation. It often occurs as pellets, or as a replacement mineral in bioclasts or other minerals (Odin & Fullaga, 1988). As glauconite matures, it becomes more enriched in potassium, and changes from a bright, yellowish green to a much darker green (McRae, 1972; Odin & Matter, 1981). In siliciclastic systems with high sediment flux glauconite formation is typically associated with sea level rise and sediment starvation (Udgata, 2007). However in the carbonate system within Waitaki, sediment flux was typically too low to supress glauconite production. Instead, high production levels were associated with lowstands, where the palaeocoastline was closer, and there was an increased supply of terrestrial clay minerals which could be altered. Because of this, erosional surfaces related to sea level fall in Waitaki are often overlain by glauconite-rich units (Thompson 2013; Thompson et al., 2014).

1.2 Geological History

New Zealand's geological development throughout the Cenozoic has been dictated by a tectonic regime which began around 85 Ma, with the late Cretaceous separation of Zealandia and Gondwana (Laird & Bradshaw, 2004). Prior to this rifting, the Zealandia crustal block had experienced a long period of compression and overthickening. The switch to extension began a long period of tectonic quiescence and slow thermal subsidence of New Zealand (Cox, 2007; Laird & Bradshaw, 2004).

The subsidence of New Zealand was accompanied by gradual marine incursion, which reached its peak in the Oligocene (Figure 1.1) (Nathan 1974; Maxwell 1975; Nathan et al. 1986; Field et al. 1989; Isaac et al. 1994). This reduced New Zealand's total land area by around 80% (King et al. 1999) (Figure 1.2). River networks were drowned, and the lack of erodible terrestrial land resulted in reduced sediment supply to marine basins (Edwards, 1991). This clastic deficit meant that carbonate clasts became the dominant sediment source, resulting in the thick limestone deposits which characterise the modern Waitaki area. The initiation of strike-slip movement along the Alpine Fault in the Miocene led to distributed deformation which caused uplift and emergence of the Waitaki Region (Norris et al. 1978).

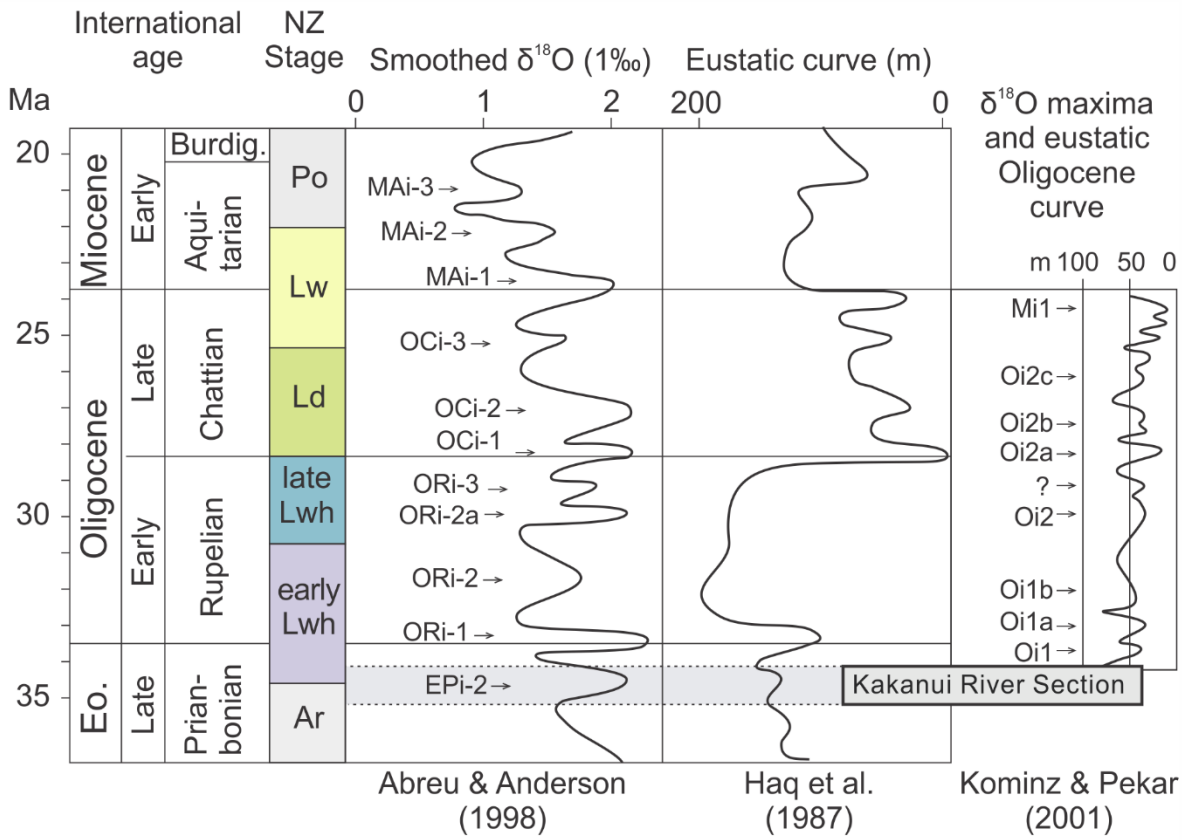

Figure 1.1: Eustatic sea level and $\delta^{18}O$ curves across the mid-Cenozoic inundation, modified from Nelson et al. (2004). Arrows show the position of oxygen isotope ($\delta^{18}O$) maxima events, which indicate relatively lowered sea level, and potential unconformity development in shelf sequences Kakanui River Section age estimates obtained from Sr isotope dating of brachiopod shells from the top and base of the section, by Nelson et al. (2004).

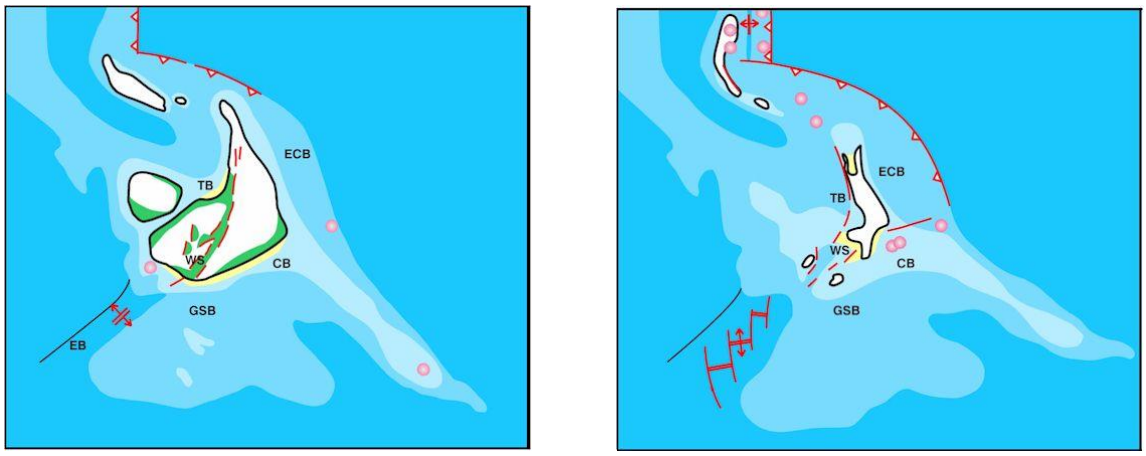

Middle Eocene c. 40 Ma Late Oligocene c. 25 Ma

Figure 1.2: New Zealand land surface during the mid-Cenozoic inundation. TB = Taranaki Basin, ECB = East Coast Basin, CB = Canterbury Basin, GSB = Great South Basin, WS = Western Southland, EB = Emerald Basin, CP = Campbell Plateau. The Waitaki study area is part of the Canterbury Basin (CB). Image taken from King (2000).

In addition to geological changes occurring within New Zealand, major global oceanographic and climatic changes took place during the mid-Cenozoic. Tectonic rifting between Antarctica and Australia caused the opening of the Tasmanian Seaway around 33.5 Ma (Exon et al., 2004; Stickley et al., 2004). Rifting between Antarctica and South America created the Drake Passage, which may have fully opened by 28.5 Ma (Lawver & Gahagan, 2003), or possibly around 24 Ma, near the Oligocene-Miocene boundary (Pfuhl and McCave, 2005; Lyle et al., 2007). These gateways allowed the formation of the Antarctic Circumpolar Current (ACC), an eastward-flowing ocean current which circles Antarctica, mixing with waters from all other oceans (Hassold et al., 2009).

The ACC thermally insulated Antarctica, leading to major cooling, and driving the glaciation of the continent. Significant amounts of water were locked up as ice sheets (Lawver et al., 1992; Zachos et al., 1992) leading to a eustatic drop in sea level of 40-75 m, at the Eocene to Oligocene boundary (Pekar et al 2002; Pekar & Christie-Blick, 2008). The large thermal gradient between the tropics and the pole created strong, temperature-driven global circulation. Increased ocean currents allowed deep, nutrient-rich water to be drawn up to the surface, which promoted biological activity (Toggweiler & Key, 2003).

The formation of the ACC triggered a major climatic shift from the "greenhouse" earth of the Mesozoic-Eocene to cooler "icehouse" conditions. Prior to the Eocene-Oligocene boundary, the Waitaki region was subtropical to marginally tropical (Lee et al., 1997), with a mean winter sea-surface temperature of around 20°C during the early Runangan (Edwards et al., 1991). This environment promoted the spread of warm-water flora and fauna, such as large foraminifera, mangrove and coconut palms. It was followed by an abrupt cooling in the earliest Oligocene, possibly associated with the development of cold-water current from Antarctica (Buening et al., 1997)

New Zealand has experienced intermittent phases of intraplate volcanism throughout the Cenozoic. This volcanism includes a variety of styles, including monogenetic volcanic fields, which occurred in Waitaki (Timm et al., 2009). The cause is debated, but may have been due to a mantle plume (Weaver et al., 1994; Storey, 1995, Storey et al., 1999), the jamming of the subduction zone along the Hikurangi Plateau (Davy and Wood, 1994; Mortimer at al., 2006; Davy et al., 2008) or detachment of lithospheric pieces, allowing the rise of hot aesthenospheric material (Hoernle et al., 2006).

1.4 Regional stratigraphy

New Zealand's Waitaki Region contains a range of mid-Cenozoic rocks, deposited in a marine basin during the inundation of New Zealand. This basin provides an important window into some of the local and regional events which have occurred in New Zealand. A simplified stratigraphy of these deposits from the Late Cretaceous to the Miocene is shown in Figure 1.3.

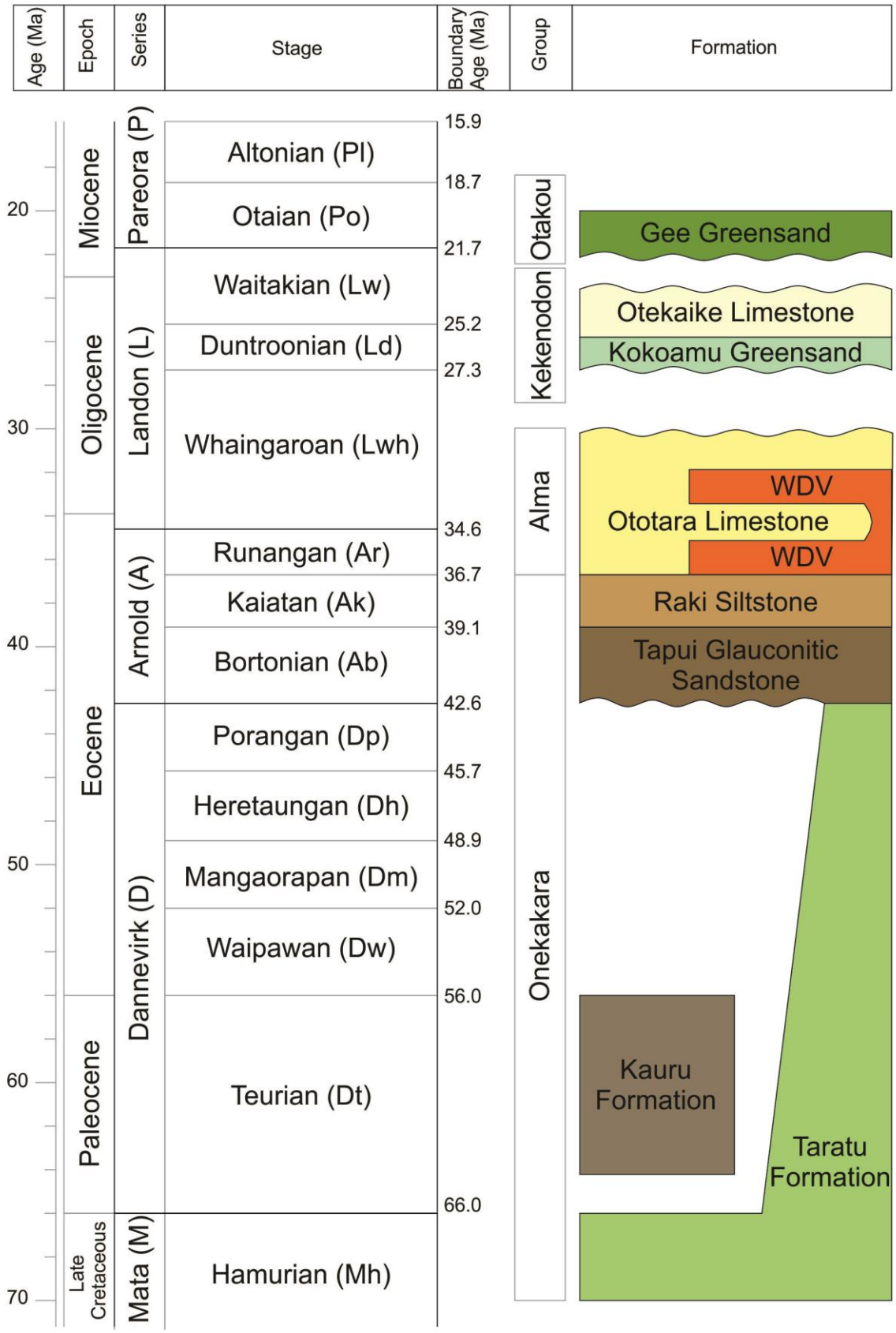

Figure 1.3: Geological stratigraphy of the Waitaki region. WDV are the Waiareka-Deborah Volcanics. Geological formation data taken from Gage (1957); Forsyth (2001); and Cooper (2004). Timescale data taken from Raine et al. (2015).

The Onekakara Group is the oldest Cenozoic group in the study area. This is a Late Cretaceous to Early Oligocene unit of terrestrial to shallow marine sedimentary rocks, which formed during the beginning of regional transgression. It includes quartzose sandstones, mudstones, marls, and coals, which were deposited in fluvial systems, estuaries, and marine environments (Forsyth, 2001). The time-transgressive Waipounamu Erosional Surface separates the terrestrial and marine units, and the Marshall Paraconformity forms the upper limit of the group. Onekakara sediments are up to 1500 m thick onshore, and up to 3000 m thick offshore. (Forsyth, 2001).

The Eocene to Oligocene Alma Group overlies the Onekakara Group. It contains carbonate marine rocks, and volcanics erupted from the monogenetic Waiareka-Deborah Volcanic Field (Forsyth, 2001). This field was located around 50-60 km offshore, extending roughly along the current coastline (Edwards, 1991). The seamounts and volcaniclastic material created an area of raised seafloor, referred to as a palaeohigh (Thompson, 2013) (Figure 1.4). This underwater topography altered ocean currents, creating sheltered zones of lower energy, and driving upwelling which brought nutrient-rich bottom waters to the surface. It also provided a solid, shallow base for organisms, allowing them to grow in an area which would otherwise have been deep water (Thompson et al., 2014).

Waiareka-Deborah deposits were produced by Surtseyan-style eruptions, in a monogenetic volcanic field, which was probably active between ~ 40 and 32 Ma (Late Eocene to Early Oligocene) (Cooper 2004; Coombs et al. 2008). The field ran roughly parallel to the northward trending palaeo-coastline, which was several tens of km away, although the actual distance varied with changes in sea level (Edwards, 1991). Originally, deposits from this field were grouped into two distinctive units, the Waiareka and the Deborah volcanics, based on their separation by limestone beds in some places (Hector, 1884; Park, 1918; Gage, 1957). However, this division is not regionally extensive; in places the two units are in contact, and the presence of tuff layers within separating limestone suggests that volcanism was continuous, if intermittent (Coombs et al., 1986; Cas et al., 1989). Waiareka-Deborah deposits include extensive basaltic tuffs, as well as agglomerate and pillow lavas, basaltic to doleritic dikes and sills, and layers of coeval sediment (Forsyth, 2001). The total volume of erupted or near-surface material was estimated to be tens, or possibly in the low hundreds of cubic kilometres. This volcanic material was an important source of sediment and elements such as silica during a period of low terrestrial sedimentation rates (Edwards, 1991).

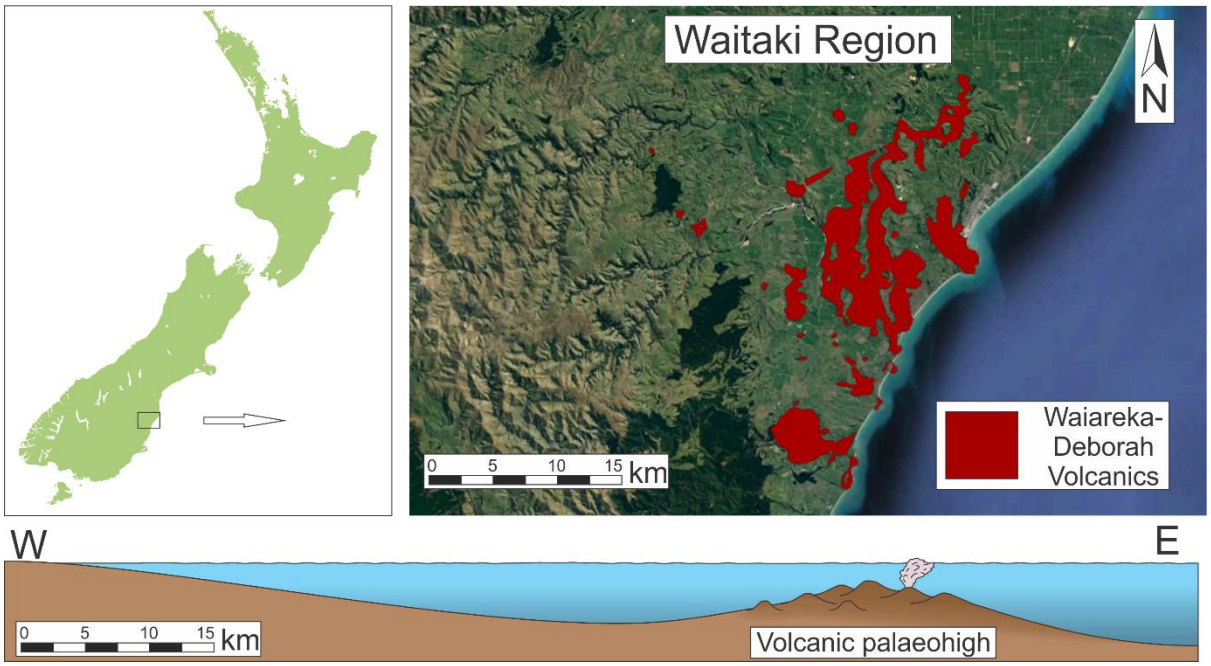

Figure 1.4: Waiareka-Deborah volcanic deposits across Waitaki, compared with the original subaqueous depositional setting in the mid-Cenozoic. Background map from GoogleEarth ("Waitaki." 45°10'23.27" S 170°51'31.61" E 10/21/2016). Geological data adapted from Forsyth (2001), ((C) GNS Science 2016).

At the same time as the development of the volcanic palaeohigh, carbonate rocks of the Runangan – Whaingaroan Ototara Limestone were being deposited. This formation is dominated by bryozoan-rich limesone, with little terrigenous material, and has a thickness which varies from a few metres, to 60 m. Minor volcaniclastic content, and macrofossils of molluscs, brachiopods, sharks teeth and rare penguin bones occur locally (Gage, 1957). Edwards (1991) estimates that the bryozoans which characterise this formation typically lived in depths of 30 – 60 m, but were often redeposited into much deeper environments. Inner to mid-shelf deposits dominate along the present coastline, around the location of the palaeohigh, while deeper-water deposits occur further inland (Gage, 1957; Forsyth, 2001).

An unconformity forms the upper boundary of the Ototara Limestone, separating the Alma Group from overlying units. This is the Marshall Paraconformity; an erosional surface which has been identified in many marine sequences across New Zealand. The layers immediately above it often contain hardground faunal assemblages and high glauconite concentrations, indicating that it represents a significant time gap (Lever, 2007). In Waitaki, the Marshall Paraconformity is present as a prominent karst surface at the coast, indicating subaerial exposure. Further inland it is represented by a submarine sedimentary hiatus (Thompson, 2013).

Following the Marshall Paraconformity, the latest Oligocene to earliest Miocene Kekenodon Group was deposited. This group represents the maximum inundation of the area. It outcrops on either side of the Waihemo Fault system, although the two sides contain different formations. The northern section, which occurs in the study area near Kakanui, includes the Kokoamu Greensand, the Otekaiki Limestone and the Gee Greensand (Forsyth, 2001).

The Kokoamu Greensand is a massive, fossiliferous, calcareous greensand. It includes quartz pebbles, occasional phosphatic nodules, and fossils of foraminifera, molluscs, ostracods, brachiopods, corals, cetaceans, penguins and sharks teeth. This greensand is up to 10 m thick, although in some localities, such as around Kakanui, it is only known from infilled borings and dissolution cavities in the underlying Ototara Limestone (McMillan, 1999).

The Otekaike Limestone appears in the study area around Kakanui as a hard, glauconitic, bryozoan limestone. The depositional environment is interpreted as middle shelf at the base, to inner shelf at the top (Ayress, 1993). An unconformity separates the Otekaike Limestone from the next unit, the Gee Greensand. This unconformity is well developed in shallow-water deposits around coastal areas of North Otago and South Canterbury, where it is present as a karsted surface. This suggests that it formed due to subaerial exposure of the Otekaike Limestone (Batt, 1993).

The Gee Greensand unconformably overlies the Otekaike Limestone. This formation contains high glauconite concentrations, and well-rounded local and exotic clasts at the base (Batt, 1993). It grades up to a calcareous greensand and glauconitic fine sand. The lower section contains phosphatised nodules, and pebbles of limestone or basalt. Fossils include foraminifera, corals, brachiopods, molluscs and shark teeth. Burrowing is common throughout the unit (McMillan, 1999).

1.5 Study Area

This thesis is based around Kakanui: a small coastal town in the Waitaki region, around 14 km south of Oamaru. It is located within the area of the mid-Cenozoic volcanic paleohigh, and is surrounded by a number of extensive outcrops. The transgressing coastline has exposed several seamounts, some of which are exceptionally well-preserved, with the original cone morphology

still clearly visible. The Kakanui River, which flows roughly southeast towards the coast, contains excellent exposures of limestones and volcanics along its banks. There are also several limestone ridges, and a quarry nearby (Figure 1.5). Because of these numerous good outcrops, the area around Kakanui is an ideal site for stratigraphic and palaeoenvironmental investigations.

Figure 1.5: The area around Kakanui, and several of the main sites of investigation for this thesis. Kakanui North Head and Kakanui South Head are remnants of seamounts. The Campbells Bay and Kakanui River Mouth outcrops contain the top of the South Head volcanics, and overlying limestones. The Kakanui River Sections is an outcrop of reworked tuff deposits and limestones. The Upriver Lapilli Tuffs are steep cliffs of lapilli tuffs which line the eastern bank of Kakanui River.

1.5.1 Kakanui Headlands

The Kakanui Township sits next to two headlands which jut out into the ocean: Kakanui North Head and Kakanui South Head. These headlands are composed of Waiareka-Deborah volcanic tuffs, categorised by Thompson (1905) into a "mineral breccia" and a "barren breccia." The mineral-rich breccia, named the Kakanui Mineral Breccia, occurs at both headland deposits, sloping inwards at Kakanui South Head, and representing the interior of the cone (Corcoran & Moore, 2008). The KMB is a nephelinitic tuff breccia rich in upper mantle xenocrysts and

xenoliths. These include the international microprobe standards for kaersutite and anorthoclase feldspar, as well as good examples of garnet, eclogite, pyrope, pyroxene, and amphibole (Reay et al., 1993). The KMB was dated to 31.6 ± 1.2 Ma (K-Ar) by Dasch (1970), and more recently to 34.1 ± 0.1 (single fusions) and 33.7 ± 0.3 Ma (step heating analyses) by Hoernle et al. (2006). The KMB is only known to have erupted at the Kakanui Headlands, although a similar, but geochemically distinct mineral breccia also occurs in the Waiareka-Deborah volcanics at Alma (Reay, 2002).

The outermost units of Kakanui North Head and Kakanui South Head are less mineralogically diverse. They consist of lapilli tuff beds which include cm-scale bombs, basaltic clasts, palagonite altered from glass, and kaersutite xenocrysts (Mellis, 2016). This exterior unit is lithologically similar to the various tuffs which occur throughout the Waiareka-Deborah volcanic field. Unlike the nephelinitic KMB, Dickey (1968b) reports that these tuffs have alkaline olivine basalt chemistry.

1.5.2 Kakanui River Section

One of the best exposures around Kakanui is a section of limestones and tuffs which runs for around 300 m along the western bank of the Kakanui River. Strontium isotope dating of brachiopods by Nelson et al. (2004) shows an age range of 35.18 Ma at the base of the section, up to 34.13 Ma near the top. The biostratigraphy indicates deposition during the Runangan - Whaingaroan stages (36.0 - 27.3 Ma), and the section contains a continuous record across this boundary (Clowes, 2009). The ~10 m thick unit of grey and brown tuff which occurs in the middle of this outcrop was used as the type section for the now defunct Deborah Volcanic Formation, since the top and base were exposed, and Ototara Limestone beds separated it from a small, disconnected outcrop mapped as Waiareka Volcanics (Gage, 1957).

The rocks in the Kakanui River Section show a persistent dip of around 15 – 20° towards the ESE (Dickey, 1968b; Corcoran & Moore, 2008). A similar, if less extreme dip is seen across the South Island's east coast, related to deformation and local folding from the late Cenozoic development of the Alpine Fault (Norris et al., 1978). However, this regional dip is only 10° (Mutch, 1963), so the Kakanui River Section either represents an area of greater deformation, or deposition on a shallow slope which was later steepened (e.g. Corcoran and Moore, 2008).

The relationship between the Kakanui River Section and Kakanui South Head is somewhat uncertain. While the river section rocks dip towards the east, the inland rocks of South Head dip

towards the west, and the contact between the two is hidden in the 200 m gap which separates them. Park (1918) inferred the presence of a syncline, and believed that the South Head and River Section volcanics represented a single unit. Corcoran and Moore (2008) attribute the dips to deposition on the slopes of two adjacent cones. They see the volcaniclastic units in each location as separate deposits, but group the limestones overlying them into one unit.

1.5.3 Upriver Lapilli Tuffs

Upriver from the Kakanui River Section, and north of the bridge, cliffs of lapilli tuff run along the river's eastern bank. These are referred to in this thesis as the Upriver Lapilli Tuffs. Park (1918) noted this area as a "strong development" of tuffs, which he grouped as part of the older Waiareka Volcanics. He speculated that this section north of the bridge probably extended to a small outcrop south of it, 300 m upriver from the Kakanui River Section, although later authors assigned only the small outcrop to the Waiareka Volcanics, and the Upriver Lapilli Tuffs to the younger Deborah Volcanics. Based on the eastward dip of 10-12°, Park speculated that the Upriver Lapilli Tuffs probably underlay the Kakanui River Section.

Dickey (1966, 1968b) made some brief observations on the Upriver Lapilli Tuffs. He estimated their total thickness to be about 120 feet (36.6 m), with a sharp discontinuity around halfway up the outcrop. The topographic prominence and the presence of a basaltic dike suggest that the eruptive centre may have been near. Further upstream, a thin exposure of mineral breccia appears to be unconformable with the lapilli tuffs, and may represent deposits from a more distant vent, such as South Head.

1.6 Previous Investigations

1.6.1 Geological mapping

The first geological reports on the Waitaki Region were written by Mantell (1850), Hector (1865), McKay (1877) and Hutton (1886). These were followed by Park (1904, 1918) who conducted in-depth field mapping of the regional geology. Regional geological studies were also conducted by Uttley (1916, 1918), Benson (e.g. 1942), and Gage (1957).

Multiple sources have been compiled to produce regional geological maps of Waitaki, typically to 1:250 000 scale. Older regional maps include those of Mutch (1963), McKeller (1966) and

Gair, 1967). A new regional map was more recently compiled by Fordyce (2001) as part of the GNS quarter million mapping (QMAP) project.

1.6.2 Palaeontology

A number of studies have investigated fossils around the Kakanui area, mainly to develop biostratigraphy. These studies include macrofossils (Gage, 1957) dinoflagellates (Wilson 1982; Clowes & Morgans 1984; Clowes 1985; Clowes 2009), and foraminifera (Finlay, 1939a, b, c; 1940; Hornibrook, 1961; 1971; Hicks, 2014). Figure 1.6 shows some of the areas sampled, and the New Zealand stage they belong to. In general, deposits are older to the west, and younger to the east.

Hicks (2014) studied foraminifera and other fossils at several sites, in order to construct a detailed palaeoenvironmental interpretation. These locations included an outcrop of mudstones in a railway cutting near Maheno, a section of limestones and volcanics along a farm track near Clark's Mill, and the bioclastic deposits which formed on the Bridge Point cone (2.5 km south of Kakanui). Depositional environments for all locations ranged from inner to mid shelf, although with anomalously high numbers of *Globocassidulina subglobosa*, which is generally a deep-water indicator. The first two sites were found to be lateral equivalents, formed from distal turbidite deposits. However, any relationship between these and the Bridge Point site could not be determined.

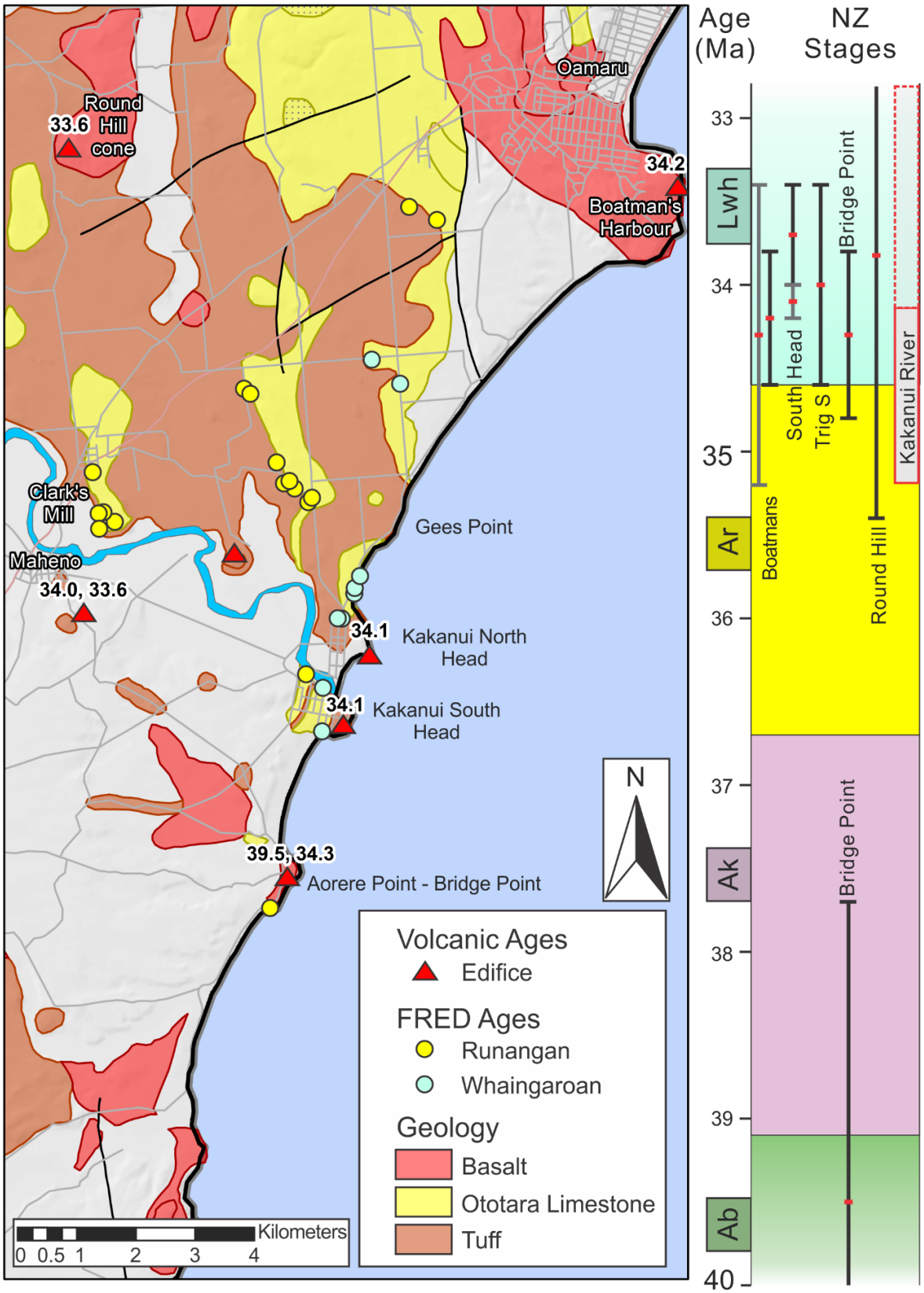

Figure 1.6: Biostratigraphy for sites around the study area (from FRED database), and volcanic ages (from Hoernle et al., 2006). The column on the right shows New Zealand stages, annotated with volcanic ages and error bars. Black error bars represent ages obtained by the $^{40}Ar/^{39}Ar$ step-heating method, and grey bars, the single fusions method. The older Bridge Point sample is from a basaltic andesite dike fragment, and possibly indicates older volcanism not exposed at the surface. The Kakanui River section date is based on Sr isotope dating of brachiopods (solid box) and pecten (dashed box) (Nelson et al., 2004).

1.6.3 Geochemistry

Volcanic deposits around Kakanui were produced by multiple volcanic cones, several of which are still evident today. These deposits include both the distinctive Kakanui Mineral Breccia, and the less mineral-rich volcaniclastics. These volcanics provide important geochemical clues to the magmatic processes that sourced them.

Hoernle et al. (2006) looked at several Waiareka-Deborah locations in their study of Cenozoic intraplate volcanism in New Zealand. They provide major and trace elements, and $^{40}Ar/^{39}Ar$ dates for some notable volcanoes in Waitaki. While Hoernle et al. (2006) note that their sample ages appear to cluster quite tightly, other authors who have investigated individual volcanoes have inferred slightly different ages, indicating that this clustering is not as strong as it appears. For example, the Bridge Point volcano, dated to 34.3 ± 0.9, is overlain by limestones of Runangan age (36.7 – 34.6) (Cas et al., 1989; Hicks, 2014), so must have erupted some time before 34.6 Ma. The Cape Wanbrow deposits, dated to 34.2 ± 0.4 and 34.3 ± 0.9 were determined by Moorhouse (2015) to represent six events, estimated to have occurred over a period from 38 – 36 Ma.

Coombs et al. (1986) sampled several Waiareka-Deborah volcanic localities, including Boatmans Harbour, Moeraki Peninsula and Lookout Bluff. They found that despite alteration and the presence of secondary minerals, microprobe analysis showed very similar magma compositions, similar to typical continental tholeiites, but with slightly higher than average alkali concentrations.

The Kakanui Mineral Breccia has received a lot of attention due to its unique mineralogy, and the preservation of upper-mantle material. Mason (1966, 1968) and Mason & Allen (1972) investigated the mantle xenoliths included in the KMB, and concluded that while the peridotite xenoliths are similar to those found elsewhere in the world, the eclogite xenoliths are unique in their chemistry. They analysed minor and trace elements in KMB augite, hornblende and megacrysts, determined that the containing magma was derived from a basaltic melt which underwent selective crystallisation following the removal of pyrope.

White and Chappell (1971) studied the chemistry of Kakanui xenocrysts, and minerals carried within eclogitic inclusions. They found that the transition from xenocryst minerals to eclogite minerals was accompanied by an increase in Fe/Mg ratio and Na_2O content in garnet and

clinopyroxene, and a change in clinopyroxene composition from more Tschermakitic to more jadeitic. They explain this as a result of fractional crystalisation, causing the parent alkali basaltic or basanitic magma to become more nephelinitic.

Several authors have constructed models to explain the magmatic developments responsible for the volcanism in Kakanui, most of these build around the same elements. Within the upper mantle, a rising nephelinitic melt, possibly triggered by an injection of alkali olivine basalt (Garden, 2001), began crystallising a variety of minerals, such as garnet, clinopyroxene and kaersutite (Mason & Allen, 1972; Merrill & Wyllie, 1975). This rising magma intersected another melt which contained mantle xenoliths of garnet and omphacite, and crystals of kaersutite (Dickey, 1968; Merrill & Wyllie, 1975), formed at high temperatures (1200° to 1350°C), and depths of 75 – 85 km (Clark et al., 1969; McCallister et al., 1976; Moorhouse, 2015). The xenoliths and xenocrysts were entrained as accidental inclusions in the rising melt (Mason & Allen, 1972; Merrill & Wyllie, 1975). The magma ascent was fairly rapid, causing the eclogitic inclusions to partially melt, but remain largely unaltered, and preventing denser xenoliths from settling out (Mason, 1966, 1968; Merrill & Wyllie, 1975).

Garden (2001) used an EMP and LAM study of KMB megacrysts to alter and refine the traditional magmatic model. This investigation determined that three magmas were involved in KMB petrogenesis. A nephelinite melt within the upper mantle formed garnet, clinopyroxene and kaersutite megacrysts, at pressures of 15 – 25kb and temperatures of 1150° – 1200°C. Magma ascent was triggered by an injection of alkali olivine basalt, which may have also added garnet xenocrysts with higher magnesium content. The ascending magma intersected a solid garnet pyroxenite pod; possibly evolved enough to contain plagioclase, trapped within lherzolite formed from an evolved nephelinite parent. The nephelinite host introduced volatiles to the lherzolite, triggering the precipitation of metasomatic kaersutite.

1.6.4 Volcanic Processes

Once magma reaches the surface, a number of factors influence the type of deposits it produces. These include eruption style, nature of erupted material, and volcaniclastic transport mechanisms. Several authors have addressed the volcanic processes occurring around Kakanui, and at other Waiareka-Deborah edifices.

Dickey (1966, 1968b) studied the volcanic deposits around Kakanui, and concluded that they represented three volcanic eruptions of the younger, now defunct, Deborah Volcanic Formation.

He grouped the less mineralogically diverse volcaniclastics which formed from alkaline olivine basalt into two units: Tuff I and II. These units outcrop along the outside of the headlands and along Kakanui River. They were followed by the eruption of the Kakanui Mineral Breccia, which formed from nephelinite magma, and outcrops at the centre of Kakanui North and South Heads.

Corcoran and Moore (2008) use facies analysis to interpret the deposits around Kakanui South head and Kakanui River mouth. They conclude that two closely spaced cones are present; one of which is well exposed along the coastline, and another further inland, with deposits which outcrop along the western bank of the Kakanui River. They attribute both volcaniclastic units in this river section to high particle density deposits from the same vent, with the fine-grained unit separating them representing a volcanic hiatus. The shelly limestone which overlies these river section volcanics is correlated with the limestone beds that overlying the South Head volcanics at Campbells Bay and Kakanui River mouth.

Volcanic processes at other Waiareka-Deborah volcanic centres have also been studied. Cas et al. (1989) investigated the volcanic edifice which outcrops at Bridge Point and Aorere Point, around 2.5 km south of Kakanui South Head. The Bridge Point/Aorere Point edifice is older than Kakanui South Head; it was dated to 34.3 ± 0.5 Ma (Hoernle et al., 2006), and overlying strata indicate an eruption before the end of the Runangan (34.6 Ma). Cas et al. (1989) found that deposits included a basal unit of lapilli tuffs and lapillistones, representing reworked fall deposits which built up a cone during an eruption period which probably only lasted several days. Overlying this is an epiclastic sequence formed during post-eruptive degradation. This overlying sequence includes layers with volcanics, bioclasts, carbonate muds and glauconite. Grainsize decreases to mudstone in the upper unit, which Cas et al. (1989) interpret as evidence of sea level rise. A tuffaceous deposit near the top of the sequence indicates the eruption of a separate, more distant volcano.

Recently, Moorhouse (2015) analysed the deposits which occur around at Cape Wanbrow, next to Oamaru. He concluded that this promontory represented at least six overlapping vents. This seems unlikely to have resulted simply from random eruption locations, and Moorhouse speculates that some factor, such as a long-lived crustal feature, or a more “meltable” zone, may have caused this area to be a preferable eruption site. The volcaniclastic deposits from these vents were determined to include subaqueous density currents, both eruption-fed and reworked;

as well as subaerial deposits formed while a cone was emergent. This shows the complexities which can be involved, even in a "monogenetic" volcanic field.

1.7 Aims

The objective of this thesis is to further the understanding of the volcanic and sedimentary environment occurring during the Eocene-Oligocene at Kakanui. It will use a multidisciplinary approach to determine palaeodepth, characterise the sediment source, and identify the factors affecting deposition. It will consider both larger-scale events, such as sea-level changes; as well as local events, such as seamount eruptions and mass-transport processes.

One of the main aims is to investigate the depositional environment of the Kakanui River Section outcrop. This will involve detailed investigation of the changes in lithology and sedimentary structures across the section, and the identification of foraminifera present within these units. Strike and dip measurements around Kakanui will help to get absolute bed thicknesses, indicate stratigraphic relationships, and reveal the influence of any structural modification. This information will be used to characterise the evolution of the depositional environment, including factors such as sea level changes, palaeocurrent direction, and supply and transport of carbonate, terrestrial and volcaniclastic sediment.

This thesis will also investigate the volcanic provenance of Waiareka-Deborah deposits, particularly the two volcaniclastic units within the Kakanui River Section. It is hoped that geochemical and mineralogical analysis of volcaniclastic deposits and volcanic edifices will uncover "fingerprints" which characterise particular eruptions. This will help to identify the sources of volcanic deposts, and can also be used to help understand the magmatic changes occurring within the Waiareka-Deborah volcanic field.

The final aim of this thesis is to integrate the palaeoenvironmental interpretations obtained from the sedimentology and palaeontology of the Kakanui River section with the volcanological interpretations derived from field research and geochemistry. This will inform a detailed model of the evolution of the study area, which will include changes in water depth, sediment supply, volcanism, and other major factors. It is hoped that this thesis will bridge some of the studies which have focused on one particular subject, to help develop a greater understanding of the overall geological evolution at Waitaki.

2. Methods

2.1 Field Investigation

The fieldwork for this thesis mainly took place on 18 - 28 March, 2016. This involved detailed site investigation at several locations around Kakanui, as well as a broader survey of outcrops around the Waiareka-Deborah Volcanic Field. Some of the main sites of investigation are shown on Figure 2.1.

The Kakanui River Section was mapped in detail, with notes made on the sedimentary structures, grainsize, and bioclast and clastic composition of each bed. Rock samples were also taken at regular intervals, for more in depth analysis. The geological changes observed in this section helped to construct a model of the evolving environment around Kakanui.

Detailed strike and dip data was recorded around the Kakanui Headlands, along the Kakanui River Section, and at accessible points on the Upriver Lapilli Tuffs. These dips were measured using a geological compass, and often a flat map board. Around the headland, bedding planes were well exposed, although care had to be taken to avoid any that had been rounded by weathering. Measurements along the river were more difficult, since bedding was sub-horizontal, and often only visible in two dimensions on the face of the outcrop. Where necessary, parts of the outcrop were excavated to get a plane that could be measured.

At the time of this investigation, the mouth of the Kakanui River was fairly narrow due to clogging and the build-up of the mouth bar. This caused high river levels, and made it more difficult to access outcrops. Additionally, at high tide the coastal outcrops became mostly submerged. However, these difficulties did not prevent these sites from being accessed and investigated.

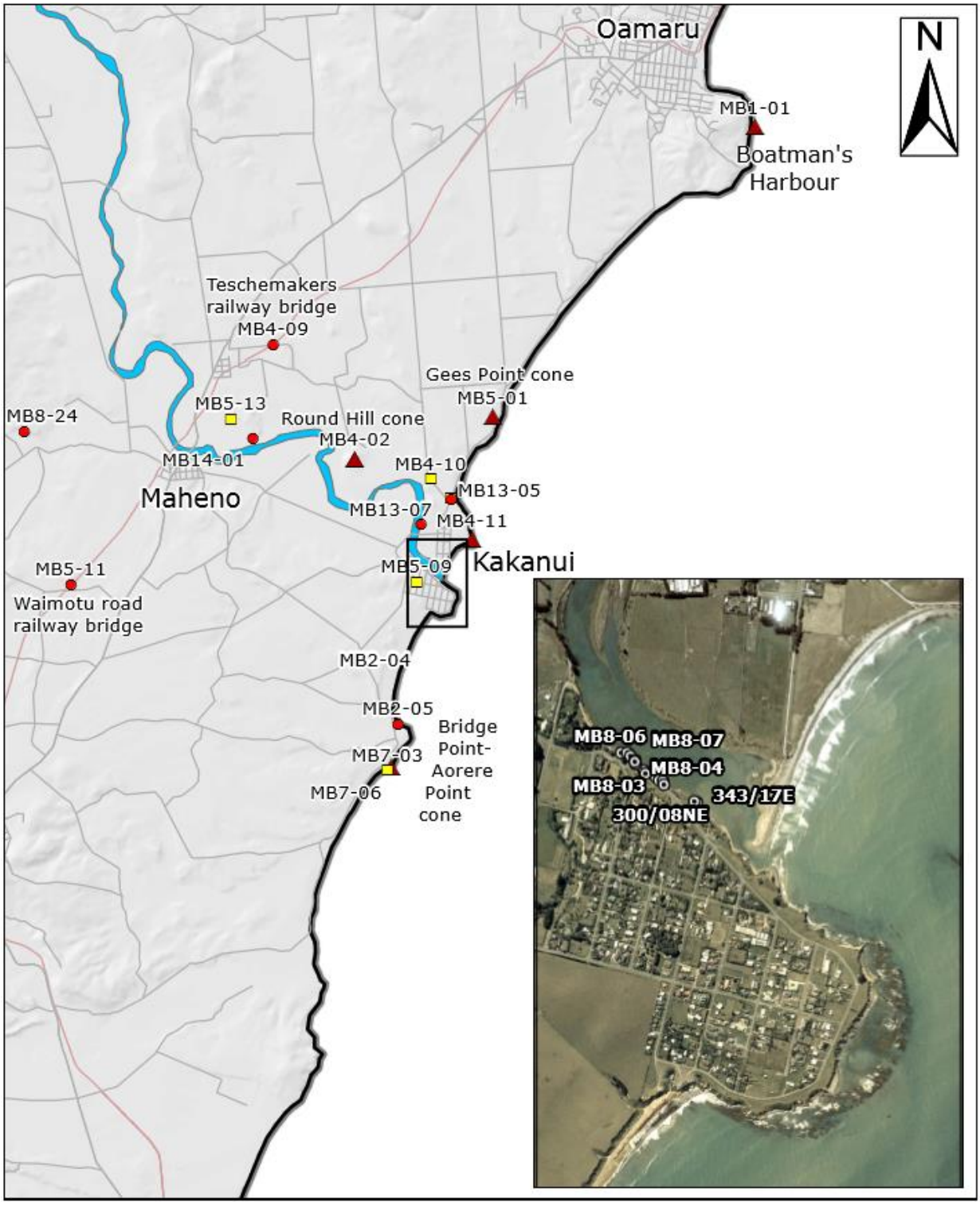

Figure 2.1: Map of the Waitaki coastline, annotated with some of the areas investigated and sampled in this study. (Red triangles – volcanic cones; red circles – tuffs; Yellow squares – limestones.)

2.2 Foraminifera counts

Rock samples from along the Kakanui River Section and at the Kakanui River Mouth were broken into small fragments, using a press. Approximately 500 mL of each sample was soaked in water for 24 hours to disaggregate it, then washed through a 350 µm sieve, to remove the finest particles. The samples were then soaked for a further 24 – 48 hours in a solution of calgon (sodium hexametaphosphate), until they had broken down to their component clasts. After this, the samples were again poured through a 350 µm sieve, dried in an oven at 50°C for 24 hours, and examined under a microscope.

Foraminifera were relatively abundant in all of the sampled limestone sequences. They were present in samples from the cross-bedded and laminated volcaniclastics, but not in sufficient numbers to get a good representation. Those samples with enough foraminifera were put through a sediment splitter and a fraction (typically 1/32), was poured into a gridded tray and examined under a microscope. A square was selected using a random number generator, and every foraminifera present within it was collected. Following this, another square was randomly chosen, until at least 100 foraminifera had been taken from each sample. These were then grouped by genus or in some cases, species, so that they could be used for environmental interpretation.

2.3 Thin section microscopy

Several samples were selected to be made into thin sections, including volcanic rocks from various sources across Waitaki, as well as samples from the Kakanui River Section, and other sites of investigation. These samples were cut into small rectangular blocks, then mounted on glass slides, diamond cut to thin slivers and ground down to a thickness of 30 – 35 µ. These thin sections were left uncovered, so that they could still be used for geochemical analysis. An epoxy resin was used to hold together some of the more poorly indurated or porous limestone and calcareous sandstone samples.

The thin sections were examined with a petrographic microscope, and photographed using a Leica DFC-295 camera attachment. Several observations were recorded, including texture, grainsize, sorting, grain rounding or crystal habit, bioclasts present, minerals present, and

matrix-to-clast ratio. The samples from the river section were used to add finer details to the stratigraphic column and aid in environmental interpretations of that area.

2.4 Microprobe analysis

Mineral-rich tuffs of Waiareka-Deborah volcanics were collected from around the study area, in order to get mineral samples for microprobe analysis. These tuffs were crushed using a press and examined under a microscope so that minerals could be picked out. Picked minerals included kaersutite, olivine and chrome diopside. These minerals were then arranged into sections on double-sided tape, sealed into epoxy disks, and polished.

The mounted minerals were taken to the Analytical Facility at the Victoria University of Wellington, and analysed using a JEOL JXA-8230 SuperProbe Electron Probe Microanalyser. Microprobe operating conditions were:

- A beam current of 10 nA
- An accelerating voltage of 15kV
- A defocussed beam diameter of 100 µm

Kaersutite analysis was calibrated against the "Hornblende" microprobe standard. Olivine and pyroxene were calibrated against the "Px1", "Hypersthene" and "Springwater" standards. Once the microprobe analysis had finished, points which had measured element totals lower than 97 % were removed. The remaining samples had totals of between 97.163 % and 101.764 %, and were considered more reliable.

2.5 X-ray fluorescence

X-ray fluorescence (XRF) was used to determine the bulk chemistry of basalt from bombs, dikes and lava flows. Good samples were obtained from sites with lavas or larger bombs. However, the Kakanui River Section was more difficult, as most volcanic clasts were less than 1 cm in diameter, and surrounded by a calcite-rich matrix (Figure 2.2). In order to get the 10 grams of material required for XRF, samples of the coarsest tuffs were taken, crushed under a rock press to break them apart, and then sieved to remove small fragments. Then, individual basalt lapilli were removed, and any calcite cement coating was scraped off. These samples are less likely to provide accurate quantification of absolute magmatic compositions than the cores of large basaltic bombs or lavas, but they should still give useful information for geochemical

fingerprinting. In order to determine the accuracy of this technique a sample from the Upriver Lapilli Tuff, which also includes a dike and large bombs, was prepared in the same way, to assess the difference between picked lapilli and solid basalt samples.

Figure 2.2: Different types of volcanic sample types. **A:** Bomb from Kakanui South Head. **B:** Basalt from dike at Taipo Hill. **C:** Ash and lapilli taken from broken Kakanui River Section Tuff A.

The selected samples were cut with a diamond saw to remove any cement or impurities. After being dried, they were crushed to fragments in a hydraulic press, and then put in a ring mill to grind them to powder. The powdered samples were analysed using the fusion bead method. A weighed portion of each sample was heated until it melted into a homogenous glass, which removed complications caused by different grainsizes and mineralogies. These glass beads were analysed for both major and trace elements.

3. Results

3.1 Field mapping

Detailed geological mapping was used to construct stratigraphic columns for several sites around Kakanui, including the Kakanui River Section, the top of the Kakanui South Head volcanics at Campbells Bay and the Kakanui River Mouth, and the scattered outcrops on the inland hillslope of Kakanui South Head. These columns contain a number of different facies, which provide important clues to the geological development of the area.

3.1.1 Kakanui River Section

The Kakanui River section contains an almost completely unbroken outcrop running along the western river bank for around 300 m. These rocks have a fairly consistent dip of around 15 - 20° to the east, and an estimated total thickness of around 50 m. A number of different facies occur within this section, described in table 5.1. Detailed field investigation was used to measure and identify the beds in the Kakanui River Section, and this information was used to construct a stratigraphic column. Thin section locations, as well as foraminiferal study locations (from this report and previous investigations) are annotated to the right of the column (Figure 3.1).

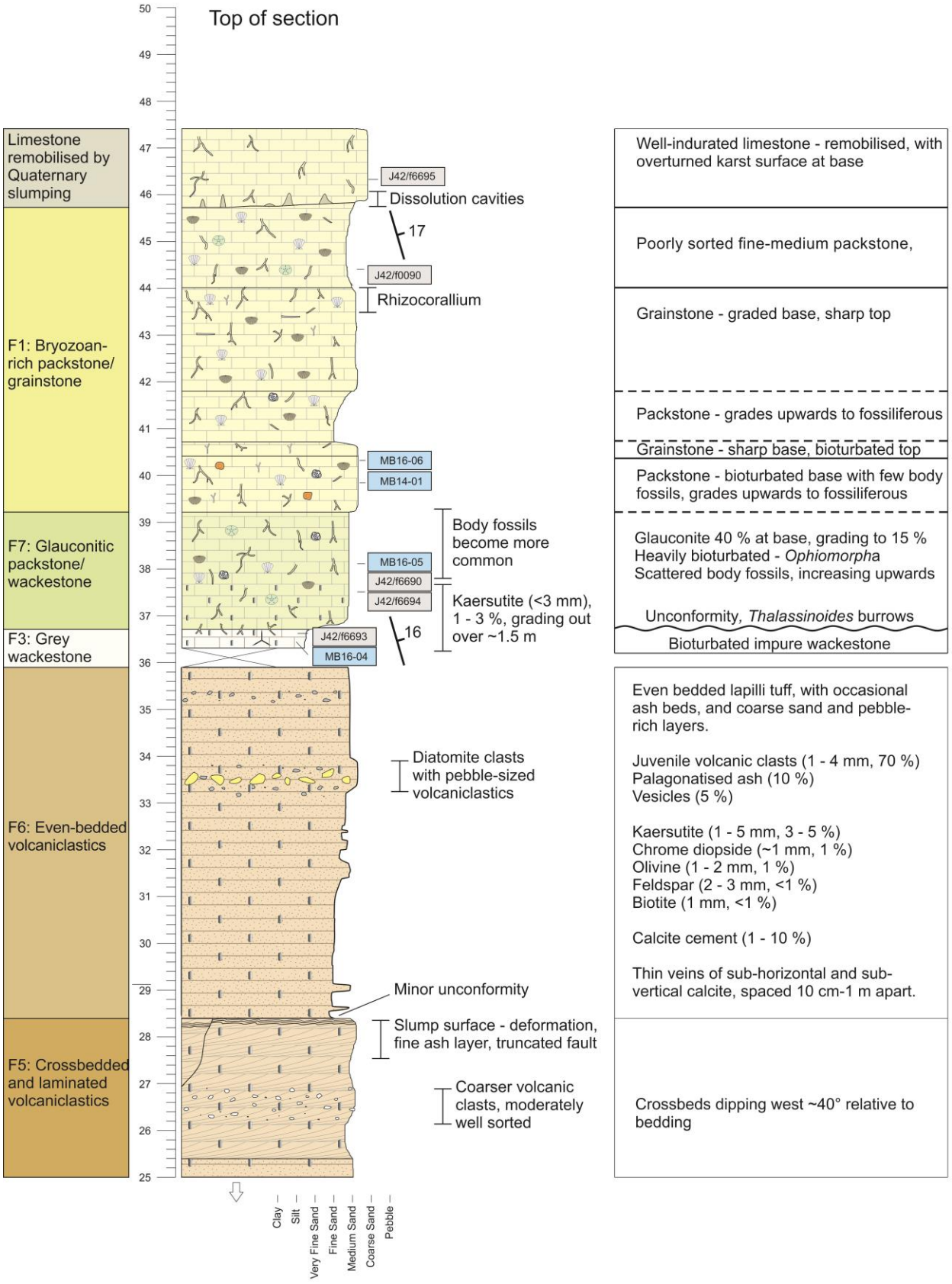
Top of section
50
49
48
47
46
45
44
43
42
41
40
39
38
37
36
35
34
33
32
31
30
29
28
27
26
25
Limestone remobilised by Quaternary slumping
F1: Bryozoan-rich packstone/ grainstone
F7: Glauconitic packstone/ wackestone
F3: Grey wackestone
F6: Even-bedded volcaniclastics
F5: Crossbedded and laminated volcaniclastics
J42/f6695
Dissolution cavities
17
J42/f0090
Rhizocorallium
MB16-06
MB14-01
Body fossils become more common
MB16-05
J42/f6690
J42/f6694
Kaersutite (<3 mm), 1 - 3 %, grading out over ~1.5 m
16
J42/f6693
MB16-04
Diatomite clasts with pebble-sized volcaniclastics
Minor unconformity
Slump surface - deformation, fine ash layer, truncated fault
Coarser volcanic clasts, moderately well sorted
Clay
Silt
Very Fine Sand
Fine Sand
Medium Sand
Coarse Sand
Pebble
Well-indurated limestone - remobilised, with overturned karst surface at base
Poorly sorted fine-medium packstone,
Grainstone - graded base, sharp top
Packstone - grades upwards to fossiliferous
Grainstone - sharp base, bioturbated top
Packstone - bioturbated base with few body fossils, grades upwards to fossiliferous
Glauconite 40 % at base, grading to 15 %
Heavily bioturbated - Ophiomorpha
Scattered body fossils, increasing upwards
Unconformity, Thalassinoides burrows
Bioturbated impure wackestone
Even bedded lapilli tuff, with occasional ash beds, and coarse sand and pebble-rich layers.
Juvenile volcanic clasts (1 - 4 mm, 70 %)
Palagonatised ash (10 %)
Vesicles (5 %)
Kaersutite (1 - 5 mm, 3 - 5 %)
Chrome diopside (~1 mm, 1 %)
Olivine (1 - 2 mm, 1 %)
Feldspar (2 - 3 mm, <1 %)
Biotite (1 mm, <1 %)
Calcite cement (1 - 10 %)
Thin veins of sub-horizontal and sub-vertical calcite, spaced 10 cm-1 m apart.
Crossbeds dipping west ~40° relative to bedding

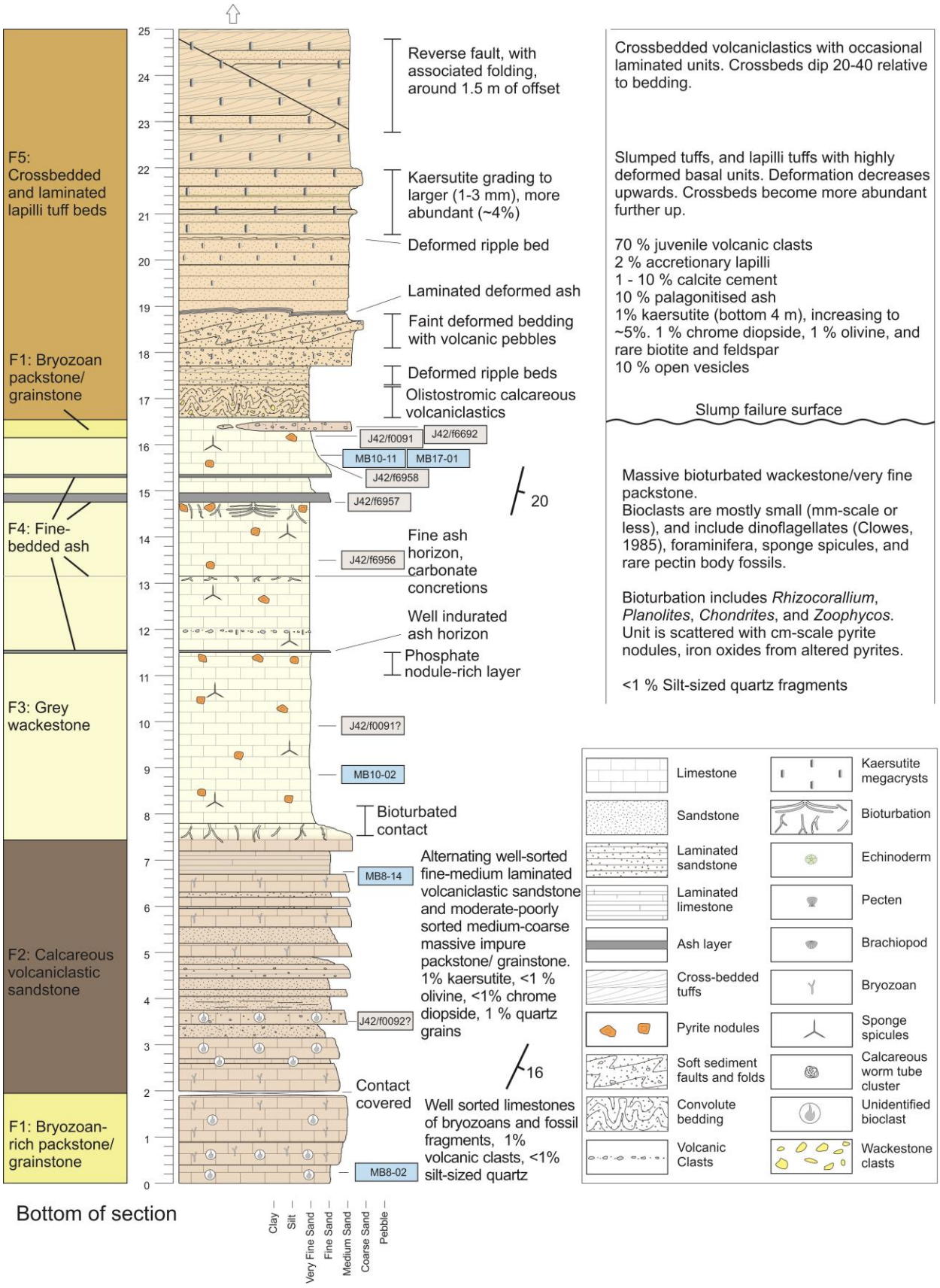

Figure 3.1: Stratigraphic column of the Main Kakanui River Section. Blue boxes are selected samples taken as part of this investigation, grey boxes are samples taken from previous investigations, recorded in the FRED database.

Section 1: Basal limestones - Bryozoan-rich packstone/grainstone facies (F1)

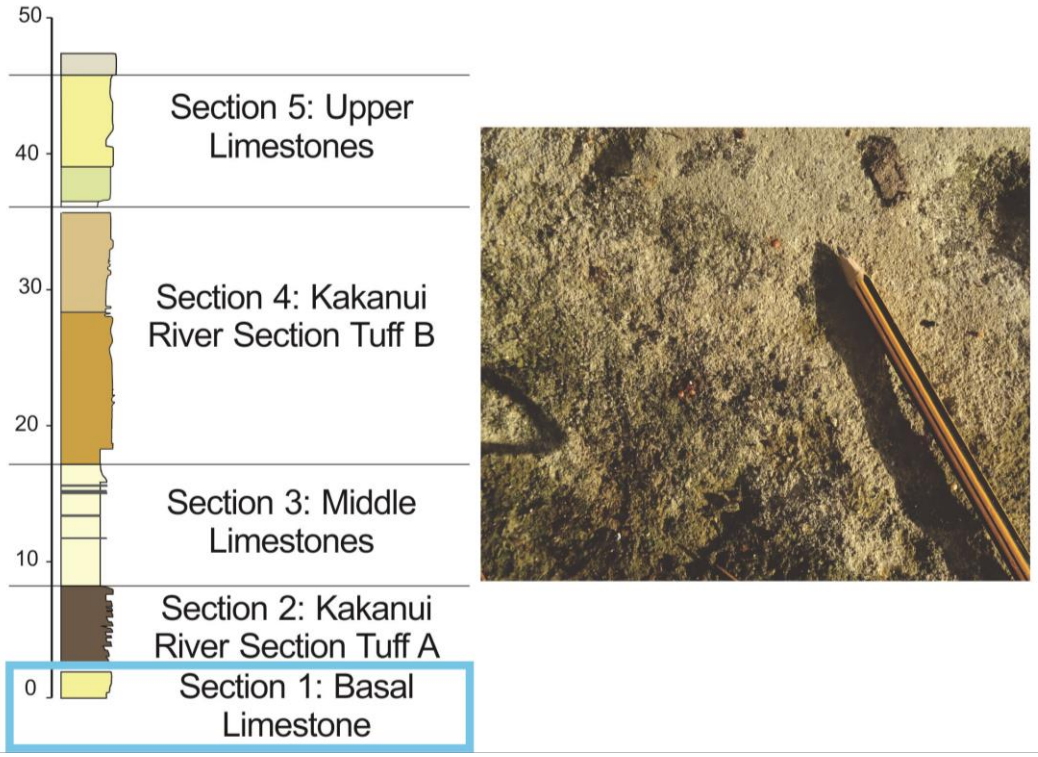

Figure 3.2: Appearance and stratigraphic position of Section 1.

The bottom-most section is composed of massive impure beds of the bryozoan-rich packstone/grainstone facies (F1) (Figure 3.2). This section is roughly 3 m thick, covered at the base by Quaternary sediments, and overlain by a gradational contact.

This bryozoan-rich packstone/grainstone unit contains medium to coarse sand-sized grains, which are moderately well sorted. This unit dominantly consists of branching bryozoan fragments (~60 %). Echinoderm plates and spines are common (~10 %), typically 2-3 mm fragments. Sand-sized volcanic fragments are present in low concentrations (~1 %). Benthic forams can be observed in thin section, although they are rare (<1 %) and difficult to notice amongst all the other bioclasts. Glauconite has formed in situ within bioclast pore spaces (15 %), and is also present as rare, variably oxidised detrital grains (1 %). Rare terrigenous clasts of very fine sand-sized quartz fragments are present (1 %). The porosity of the rocks can be seen in thin section, with both inter- and intragranular void spaces present (10%). All beds are grain-supported, but many layers contain small amounts of micritic mud (Figure 3.3).

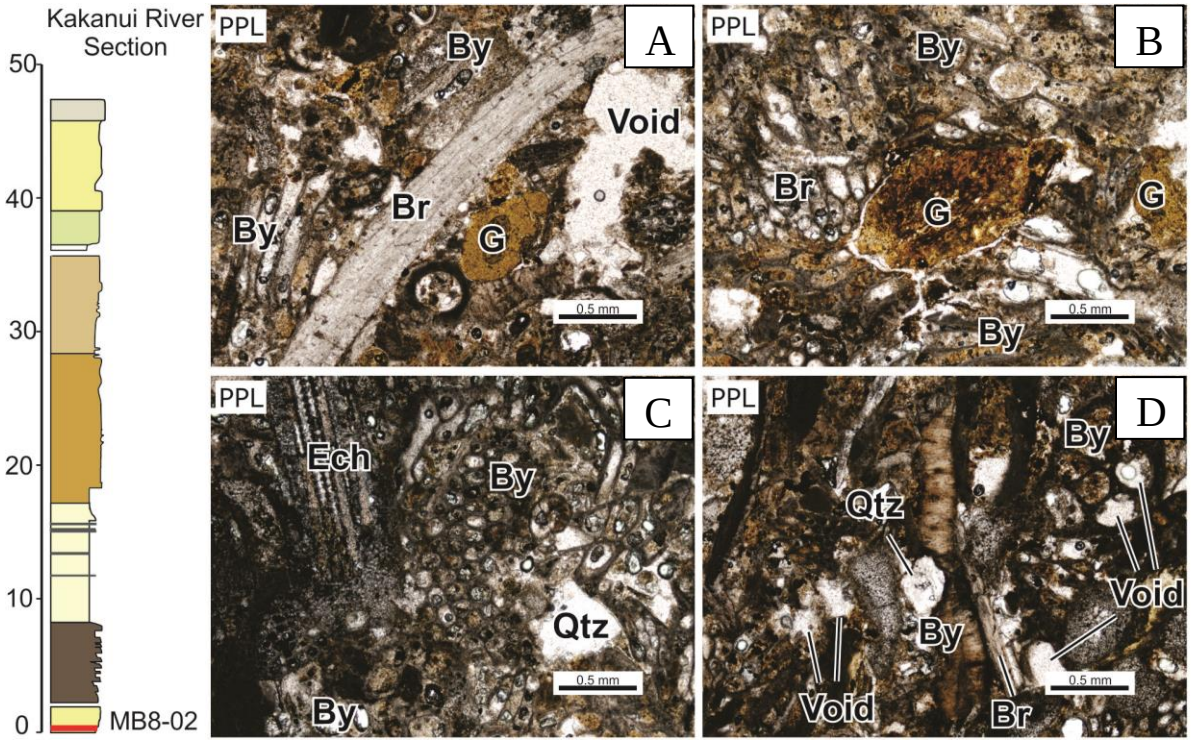

Figure 3.3: Thin section of MB8-02, from the bryozoan packstone/grainstone at the base of the river section. This thin section contains tightly packed branching bryozoan fragments, with rounded glauconite clasts, and in situ glauconite intraclasts are present. Grains are moderately well sorted and sub-angular., with one large void space. Top left contains a 5 mm brachiopod shell fragment
By = Bryozoan; Br = Brachiopod; Ech = Echinoderm; G = Glauconite; Qtz = Quartz, Void = Void space

Interpretation:

This bryozoan-rich packstone/grainstone unit contains an assemblage of inner-mid shelf bioclasts, including branching bryozoans and benthic foraminifera. Within the study area, this facies is sourced from volcanic highs colonised by marine organisms. The formation of glauconite within pore spaces implies that this deposit experienced semi-reducing conditions with low reasonably low sedimentation rates. The rare fine sand-sized quartz fragments are likely terrigenous clasts eroded from the Otago Schist basement rock. They are very rare in this section, reflecting only a minor supply of sediment from the palaeoshoreline.

Section 2: Kakanui River Section Tuff A - Calcareous volcaniclastic sandstone facies (F2)

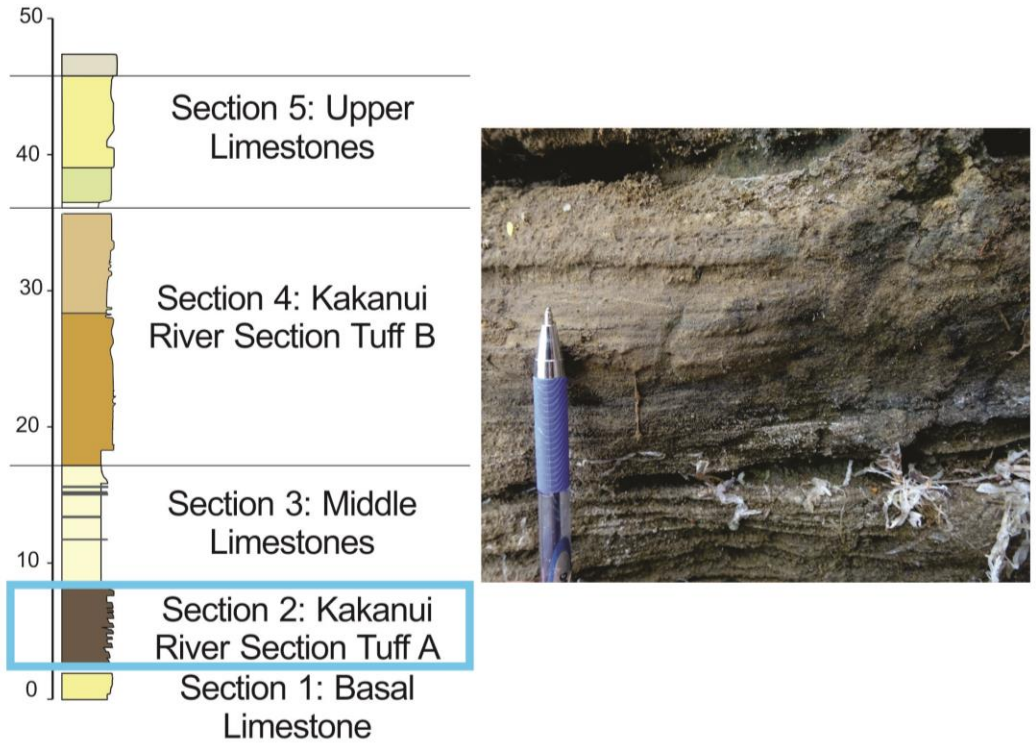

Figure 3.4: Appearance and stratigraphic position of Section 2.

The underlying bryozoan limestones transition gradationally into the next section (Figure 3.4), which contains a more tuffaceous unit of alternating massive and laminated very fine to medium calcareous sandstone (Figure 3.5). The massive beds are moderately sorted, and tend to contain sub-angular to sub-rounded clasts, while the laminar beds are typically well sorted within lamellae, and contain rounded to sub-rounded clasts. This unit is one of the deposits investigated for geochemical fingerprinting in Section 3.4, where it is named "Kakanui River Section Tuff A". Near the bottom of this section, the beds are mainly fine to very fine sand-sized calcareous volcaniclastics. Further towards the top, the beds become more fossiliferous and coarser-grained (fine to medium sand-sized). Volcanic clasts occasionally exceed 1 cm, but most are ash-sized.

The upper, more fossiliferous beds have less volcanic material (<20 %), and similar bioclast assemblages as those from the underlying bryozoan-rich packstone/wackestone. Bryozoan fragments are dominant (~40 %). Benthic foraminifera (1 – 3 %), and fragments of bivalves (5 – 10 %), bryozoans (1 – 5 %), echinoderms (~10 %) and unidentified fossils (15%) are also present. A thin grain bounding calcite is present in some beds (up to 15 %). Very fine sand-sized quartz fragments occur rarely (1%). In situ glauconite is present in some bioclast pores (1 %) (Figure 3.6).

Figure 3.5: Alternating massive (A) and laminated (B) beds of calcareous volcaniclastic sandstone.

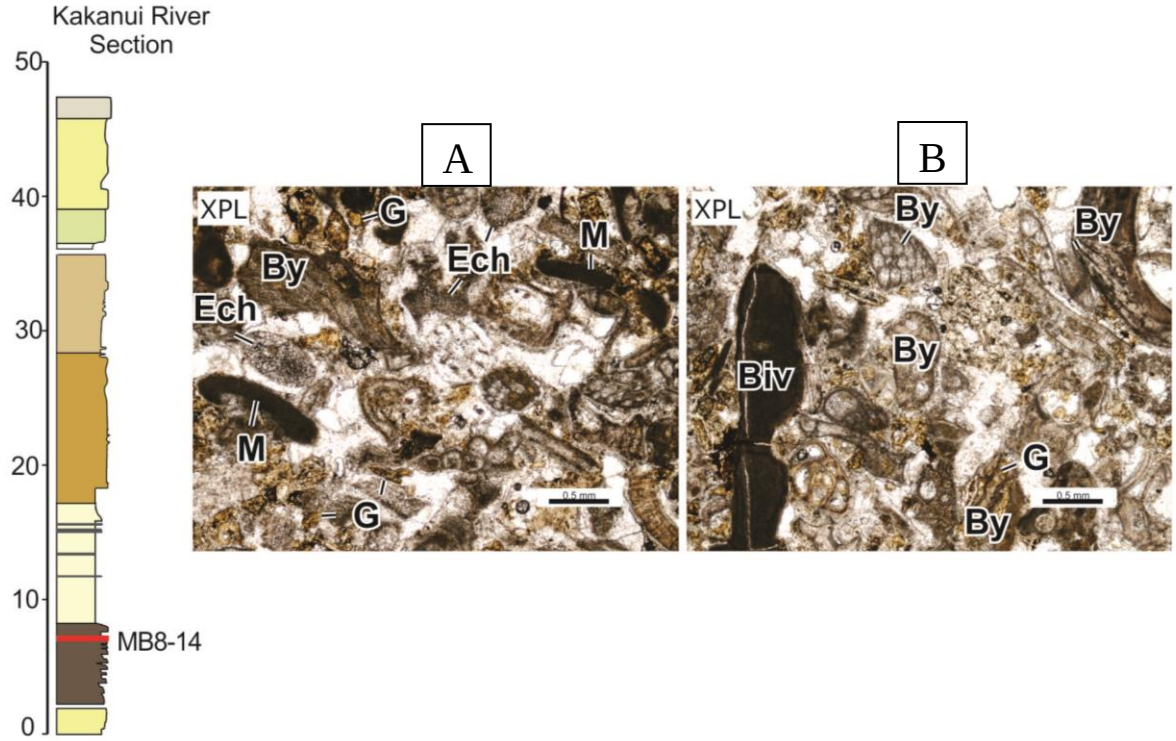

Figure 3.6: Thin section from MB8-14, a fossil-rich layer from the turbidite deposits of calacareous volcaniclastic sandstone. Bioclast fragments are subrounded, and include bryozoans, bivalves, echinoderms and foraminifera. Isopachous cement is very common. Interclast and intraclast calcite cement is also present; this has formed syntaxially with echinoderm bioclasts.
By = Bryozoan; Biv = Bivalve; Ech = Echinoderm; G = Glauconite

Interpretation

This facies contains massive and laminar beds, characteristic of the bottom layers of a turbidite Bouma sequence. The well-rounded and sorted clasts are consistent with transport in turbidity currents. The mixture of carbonate and volcanic clasts suggests that the sediment source was a volcanic cone which was colonised by marine organisms, then began to collapse and be reworked. Following deposition, this facies underwent diagenesis which produced fine isopachous cement, interstitial blocky cement, and syntaxial overgrowths on echinoderm bioclasts. Isopachous cements are typical of marine environments, indicating that this section remained submerged for some time.

Section 3: Middle limestones - Grey wackestone facies (F3), thin bedded ash facies (F4)

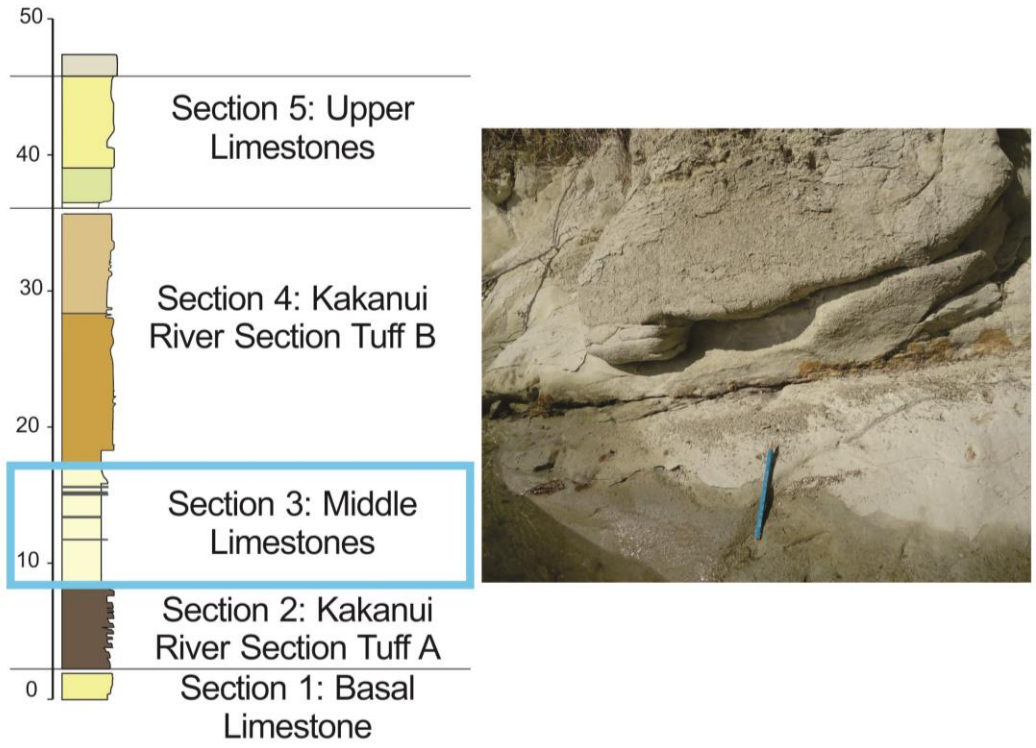

Figure 3.7: Appearance and stratigraphic position of Section 3.

Above the turbidite beds, there is a thick (~7 m) section of grey wackestone (F3) (Figure 3.7). The contact between the turbidite beds and this wackestone has been destroyed by intense bioturbation, but its location can be narrowed down to within 1 m. The wackestone itself is massive and fairly homogeneous. It is occasionally broken by thin ash layers (F4) and pebble-

rich horizons. Occasional rusty orange spots are present across the outcrop; this is likely iron staining from pyrite nodules.

In thin section, this grey wackestone unit is mostly composed of micritic mud (80 – 90 %). Planktic (1-2 %) and benthic foraminifera (3 – 5 %) are present, though with the exception of a few larger specimens, these are quite difficult to distinguish from the matrix. Well preserved siliceous sponge spicules are present (2-5 %), some of which show glauconitisation along their central hollow axis. Glauconite is also present as very fine sand-sized grains (2-5 %). Silt-sized quartz fragments are present in low amounts (<1-2 %) (Figure 3.8).

The thin bedded ash facies (F4) occurs in several places throughout this section. This facies is characterised by reasonably thin beds (mm- to cm-scale), with sharp boundaries. The grainsize is silt to fine sand, although thinner ash lenses are often associated with volcanic pebbles. The darker colour of this facies contrasts with the grey wackestone it occurs alongside, and bioturbation which mixes the two sediment types stands out strongly. Obvious *Planolites*, *Chondrites* and *Zoophychos* trace fossils are highlighted along the boundaries between F3 and F4 (Figure 3.9).

The thin bedded ash layers are often less permeable than the rocks surrounding them, forming an aquitard. This causes groundwater to be channelled along the edge of the ash beds, resulting in a zone of increased mineralisation, with a higher abundance of pyrite nodules.

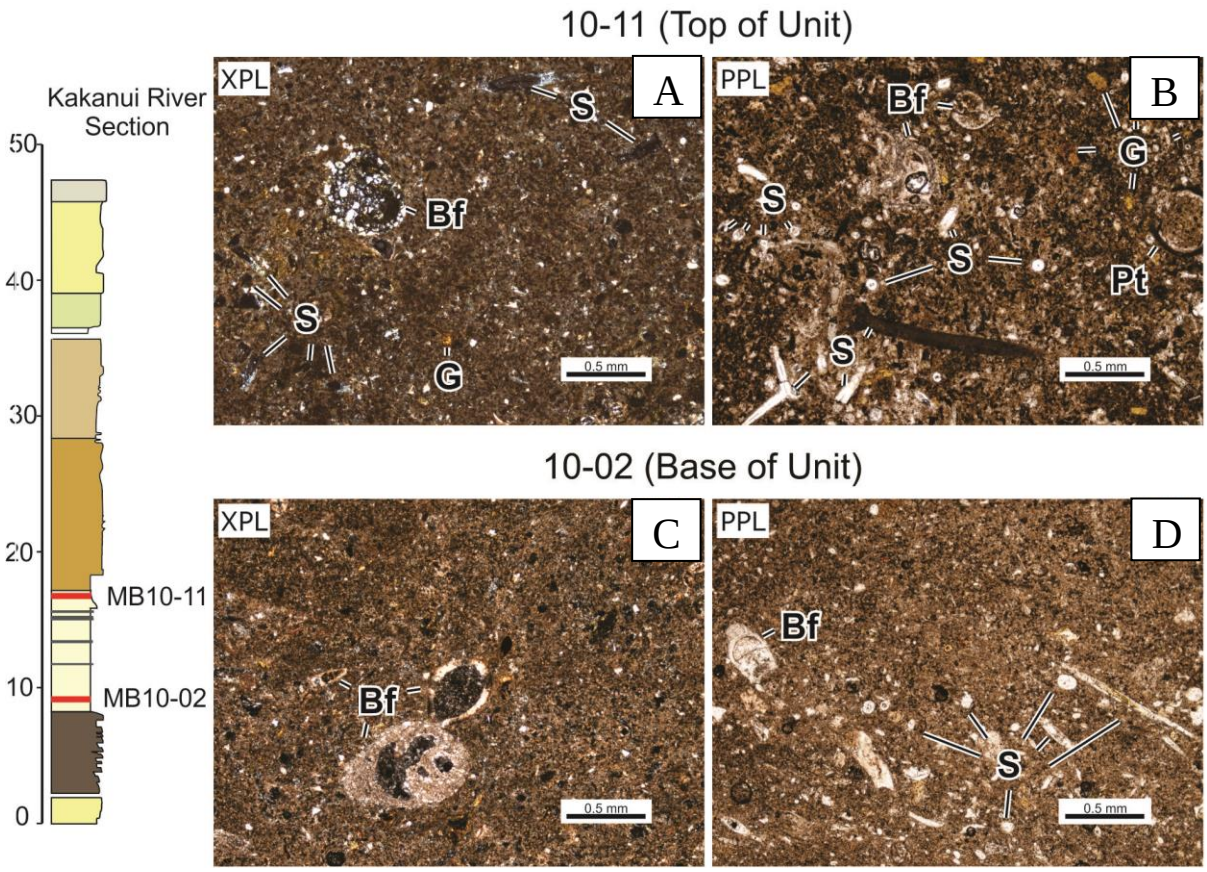

Figure 3.8: Thin sections from samples MB10-11 and MB10-02, from near the top and base of the very fine packstone/wackestone facies. Both thin sections contain similar bioclasts in a calcareous mud matrix.
A: shows sponge spicules, and a benthic foraminifera.
B has a higher concentration of bioclasts, including siliceous sponge spicules, benthic forams, a circular pteropod, as well as glauconite clasts.
C shows intraclast porosity within benthic foraminifera.
D has a uniserial benthic foraminifera, and several siliceous sponge spicules, some of which are internally glauconitised
Bf = Bethic foraminifera; S = Sponge spicule; Pt = Pteropod; G = Glauconite

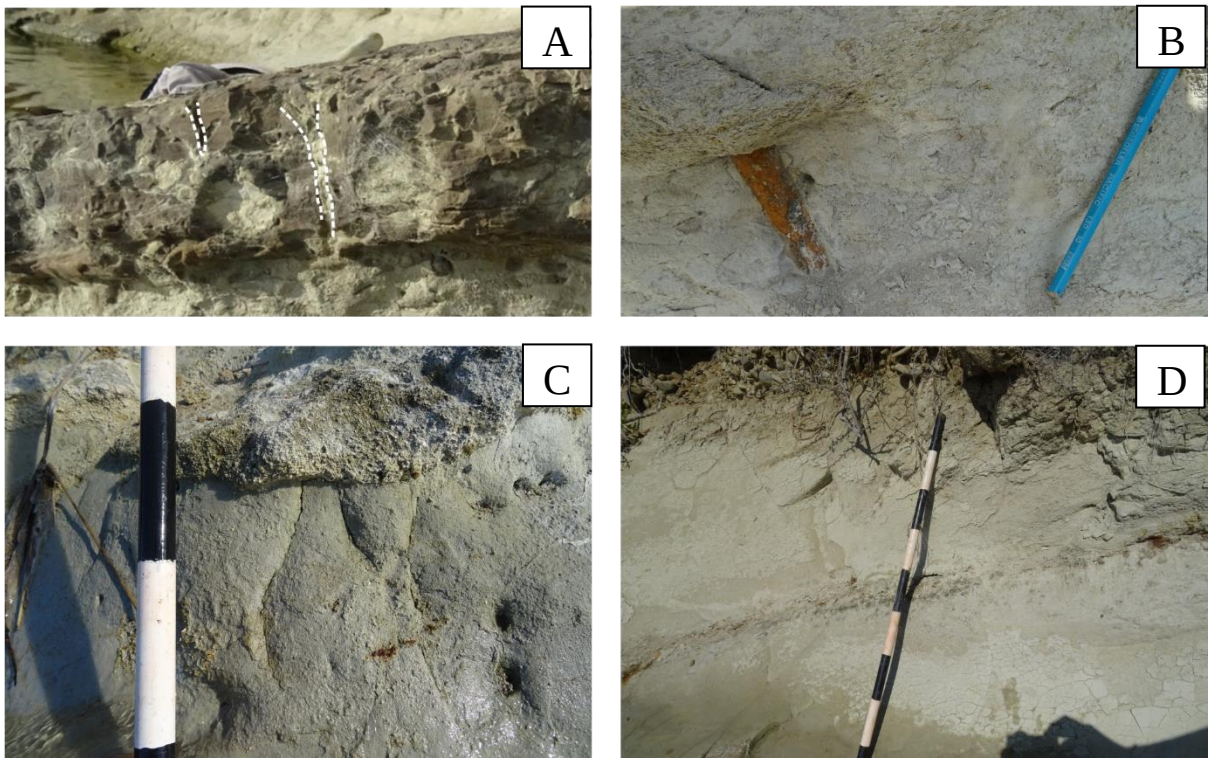

Figure 3.9: Photos from the grey wackestone unit. **Top left:** Bottom: Burrows perpendicular to a thin bedded ash layer. **Top right:** burrow infilled with pyrite. Top right: *Zoophycos* trace fossils on the surface of a grey wackestone layer. **Bottom left:** Discontinuous layer of bryozoan-rich packstone/wackestone. **Bottom right:** volcanic-rich horizon, possibly from a storm event or distant eruption. **Middle right**: *Zoophycos* burrow outlined by material from the overlying thin bedded ash.

Interpretation

The grey wackestone facies (F3) appears to have been deposited in a relatively deep sheltered environment, by suspension sedimentation. The fine sand to clay grainsize is not as diagnostic as it would be in a high sediment flux siliciclastic system, but it still indicates a low-energy environment. Sedimentary structures have been obscured by the intense bioturbation; typical of a low-energy setting. Bioclasts, such as siliceous sponge spicules and higher numbers of planktic foraminifera are consistent with deep mid-shelf to outer shelf.

The thickest occurrences of the thin bedded ash facies (F4) probably represent nearby eruptions, which provided a brief influx of volcanic material, either through direct ashfall or by triggering turbidity currents. Storm events also tend to deposits lenses of ash, but these are typically thinner, and associated with pebbles, which must have been deposited by high energy processes.

Section 4: Kakanui River Section Tuff B - Cross-bedded and laminated volcaniclastics (F5), and even-bedded volcaniclastics (F6)

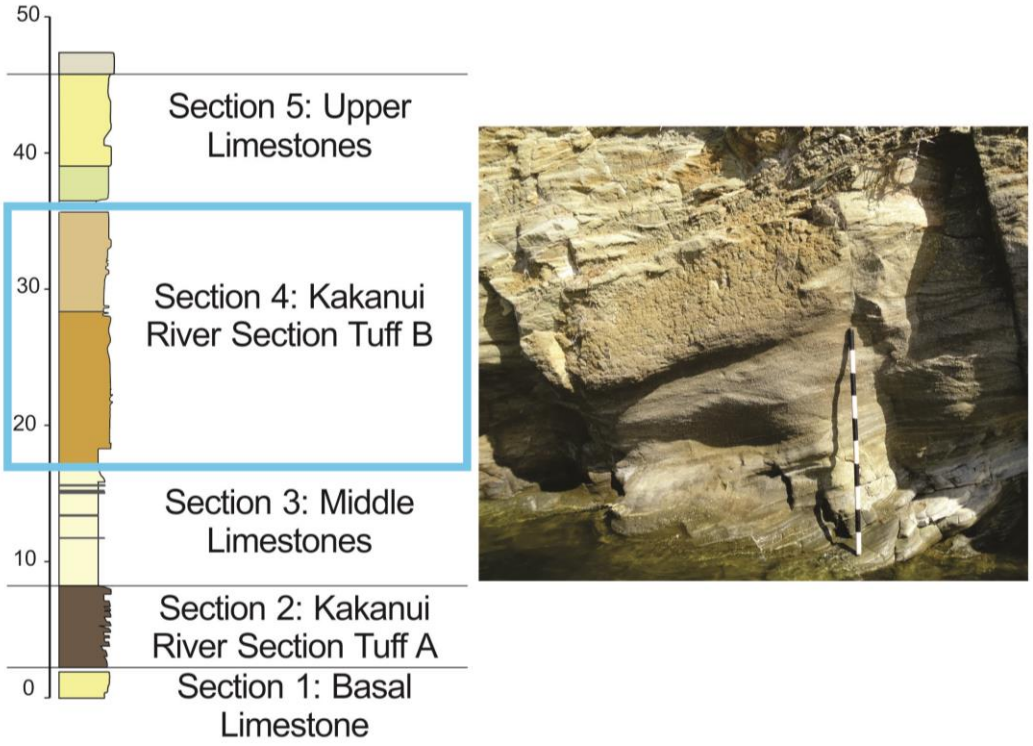

Figure 3.10: Appearance and stratigraphic position of Section 4.

The Kakanui River Section Tuff B deposit (Figure 3.10) contains ~20 m of tuffs and lapilli tuffs, which begins with ~12 m of cross-bedded and laminated volcaniclastics (F5), overlain by 7.5 m of even-bedded volcaniclastics (F6) (Figure 3.10). These facies are structurally distinct, but contain very similar material. This section has an overall dip of around 20° ESE, although a gentle fold alters this in the middle of the outcrop. This outcrop was used by Gage (1957) as the type section for the Deborah Volcanics, as both the top and the base are exposed. It is one of the deposits examined for geochemical fingerprinting in Section 3.4, where it is called "Kakanui River Section Tuff B".

This facies is dominated by juvenile volcanic clasts, typically 1 – 2 mm, occasionally >1 cm (50 – 70 %), with rare accretionary lapilli (~1 mm, 1 – 2 %), and palagonatised ash (10 - 20 %). Minerals include cleavage fragments of kaersutite, which are rare and small at the base of the section (1 – 2 mm, <1 %), but become larger and more abundant around 3 m up (3 – 5 mm, 2 – 5 %). Other minerals include ~1 mm fragments of chrome diopside (1 %), olivine (1 %), feldspar (<1 %), and biotite (<1 %). Calcite cement concentration can vary between different beds, with cement-poor layers and well cemented layers (1 – 10%) (3.11).

The cross-bedded and laminated volcaniclastics facies contains cm to m-scale beds which are dominantly cross-bedded, but also include bedded layers, and occasional low angle antidunes.
The cross-beds dip towards the west, in the opposite direction from the outcrop dip, while antidunes show both eastward and westward migration. The cross-beds showed wavelengths of 10 – 80 cm, amplitudes of up to 30 cm, and an average dip of 25 – 40° relative to their bedding plane. Tabular sets of horizontally extensive cross-beds are most common, although tapering layers and sigmoidal lenses also occur (Figure 3.12).

At the base of the cross-bedded and laminated volcaniclastic unit, tuff beds are most common, but lapilli tuffs come to dominate around 2 m up. Grainsize varies between beds, but the clasts are moderately- to well-sorted within these beds. These clasts are dominantly sub-angular, up to sub-rounded, and some are still mostly coated by their original chilled margins, indicating only minor modification since eruption.

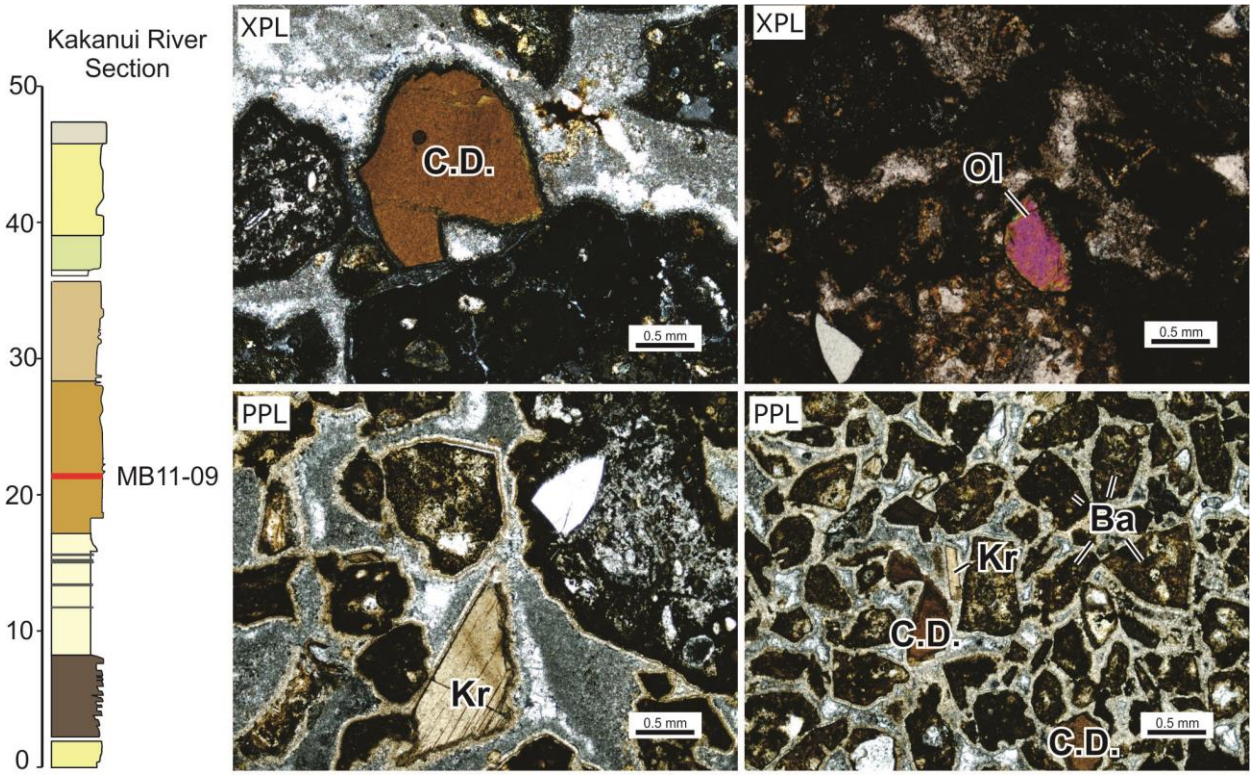

Figure 3.11: Thin section from cement-rich sample of Kakanui River Section Tuff B. **A**: A grain of the orthopyroxene mineral chrome diopside. **B**: A grain of olivine. **C**: A fragment of kaersutite, showing one good cleavage direction. **D**: Components of the crossbedded and stratified volcaniclastic facies; kaersutite, chrome diopside, clasts of juvenile basalt. Clasts are surrounded by grain-bounding and interstitial cement.
Kr = Kaersutite, C.D. = Chrome diopside, Ol = olivine, Ba = Juvenile basalt clasts

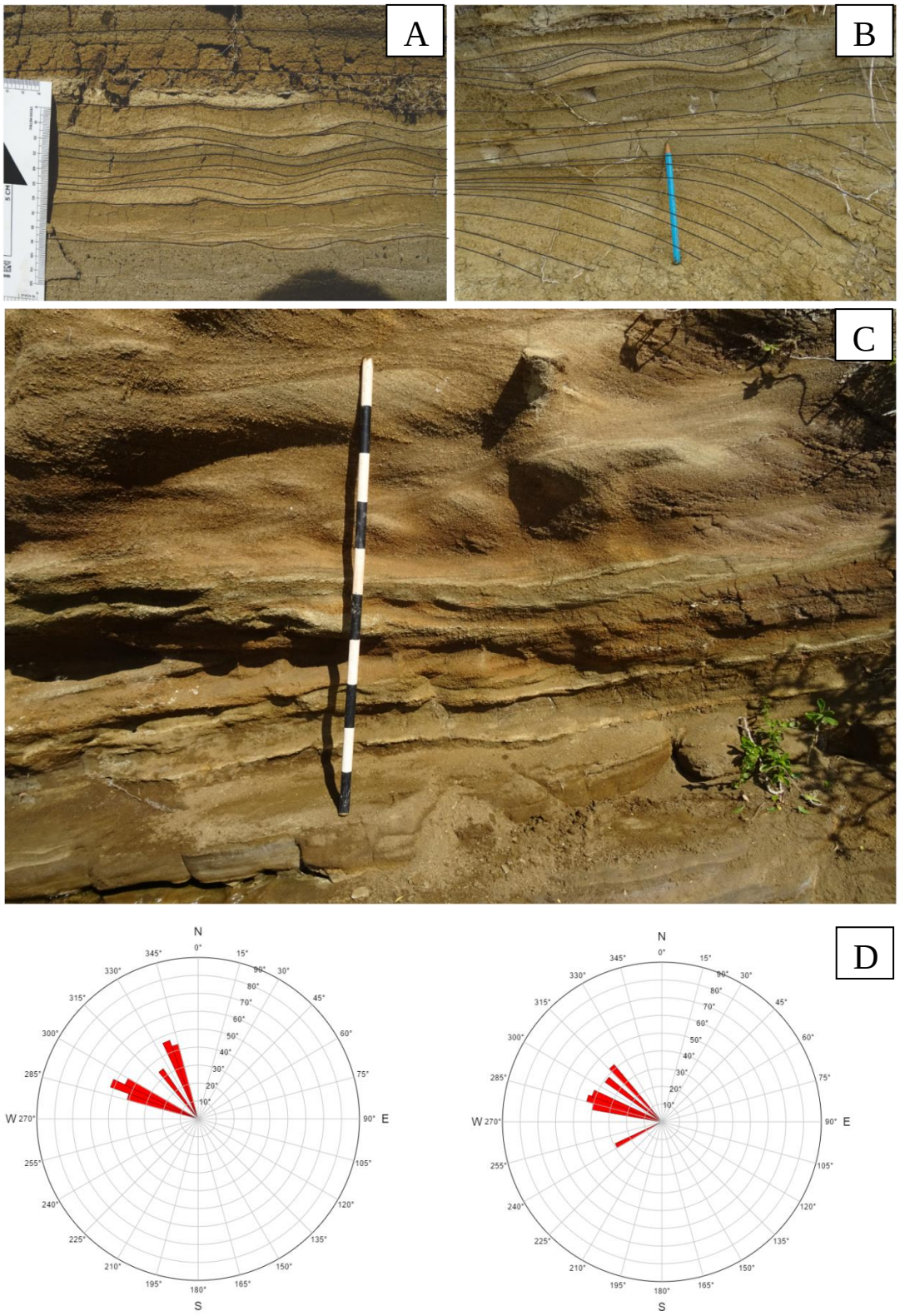

Figure 3.12: Cross-beds from the cross-bedded and laminated volcaniclastics. **A** and **B:** Low angle antidune cross-stratification migrating both east and west. **C:** High- and some low-angle cross-stratification, showing westward migration. **D:** Palaeocurrent indicators from near the base (left) and the top (right) of the cross-bedded layers.

A sharp erosive contact occurs at the base of this section, and the bottom-most beds contain rip-up clasts of wackestone. The bottom beds are strongly deformed; exhibiting convolute bedding, faulting, soft-sediment folding, and flame structures (Figure 3.13). The deformation becomes less pronounced further above the base, and it is not evident in the even-bedded volcaniclastic facies (F6) which occurs at the top of this section.

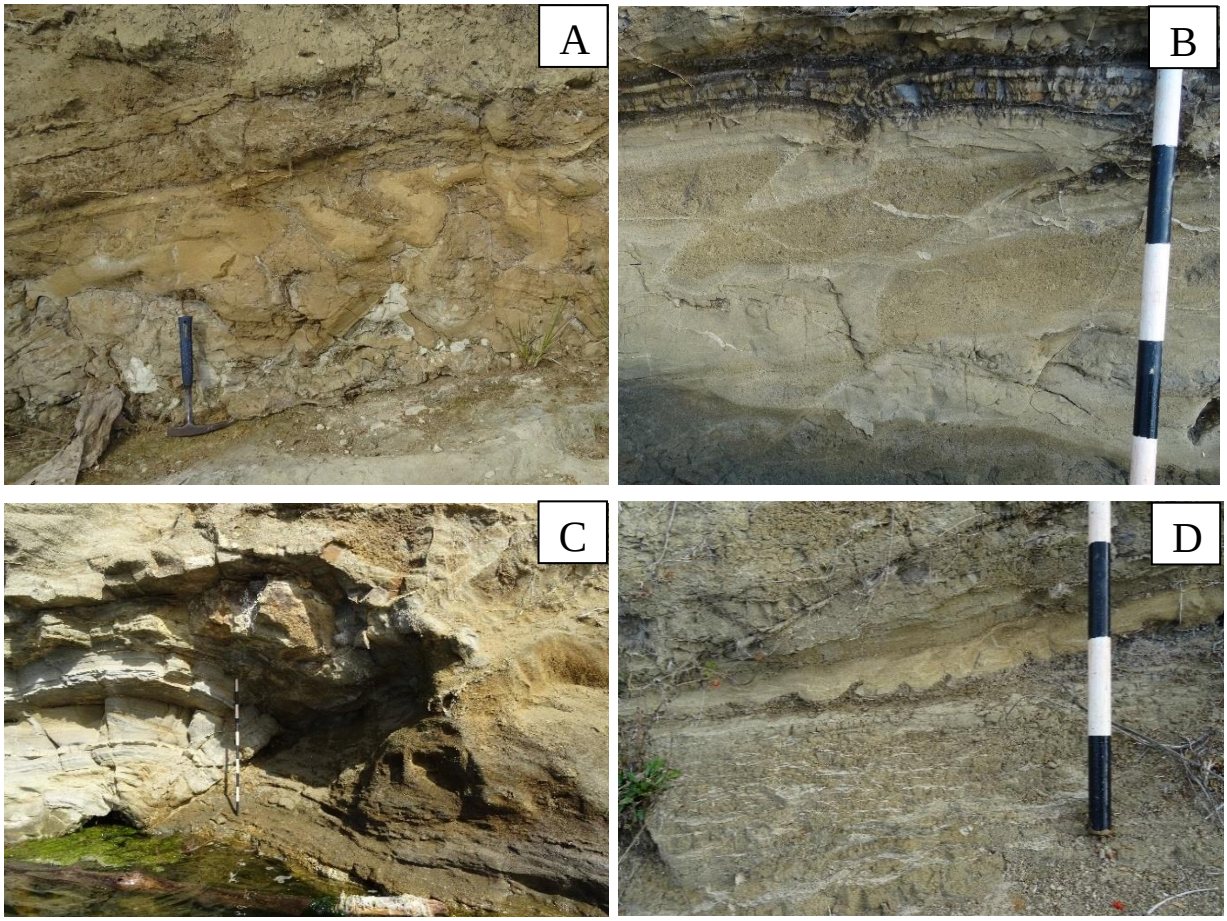

Figure 3.13: Deformation structures in the cross-bedded and laminated volcaniclastics. **A**: Sharp boundary at the base of the section, overlain by units showing convolute bedding, and containing rip-up clasts of wackestone. **B**: Soft sediment faulting and folding, roughly 2 m above the base of the section. **C**: a thrust fault with associated folding of the hanging wall beds. **D**: flame structures, with tips bending towards the west.

Around two thirds of the way up this section, the cross-bedded and laminated volcaniclastics sharply transition to even-bedded volcaniclastics (F6). The contact between the two is erosive, and cuts across the crests of deformed beds and truncates faults in the underlying unit (Figure 3.14). The even-bedded volcaniclastic unit has laminar bedding and a slightly finer average grainsize, but is compositionally similar to the underlying unit, except for a higher calcite content.

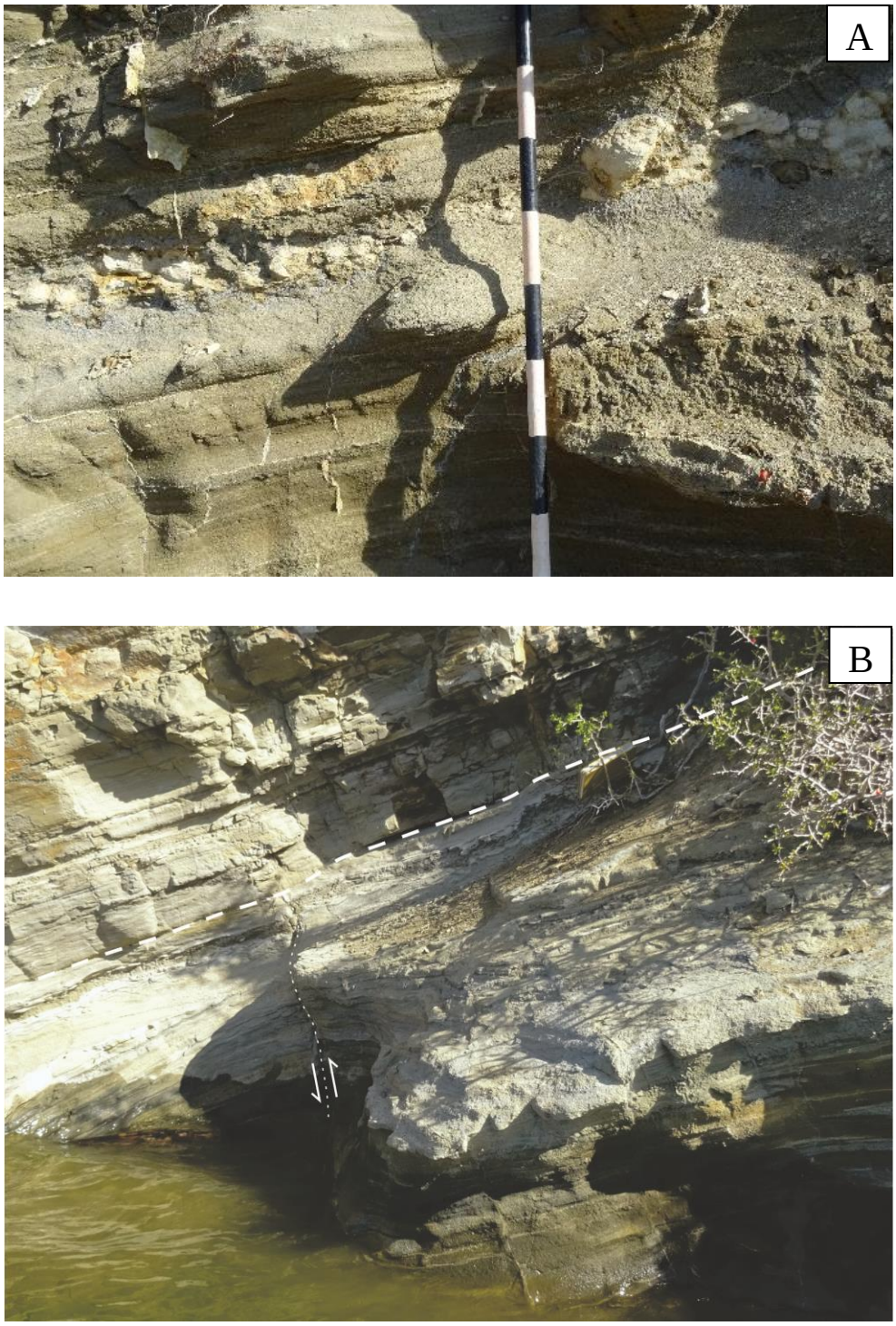

Figure 3.14: Units of even-bedded volcaniclastics. **A:** Contact between underlying deformed units of cross-bedded and laminated volcaniclastics, and overlying competent units of even-bedded volcaniclastics. Slump-related faulting does not extend past the contact, which is a minor unconformity. **B:** Laminated kaersutite-rich lapilli tuff beds, with one bed containing large wackestone clasts. Fractures infilled with calcite run roughly parallel to, and perpendicular to bedding.

Interpretation

The cross-bedded and laminated volcaniclastic unit was deposited by high-concentration grain flows, which may have been triggered by column collapse or failure of an oversteepened volcanic pile. The cross-beds formed from stoss-erosional, lee-depositional, net-positive deposition, with reasonably high sediment supply and flow rates. After this unit was deposited, it was mobilised again in a slump, as evidenced by the erosive lower contact, convolute bedding, faulting, folding, and soft sediment deformation which decreases upwards, moving away from the glide plane (Bull et al., 2009). Slumps are common around Surtseyan seamounts (Maicher, 2000), and it is likely that the Kakanui River Section deposits detached from the slope of their source edifice.

The even-bedded volcaniclastic unit does not show deformation structures, and although it is almost conformable with the underlying cross-bedded and laminated volcaniclastic unit, the contact cuts across the crests of hummocks, and decapitates slump-related faults. Therefore, this overlying unit must have been deposited post-slumping.

The even-bedded volcaniclastic unit formed from turbidity currents depositing in the upper plane bed regime. It shows a slightly finer grainsize than the underlying unit, and contains stratified beds, rather than cross-beds. This may be because the underlying unit was originally a more proximal deposit, before being remobilised in a slump, or because eruption energy waned over time.

Section 5: Upper limestones - Grey wakestone (F3), glauconitic packstone/wackestone (F7), bryozoan-rich packstone/grainstone (F1)

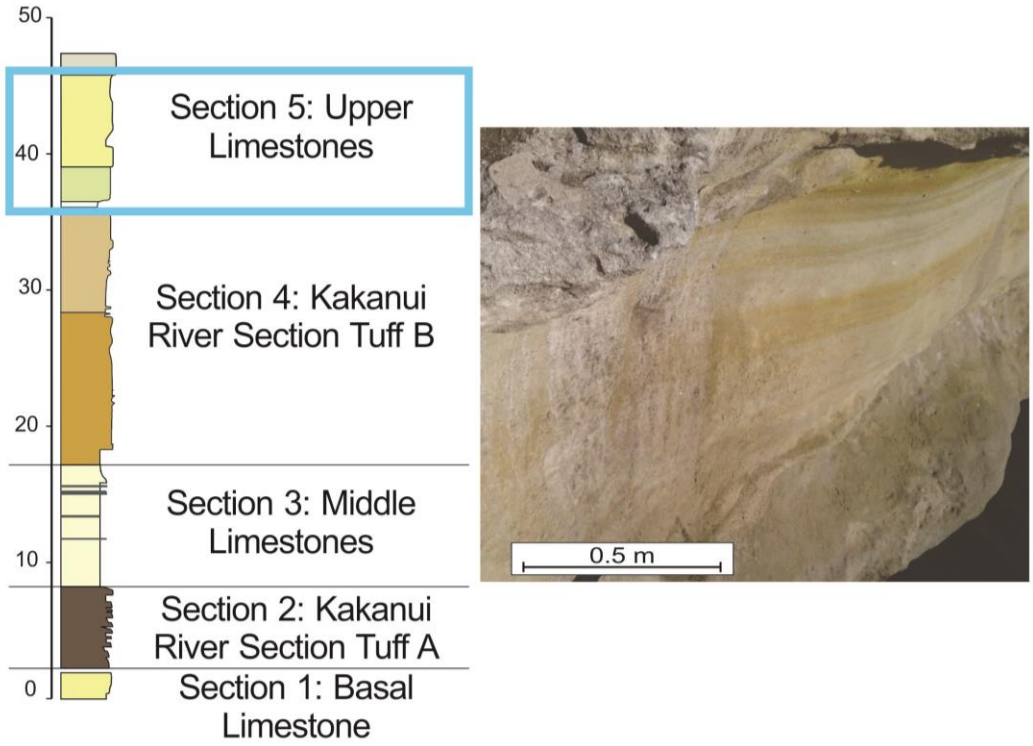

Figure 3.15: Appearance and stratigraphic position of Section 5.

The volcaniclastic section is overlain by a series of carbonate facies (Figure 3.15). The first of these is a thin unit of grey wackestone (F3), which is the same as the grey wackestone occurring below the volcaniclastics, but with the addition of kaersutite fragments. This unit is around 60 cm thick, and terminates in a sharp boundary which has been bioturbated with *Thalassinoides* burrows.

A 2.4 m thick unit of glauconitic packstone/wackestone (F7) unconformably overlies the grey wackestone. It is rich in detrital glauconite; concentrations are as high as 40 % near the base, but grade to 15 % over the first metre. This glauconite appears fairly bright green and immature. This unit is heavily bioturbated with *Ophiomorpha* burrows, destroying any bedding which might have existed. These burrows are mucus-lined, and indicate unconsolidated sediment, where lining is required to prevent burrows from collapsing. Body fossils become more common further up, and include brachiopods, echinoderms, worm fossils and pecten. Kaersutite occurs above the basal unconformity but grades out around 1 m above it.

The glauconitic packstone/wackestone grades to beds of bryozoan rich packstone/grainstone (F1). This facies is present as thick bioturbated beds, which are mostly packstone, with some

thinner bryozoan grainstone units. Bioturbation has mostly obscuring sedimentary structures, but fossil alignment indicates bed orientations, and yellow staining from groundwater flow shows the distribution of more and less permeable layers. Faint low-angle cross-beds can be seen in places, dipping towards the west. Large body fossils are present throughout this unit, including lentipectens, brachiopods, worm tube clusters and echinoderms. Smaller bioclasts include planktic and benthic foraminifera, and bryozoan, echinoderm, and molluscan fragments (Figure 3.16).

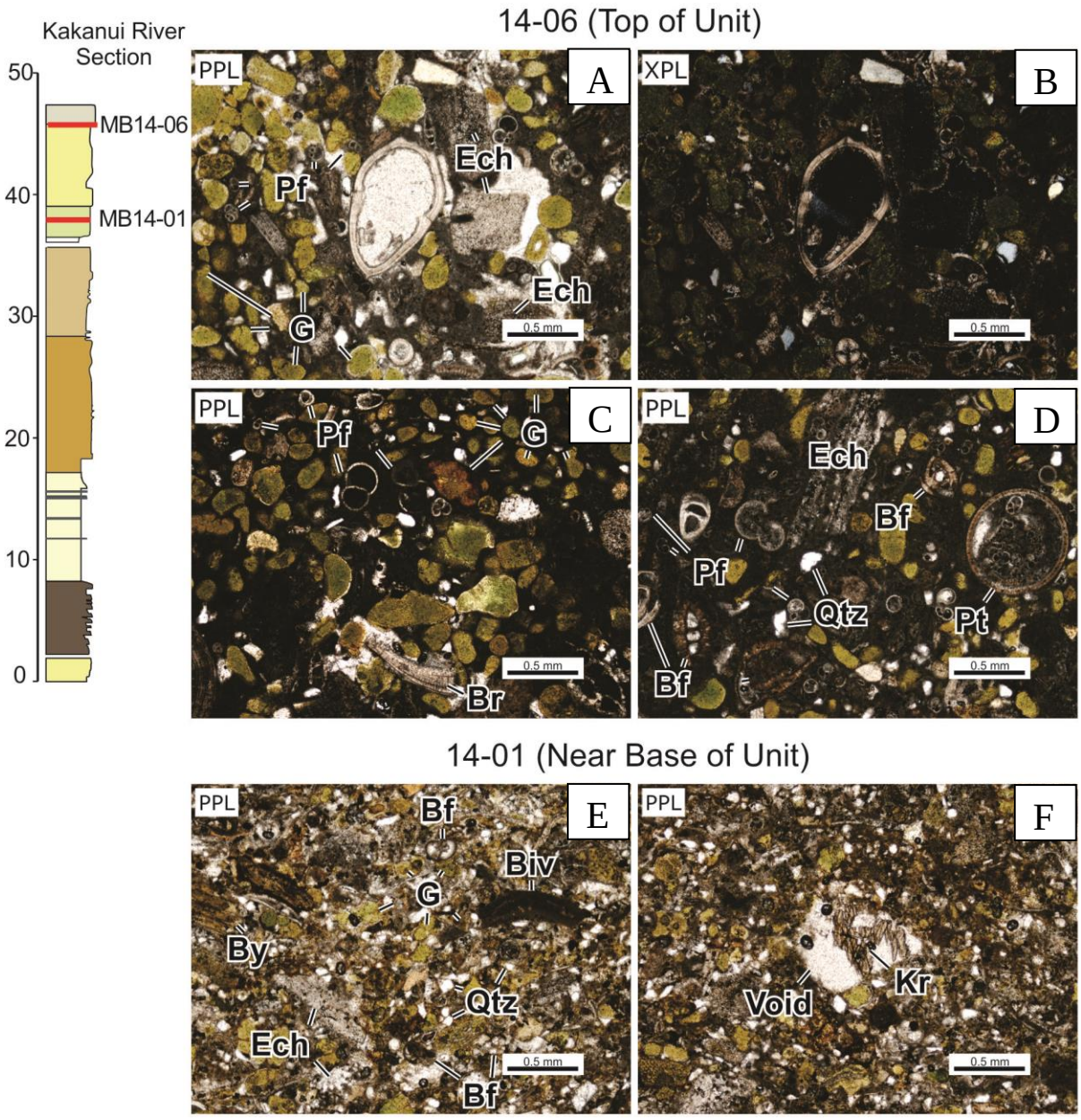

Figure 3.16: Thin sections from the limestone beds at the top of the river section.
A and **B**: Glauconite-rich horizon from the bryozoan-rich packstone/grainstone facies. Glauconite is rounded and detrital. Bioclasts contain void space, and are not glauconitised.
C and **D**: Bioclasts from the bryozoan-rich packstone/grainstone facies, including planktic and benthic foraminifera, echinoderms, brachiopods and pteropods.
E and **F**: Sample from the glauconitic packstone/wackestone facies. This sample has silt to very fine sand-sized grains glauconite (15 – 20 %), much of which is bright green and immature and quartz (10 %) with slightly larger bioclasts of benthic foraminifera (10 %), echinoderms (2 %) and bivalves (<1 %). Kaersutite occurs rarely (<1 %).
Planktic = planktic foraminifera; Brach. = brachiopod; Echi. = echinoderm; Benthic = benthic foraminifera; Ptero. = pteropod; Glau. = glauconite; Qtz = quartz; Amph. = amphibole.

Interpretation

The presence of the grey wackestone facies both above and below the volcaniclastic section indicates that the eruption merely provided an influx of material to an otherwise consistent depositional environment. The sharp contact overlying this top grey wackestone unit, however, indicates a significant change. It is associated with *Thalassinoides* burrows, which are unlined, and form in partially lithified substrate. This contact is an unconformity which represents a significant period of non-deposition.

The glauconitic packstone/wackestone facies contains relatively immature glauconite, scattered large body fossils, and reasonably abundant silt-sized terrestrial quartz. The glauconite probably formed nearby during the time gap represented by the unconformity. The body fossils are probably not majorly reworked, and are reasonably representative of the depositional environment. The fine sand grainsizes indicate that this was a fairly low-energy, likely mid-shelf environment.

The bryozoan-rich packstone/grainstone facies seems to have been sourced from a shallow, current-swept environment. Evidence for this includes the coarse sand grainsize with large shell fragments, the presence of shallow water and photic zone organisms, and the rounding of glauconite and other detrital grains. The well sorted, rounded nature of the facies indicates that it has been transported. The outsized shell fossils represent storm deposits. Palaeoflow was likely towards the WNW, based on the dip of the cross-beds.

Outcrop observations

Figure 3.17 shows the Kakanui River Section outcrop, photographed from the opposite side of the river. From this distance, large-scale features such as structure, bedding, and the overall character of the different units become obvious.

The bryozoan-rich packstone/grainstone of Section 1 is not shown on this photo. This unit, along with the calcareous volcaniclastic sandstone (Section 2) and the grey wackestone (Section 3), do not have many observable features at this scale. These deposits are the most easily weathered, resulting in smoother features and more vegetation cover. By contrast, the uppermost units form steep, relatively tall cliffs, which exhibit a number of large-scale features

The cross-bedded and laminated volcaniclastics exhibit minor shortening, as a result of the slumping. This is seen in the gentle folding of the bedding, and the reverse fault which cuts across the outcrop. This section was probably located near the toe of the slump, and experienced compression as slumping slowed and stopped. The trend of the fold and strike of the fault are roughly orthogonal to the face of the outcrop, and quite possibly represent the strike of the original slope (Lewis, 1971). The even-bedded volcaniclastics have a much more consistent dip than the underlying slumped unit. Limestone is seen sitting above the top of this unit, but this is probably more recent rock fall from further uphill.

The top carbonate unit (yellow outline) does not contact the underlying volcaniclastics, but the contact can be inferred. This section contains thick, laterally continuous beds with a consistent dip. Some bed boundaries are visible, mostly due to differences in cementation and grainsize, which have caused differential weathering. Vegetation tends to run along these bed boundaries.

Figure 3.17: Rock exposed along the Kakanui River Section. The brown outline (bottom image, right side) highlights the top of Section 2: Kakanui River Section Tuff A. This unit transitions to Section 3: Middle Limestones, outlined in pale yellow. A sharp contact separates this from Section 4: Kakanui River Section Tuff B, outlined in orange. This begins with slumped cross-bedded and laminated volcaniclastics, overlain by even-bedded volcaniclastics. Section 5: Upper Limestones begins with a thin grey wackestone unit (too small to distinguish), sharply overlain by glauconitic packstone/wackestone, transitioning to bryozoan-rich packstone/grainstone.

3.1.2 Kakanui Western Slope

Other than the excellent exposures along the coast and along the riverbanks, Kakanui South Head is largely covered by quaternary sediment. However, on the inland slope, uphill from the highway, small, isolated outcrops of rock can be found. These exposures are reasonably weathered, but their lithology can still be determined. The outcrop positions, elevations, and measured dip of 12° to the east, have been used to construct a stratigraphic column (Figure 3.18).

The basal unit of the Kakanui Western Slope is a unit of calcareous volcaniclastic sandstone. Bedding is present, but difficult to detect, due to the crumbly nature of the outcrop. Grainsize varies across the outcrop, ranging from fine to coarse sand, with occasional outsized shells, depending on the layer. However, sorting within these layers is good. The main components are bryozoans, broken pecten and brachiopod shells, and unidentified calcareous material, as well as volcanic clasts, which range from fine to coarse sand-sized, with granules present in some of the coarser layers. This unit appears similar to Kakanui River Section Tuff A, and extending the strike of the beds comes close to intersecting this outcrop. This indicates that the two exposures are part of the same deposit.

Slightly uphill from the calcareous lapilli tuff beds, the contact between two new units is exposed. The underlying unit is a soft white calcareous rock, which appears fibrous under a hand lens. No bedding is evident, although there are traces of bioturbation, which may have destroyed it. The grainsize is clay to silt; finer than most other rocks around Kakanui. No foraminifera could be located in this unit, but it appears to be rich in sponge spicules and very fine-grained components. It resembles rocks of the Oamaru Diatomite, a lateral equivalent of the Ototara Limestone which formed in deeper environments. It is associated with early volcanic eruptions, where the influx of silica led to an increase in diatom numbers.

Beds of tuff, with lenses of lapilli tuff directly overlie the diatomite, and are separated from it by a sharp boundary. The lapilli tuff lenses are slightly wavy and may have been deformed, although the small size, and weathering of the outcrop make larger-scale structures difficult to determine. This unit is well-sorted, with finer and coarser sections. Crystals of small, weathered kaersutite are present, as well as olivine and chrome diopside. This unit seems lithologically similar to the base of the cross-bedded and laminated volcaniclastics unit which outcrops in the

Kakanui River Section. However, if it is part of the same slump, it shows less severe deformation than the base of that outcrop.

An exposure of bryozoan-rich packstone/grainstone outcrops around the hillslope and slightly further north from the other Kakanui Western Slope deposits. The dip of the underlying beds indicates that the absolute thickness of the covered area is at least 16 m. This outcrop is a cemented packstone, grading to grainstone near the top. It contains bryozoans, echinoderms, large benthic foraminifera and shelly fragments, with rare detrital glauconite. This unit is inferred to be a lateral continuation of the limestones which overlie Section 5 of the Kakanui River Section.

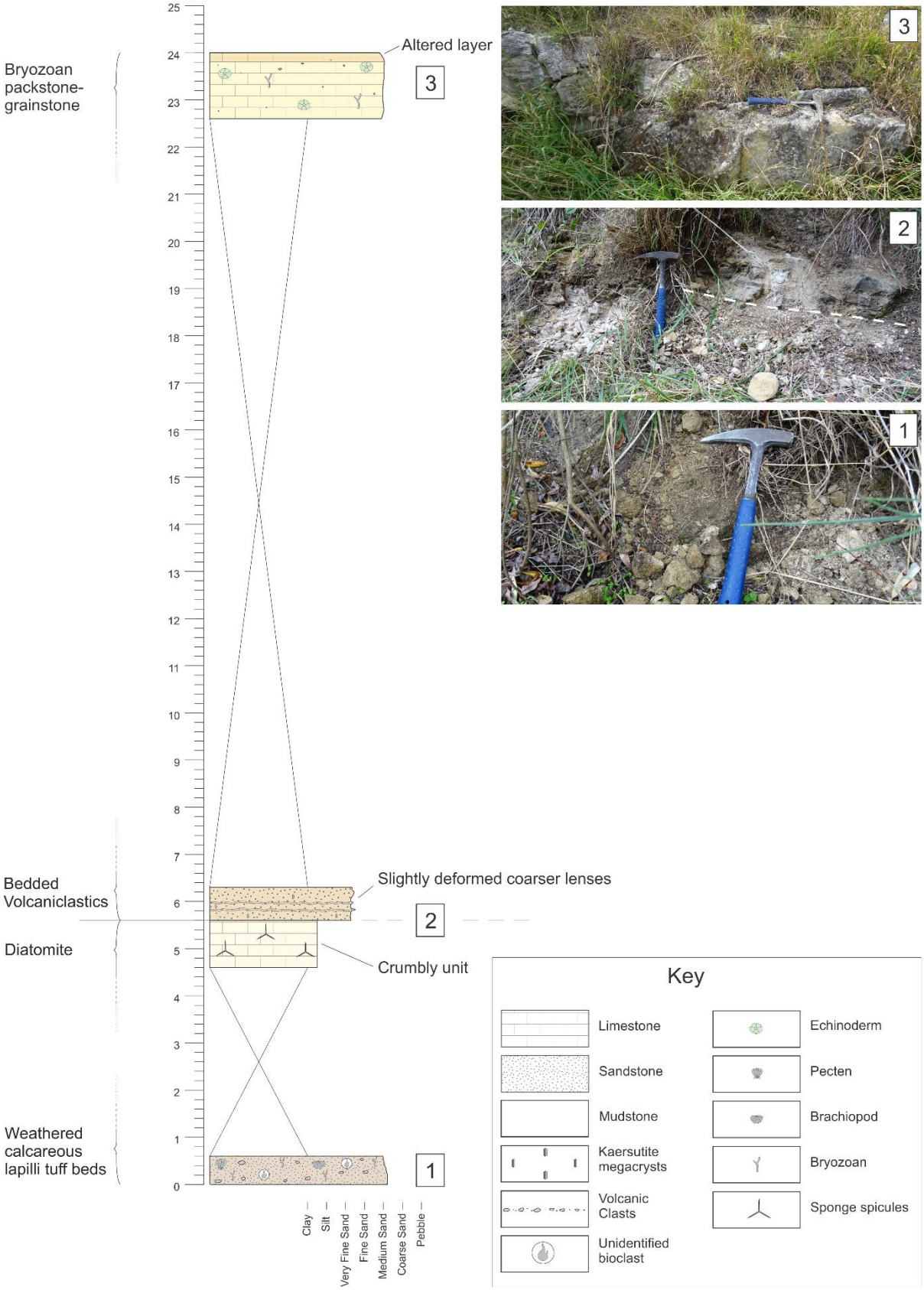

Figure 3.18: Stratigraphic column of Kakanui Western Slope; the inland slope of Kakanui South Head. This area was largely concealed, and the stratigraphy has been pieced together from isolated outcrops. The geological succession roughly matches that of the Kakanui River section to the north.

3.1.3 Kakanui South Head

The top of the Kakanui river section terminates around 200 m upriver from the next section: Kakanui South Head. This seamount has been well exposed by coastal erosion, and strike and dip measurements reveal an obvious cone structure (Figure 3.20). The cliffs and beach form a large continuous outcrop, extending from the mouth of the Kakanui River in the north, to Campbells Bay in the south. At both of these points, the volcanic deposits are overlain by limestones, and they have been used to construct stratigraphic columns (Figure 3.21).

An angular unconformity separates the exterior and interior beds of the cone (Figure 3.19). These interior beds dip steeply in an inland direction and contain large volcanic clasts, xenoliths and crystals. This unit is the much-studied Kakanui Mineral Breccia, and probably represents the final stage of the Kakanui South Head eruptions.

Figure 3.19: Unconformable contact between westward-dipping Kakanui Mineral Breccia deposits (left) and submarine tuff deposits (right) at Kakanui South Head. These deposits represent the interior and exterior beds of a Surtseyan cone. Measuring stick is 1 m.

Figure 3.20: Strike and dip data recorded around Kakanui South Head, revealing the exterior and interior cone structure.

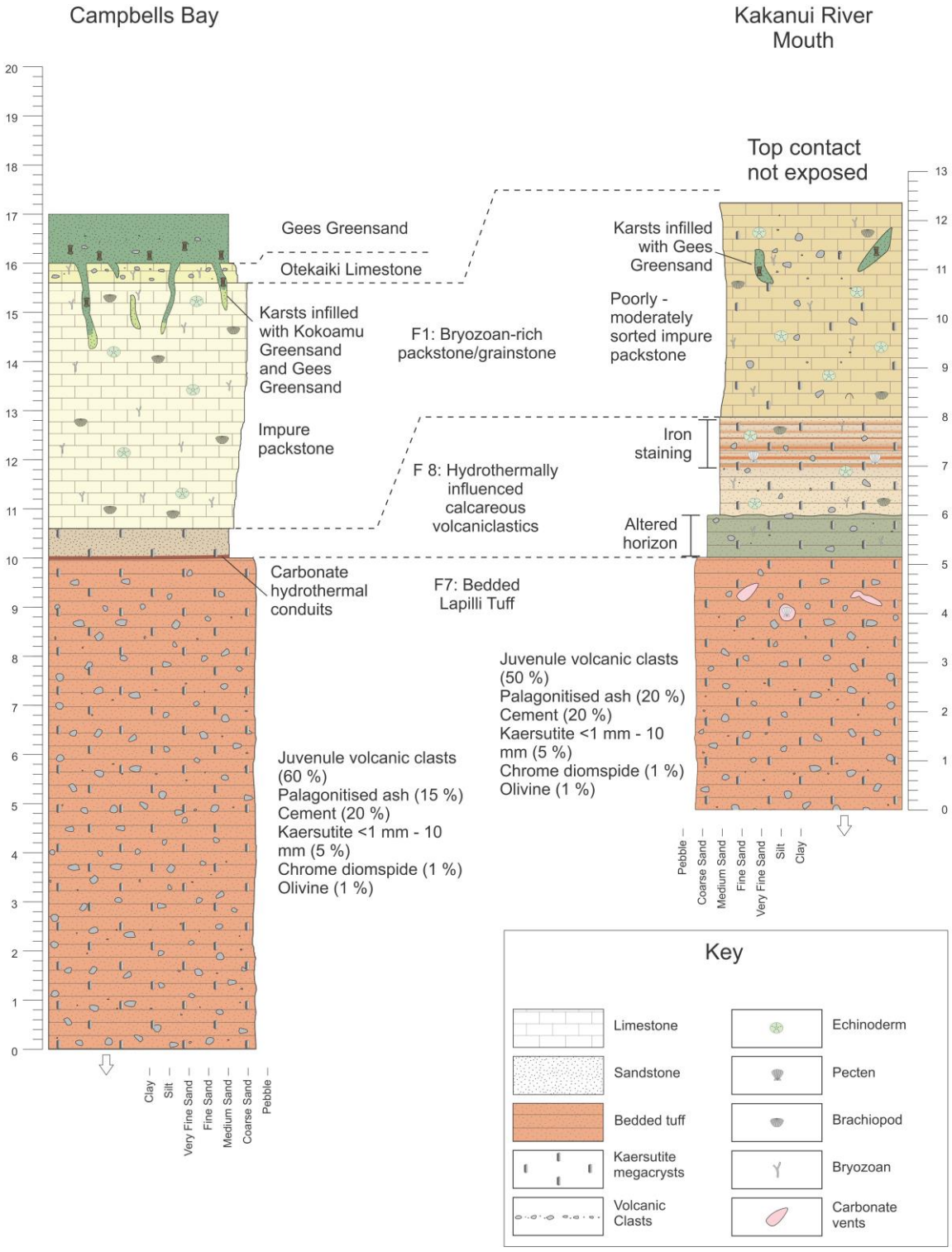

Figure 3.21: Stratigraphy from Campbells Bay, at the south end of Kakanui South Head and Kakanui River Mouth, at the north end. These outcrops show the top of the South Head cone, and the limestones which overlie it.

The top of the headland volcanics and a number of overlying units are exposed at Campbell's Bay. This bay is located at the southern end of Kakanui South Head, where the steep headland cliffs meet the sandy coastline. Here the bedded lapilli tuffs (F7) are overlain by a 60 cm thick unit of hydrothermally-influenced calcareous volcaniclastics (F8). Brown hydrothermal conduits formed by precipitated carbonate occur along the contact between the two units. The calcareous volaniclastics are a lighter greyish green, and contain fossils, including echinoderms.

A 5 m thick layer of bryozoan-rich packstone/grainstone overlies the calcareous volcaniclastics. This limestone is coarse sand-sized, and contains bryozoans, echinoderms, and shell fragments of pecten and brachiopods. A karsted surface, the Marshall Paraconformity, overlies the Ototara Limestone, indicating that it was subaerially exposed. Dissolution cavities in the top 2 m of the limestone have been infilled with lithified sediment from younger units.

Several calcareous units occur above the Ototara Limestone at Campbells Bay, but not always as simple beds. After the Marshall Paraconformity, the next stratigraphic unit is the Kokoamu Greensand. This is present within dissolution cavities of the karst surface, but the original beds have been eroded away. Instead, here the Ototara limestone is overlain by a layer of Otekaiki Limestone, which is itself bounded at the top by another karst surface. This is followed by outcrops of Gees Greensand, which line the coast towards the south. The dissolution cavities of the younger karst surface also reach into the Ototara Limestone, resulting in infill of both Kokoamu Greensand and Gee Greensand within this unit (Figure 3.22).

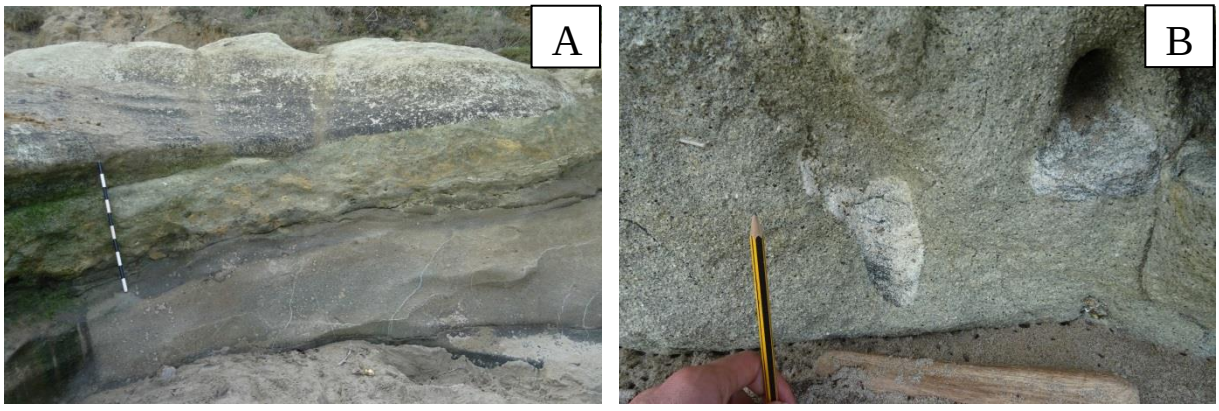

Figure 3.22: Outcrop at Campbells Bay. **A**: Headland volcanics, overlain by a green-coloured unit of calcareous volcaniclastics, and then a unit of Ototara Limestone. **B**: Infilled dissolution cavity in Ototara Limestone. Measuring stick is 1 m.

At the northern end of Kakanui South Head, at the Kakanui River Mouth, the top of the bedded lapilli tuff units is exposed. This outcrop is similar to Campbells Bay; with the same succession of volcanic beds, overlain by hydrothermally influenced calcareous volcaniclastics, and then bryozoan-rich packstone/grainstone. Here around 3 m of calcareous volcaniclastics are exposed, as opposed to the 60 cm thickness at Campbells Bay. This unit is followed by around 4.5 m of bryozoan-rich packstone/grainstone, with abundant bryozoans, volcanic clasts, echinoderm plates and spines, and rare brachiopods.

Although the top boundary of the Ototara is not preserved at this location, there is evidence that it was not far above the existing outcrop. Near the top, small infilled dissolution cavities begin to appear. The infill is glauconite-rich, and contains melitodes fossils, indicating that it is Gee Greensand.

The interpretation of this outcrop is very similar to Campbells Bay. The calcareous volcaniclastics show reworking of the edifice following colonisation, followed by deposition of much more bioclast-rich material. The karsting in the bryozoan-rich packstone/grainstone formed from the same subaerial exposure as the Campbells Bay section, and was followed by re-submergence, and the deposition of the Kekenodon Group.

3.1.4 Kakanui North Head

While Kakanui South Head has an obvious cone structure, the volcanic deposits at Kakanui North Head are more narrow and elongate. These deposits line the coast, with reasonably steep dips, which strike roughly parallel to the coastline (Figure 3.23).

Figure 3.23: Kakanui North Head, showing an elongate structure and outward dipping beds. Some measurements taken from Dickey (1966)

The distribution of the reworked volcanic beds at Kakanui North Head suggests that they may have been sourced by a fissure eruption. This fissure could have been linked to the Kakanui South Head cone, explaining the occurrence of Kakanui Mineral Breccia at both sites.

3.1.5 Upriver Lapilli Tuffs

Around 600-700 m upriver from the base of the Kakanui River section, steep bluffs of volcaniclastics line the river's eastern bank. These volcaniclastics are planar-bedded and cross-bedded, typically with cm-scale bedding, but occasional m-scale blocky layers. The beds dip at around 15° - 25° towards the east, suggesting that they underlie the Kakanui River Section. The strike runs roughly parallel to the line of the river, dipping slightly south-east in the southern-most exposures, and north-east in the northern sections.

These upriver volcaniclastics are dominantly lapilli-tuffs, with occasional ash layers, and numerous cm-scale bombs, with rare examples up to 2 m long (Figure 3.24). Some of these bombs exhibit minor breadcrust textures. Minor bomb sags occur beneath the largest bombs, confirming that they fell as ballistics during deposition of the volcaniclastics. The depositional environment was subaqueous, which lessened the impact of ballistic material, and reduced the deformation. Bombs tend to be concentrated along particular horizons, which probably reflect periods of increased eruption intensity. The large size of some bombs makes it likely that the source vent was fairly close. The closest known cones, at Kakanui North and South Head, are each roughly 1 km away; probably too far to be the source.

Cross-beds are present in some layers of the Upriver Lapilli Tuffs. These are mostly low-angle, within gently tapering sigmoidal lenses. However they also include steeper cross-beds which dip to the southeast, seen on rare east-west striking surfaces (Figure 3.25). This indicates that deposition was from the west.

Figure 3.24: Large bomb within the lapilli tuff beds of the northern Kakanui River outcrops. Image shows clear, although relatively minor deformation of underlying bedding layers, and the formation of a hummock in overlying bedding.

Figure 3.25: Cross-beds in the Upriver Lapilli Tuffs. Bedding dips 18° to the NW, while cross-beds dip 32° to the SE

A dike cuts through the Northern River Section tuffs, just north of the bridge. This dike is irregular, and thickens upwards. Because of this, the orientation is difficult to determine, but likely between 120° and 160°, trending NW-SE. This may indicate that the source vent was to the northwest or southeast

Figure 3.26: Amorphous dike, cross-cutting the Upriver Lapilli Tuff

3.2 Foraminifera Investigation

Foraminifera were abundant throughout the calcareous units of the Kakanui River Section. Certain genera, such as *Cibicides*, *Globocassidulina*, Cassidulina and *Globogerina* were dominant, but overall diversity was high. Most of the tests were fairly well-preserved, although several specimens were fragmented, or had lost too much ornamentation to be reliably identified.

Although care was taken to get a representative sample of foraminifera, it is likely that this does not completely match the original assemblage. Glauconite moulds of foraminiferal tests were found, indicating that some foraminifera which were originally present had been dissolved. The general paucity of miloilid foraminifera in the Kakanui River Section samples is likely a result of dissolution, which their high Mg/Ca ratio, combined with relatively warm oceanic temperatures, makes them particularly prone to (Budd, 1992).

Foraminiferal environmental preference was determined using the Modern Analogue Techinique of Hayward et al., 2010. This was combined with the planktic foraminiferal percentage with depth diagram, in order to characterise depositional environments (Figure 3.27).

The foraminiferal samples show a somewhat anomalous abundance of *Globocassidulina subglobosa*, since modern analogues are restricted to depths of >190 m (Hayward et al., 2010). Several authors have noted this species within shallow-water limestones in this area. Hicks (2014) speculates that either there has been some change in environmental preference from the Eocene *Globocassidulina* to the modern analogue, or upwelling brought up juvenile forms from depth, which were still able to survive in the shallow conditions. It is worth noting that benthic foraminiferal distribution is mainly controlled by oxygen and organic flux, rather than directly by depth (Zwaan et al., 1999). The appearance of *Globocassidulina subglobosa* might be unlikely in most inner shelf environments, but while this area was fairly shallow due to the palaeohigh, it was still far offshore, adjacent to deep ocean environments and exposed to strong currents which could have remobilised species.

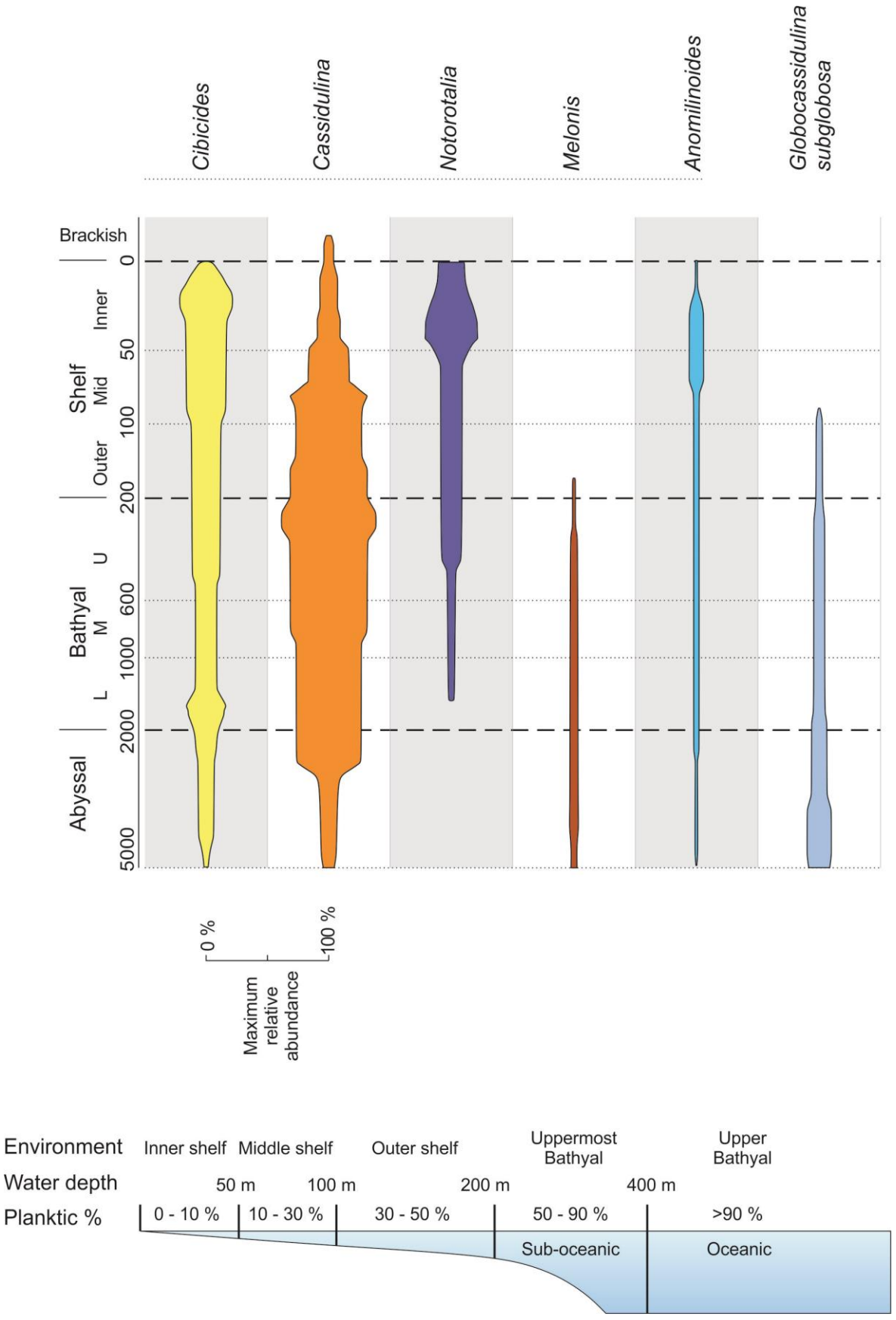

Figure 3.27: Diagrams of foraminiferal abundance, modified from Hayward et al., 2010. **Top**: Maximum relative abundance of foraminifera at certain depths, based on modern analogues. **Bottom**: Planktic foraminiferal percentages at different water depths.

Section 1: Basal limestone - Bryozoan-rich packstone/ grainstone

Table 1: Most abundant foraminiferal genera – MB8-02.

Sample	Foraminifera
MB8-02 0.22 m Bryozoan-rich packstone/ grainstone	*Cibicides* – 58 % *Globocassidulina* – 11 % *Globigerina* – 11 % *Melonis* – 2 % *Anomalinoides* – 8 % *Notorotalia* – 2 % Rare taxa (benthic foraminifera) – 5 % Rare taxa (planktic foraminifera) – 3 %

Cibicides dominate this section, including *Cibicides parki*, which is a characteristic species of the Arnold Series. *Cibicides* have a wide palaeodepth distribution, but their greatest relative abundance is in inner and mid shelf environments (Hayward et al., 2010.) (Figure 3.27). Species restricted to the photic zone were not identified, making it unlikely that this deposit represents the inner shelf. The deep water *Globocassidulina subglobosa* and *Melonis* are present, but not in high enough concentrations to be diagnostic. Planktic foraminifera make up 14 % of the assemblage, which plots in the middle shelf on the planktic percentage diagram.

This assemblage is interpreted as a mid-shelf source, which has been reworked into an environment of unknown depth.

Section 3: Middle limestones - Grey wackestone

Table 2: Most abundant foraminiferal genera – MB17-02.

Sample	Foraminifera
MB17-02 8.81 m	*Cibicides* – 32 % *Globocassidulina* – 8 % *Globigerina* – 12 % *Melonis* – 1 %

Grey wackestone	*Gyroidinoides* – 2 % *Anomalinoides* – 4 % *Stilostomella* – 1 % Rare/unidentified taxa (benthic foraminifera) – 39 % Rare/unidentified taxa (planktic foraminifera) – 1 %

Table 3: Most abundant foraminiferal genera – MB17-01.

Sample	Foraminifera
MB17-01 15.79 m Grey wackestone	*Cibicides* – 14 % *Globocassidulina* – 25 % *Globigerina* – 21 % *Melonis* – 1 % *Gyroidinoides* – 2 % *Stilostomella* – 4 % Rare/unidentified taxa (benthic foraminifera) – 33 % Rare/unidentified taxa (planktic foraminifera) –

This section has fairly high diversity. *Cibicides* is still abundant, but it decreases in from the base (MB17-02) to the top (MB17-01). The deep-water *Globocassidulina subglobosa* increases in abundance across the section, and planktic foraminiferal percentages increase from 13 % to 21 %. On the planktic percentage diagram, this plots as a deepening middle shelf environment.

This section is interpreted as a mid-shelf deposit, with a deeper source than the bryozoan-rich packstone/grainstone from section 1.

Section 5: Grey wackestone – Upper limestones

Table 4: Most abundant foraminiferal genera – MB16-04.

Sample	Foraminifera

MB16-04 36.42 m Grey wackestone	*Cibicides* – 25 % *Globocassidulina* – 26 % *Globigerina* – 13 % *Melonis* – 1 % *Anomalinoides* – 1 % Rare/unidentified taxa (benthic foraminifera) – 30 % Rare/unidentified taxa (planktic foraminifera) – 4 %

This section contains another unit of grey wackestone which overlies the volcaniclastic deposits of section 4, but is lithologically the same as MB17-02 and MB17-01. It has a similar foraminiferal assemblage as those samples, with intermediate percentages of *Cibicides* and planktic foraminifera, and high percentages of the deep-water *Globocassidulina*. It is interpreted as a continuation of the mid-shelf depositional environment which existed before the eruption, with minor shallowing probably related to volcaniclastic accumulation.

Section 5: Glauconitic packstone/wackestone – Upper limestones

Table 5: Most abundant foraminiferal genera – MB16-05.

Sample	Foraminifera
MB16-05 38 m Glauconitic packstone/ wackestone	*Cibicides* – 14 % *Globocassidulina* – 19 % *Globigerina* – 10 % *Melonis* – 1 % *Gyroidinoides* – 3 % *Stilostomella* – 3 % *Notorotalia* – 7 % Rare/unidentified taxa (benthic foraminifera) – 45 % Rare/unidentified taxa (planktic foraminifera) – %

This glauconitic packstone/wackestone unit contains a diverse assortment of foraminifera, which is less dominated by a few genera than underlying samples. The deep-water *Globocassidulina* is rarer than in the underlying MB16-04, and only 10 % planktic foraminifera are present. This deposit represents an inner – mid-shelf environment, which is notably shallower than the grey wackestone underlying it.

Section 5: Bryozoan-rich packstone/wackestone – Upper limestones

Table 6: Most abundant foraminiferal genera – MB16-06.

Sample	Foraminifera
MB16-06 40.36 m Bryozoan-rich packstone/ grainstone	*Cibicides* – 16 % *Globigerina* – 8 % *Cassidulina* – 47 % *Melonis* – 7 % *Gyroidinoides* – 2 % *Stilostomella* – 2 % *Amphistegina* – 2 % Rare taxa (benthic foraminifera) – 18 % Rare taxa (planktic foraminifera) – %

This section is rich in *Cassidulina* which is abundant at shallower depths than *Globocassidulina* (Figure 3.27). *Cibicides* species include *Cibicides pseudoconvexus*, which is characteristic of shallow water facies, probably with an attaching habitat (Hornibrook et al., 1989). Planktic foraminifera are uncommon (8 %), and plot in the inner shelf on the planktic-percentage diagram. The large benthic foraminifera *Amphistegina* has symbiotic zooxanthellae, which need light to photosynthesise. Therefore, the appearance of *Amphistegina* indicates that the sediment source was within the photic zone, with a maximum depth of up to 80 m, depending on turbidity.

The source for this section was an inner shelf environment with a solid substrate; likely a local volcanic high. Bioclasts were remobilised into the Kakanui River Section area, although this depositional environment had an unknown depth.

Figure 3.28 shows the most abundant foraminifera for each of the sites sampled along the Kakanui River Section, and from the calcareous layers at the river mouth, overlying the headland volcanics. This succession spans two biostratigraphic stages, and probably represents around 1 – 2 million years of deposition (Nelson et al., 2004; Edwards, 1991; Raine et al., 2015; Hoernle et al., 2006). Over this time, there is evidence of sea level fall, relating to the accumulation of Kakanui River Section Tuff B, and to the unconformity overlying the grey wackestone unit in the Upper Limestones.

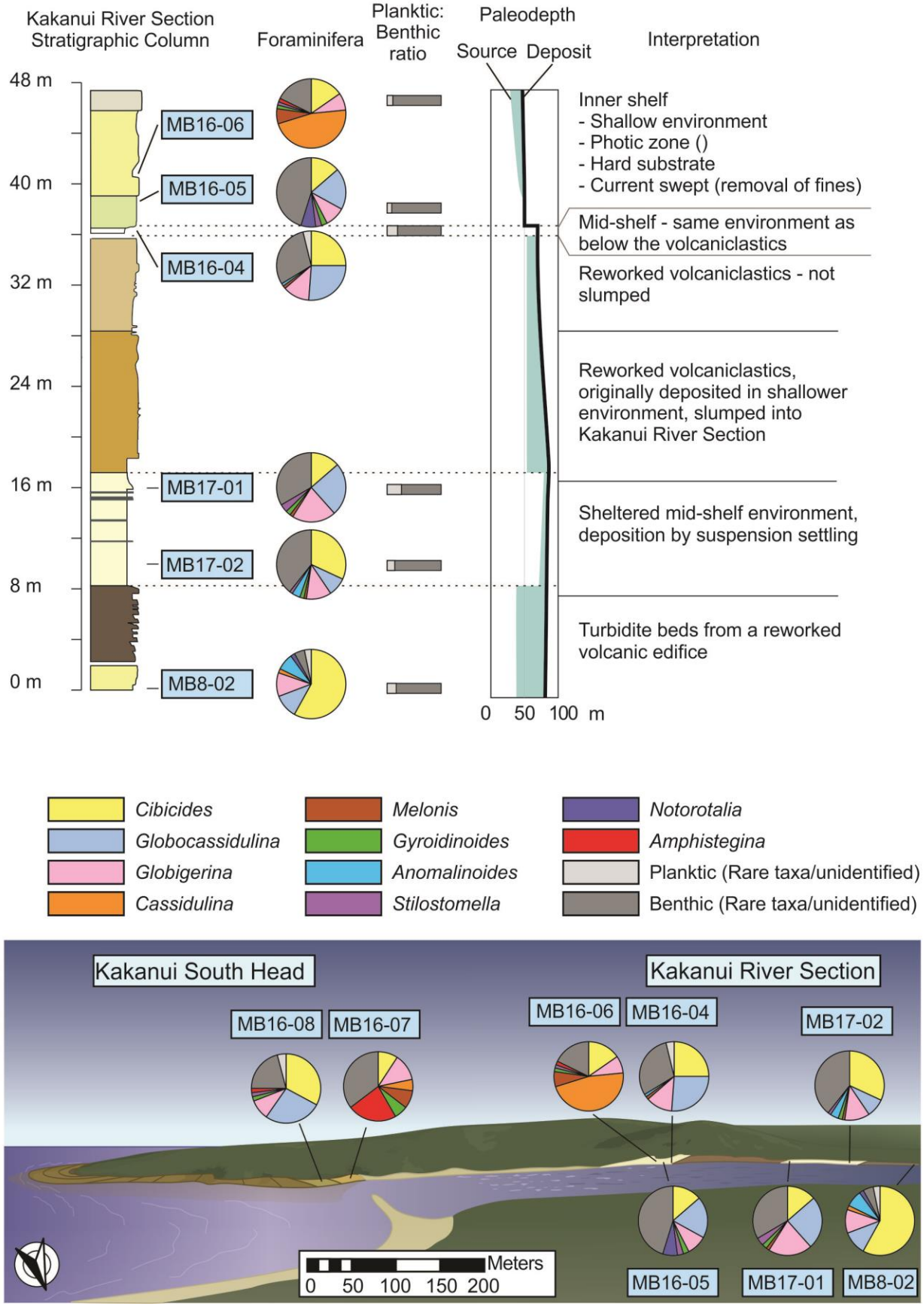

Figure 3.28: Foraminiferal percentages and sample locations, shown on a stratigraphic column and an outcrop diagram

3.3 Mineralogy

The mineralogy of different volcanic deposits was investigated using thin sections and crushed rock samples. Based on this, several conclusions could be drawn:

- The most common minerals across all sites are kaersutite, olivine, and chrome diopside (Figure 3.29)
- Feldspar, quartz and biotite were also discovered in some tuff samples, but were fairly rare (<1 %)
- The Kakanui Mineral Breccia (Kakanui North and South Head) contains a much more diverse mineralogy.
- The kaersutites of Kakanui River Section Tuff B are very smooth, clean, elongate cleavage fractures of larger crystals.
- Other lava and tuff localities, including the Kakanui River Section Tuff A, the Kakanui Western Slope, and the lavas at Pine Tree Hill contain much more irregular, granular kaersutites (Figure 3.30).

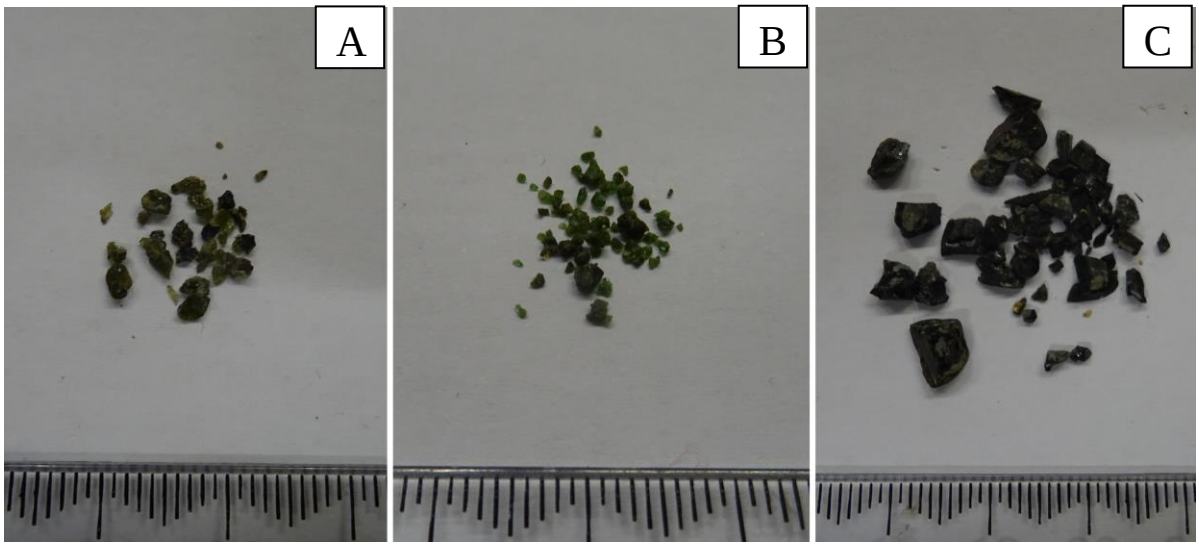

Figure 3.29: Common minerals in Waiareka-Deborah volcanic deposits. **A**: Olivine, **B**: Chrome diopside, **C**: Kaersutite.

Two distinct kaersutite varieties occur at Kakanui: those which were included in eclogitic nodules, and those which formed as megacrysts from the nephelinitic host magma (Merrill & Wyllie, 1975). Microprobe analysis indicates that the chemistries of kaersutites from the Northern River Section, the Main River Section, the flanks of the headlands, and the lavas of Pine Tree Hill match this megacryst type, while the eclogitic type is restricted to the Kakanui Mineral Breccia.

Microprobe analysis of the picked minerals showed that they were fairly homogeneous, with no obvious zoning, and only rare, small inclusions. However, as they are fragments of larger crystals, it is possible that they are too small to be representative. Figure 3.30 shows characteristic examples of the olivine, chrome diopside and kaersutite which were examined with the microprobe.

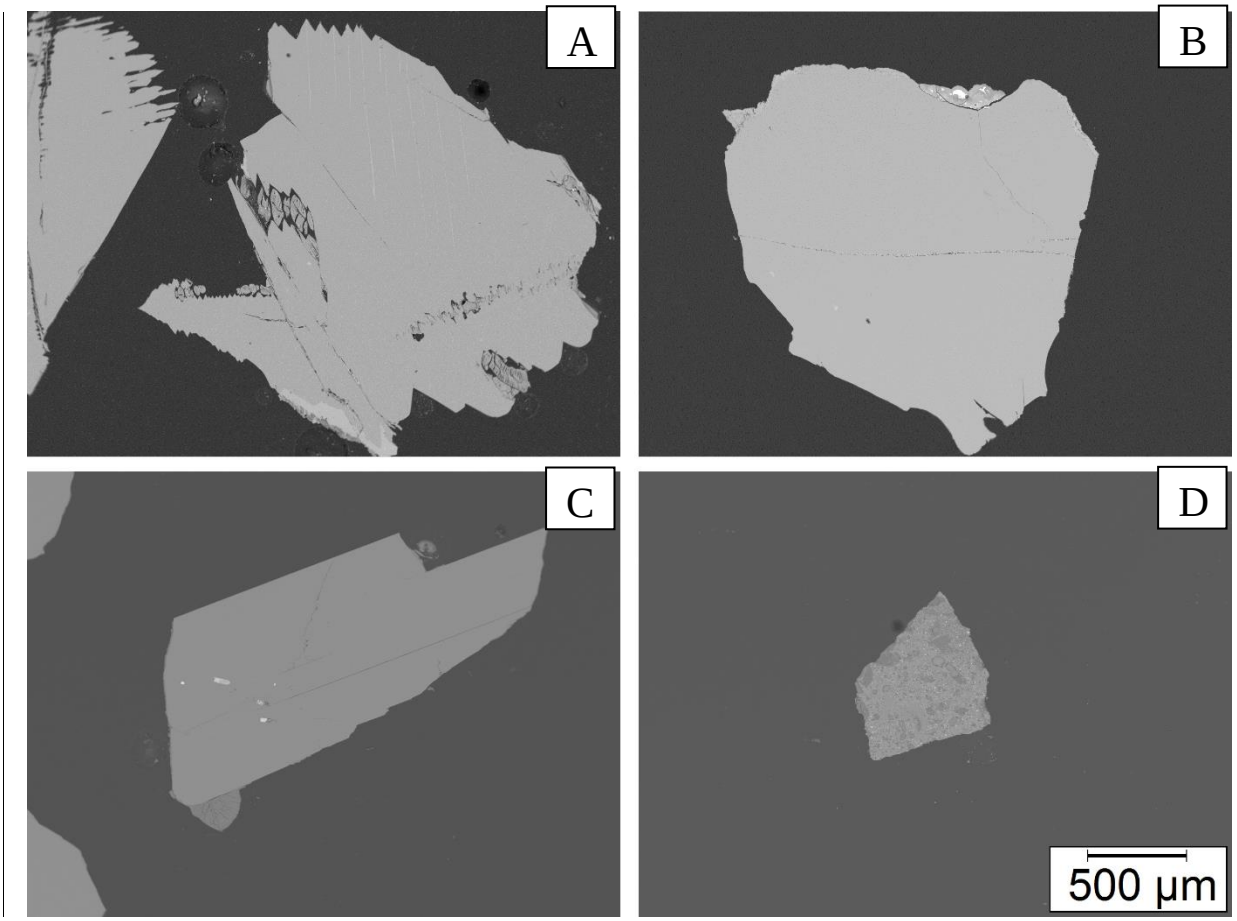

Figure 3.30: Microprobe photos of some of the most abundant minerals found in Waiareka-Deborah deposits.

A: Olivine picked from Upriver Lapilli Tuffs, showing distinctive jagged outlines due to conchoidal fracture. **B:** chrome diopside, which is typically granular and equant. **C:** Cleavage fragment of kaersutite from the Kakanui River Section, with sharp, smooth edges parallel to cleavage. **D:** Small, altered grain of kaersutite from Kakanui Western Slope. Kaersutite from this location was too weathered to be used for microprobe analysis.

Although XRF of basalt showed strong site-specific trends, microprobe analysis of minerals showed smaller variation between sites. This matches the observations of Moorhouse (2015), who found that feldspar compositions from different tuffs were remarkably uniform, and

Coombs et al. (1986) who recorded little variation in KMB crystals. Despite the closely matching compositions of the sampled minerals, there were some site-specific trends that could be observed.

The Mg# of a crystal (=100 x Mg / (Mg + Fe)) is a good indicator of the magmatic properties of the melt that formed it. Pristine mantle has an Mg# of ~89 (von Seckendorff & O'Neill, 1993; Moorhouse, 2015), and deviations from this can be evidence of magma evolution or enrichment. The average Mg# of olivine and chrome diopside was calculated for each sampling site. These returned values of <89, showing that the host magma had some degree of enrichment in Fe. The Mg# of chrome diopsides was higher and more variable, ranging from 85.6 – 89.8. These values seemed to decrease as deposits got higher in the inferred stratigraphy (Figure 3.31). The Mg# of olivines was lower, and more consistent; tending to plot around 84.6. However, this value showed the opposite trend from the chrome diopsides, seeming to increase slightly as deposits got younger (Figure 3.32).

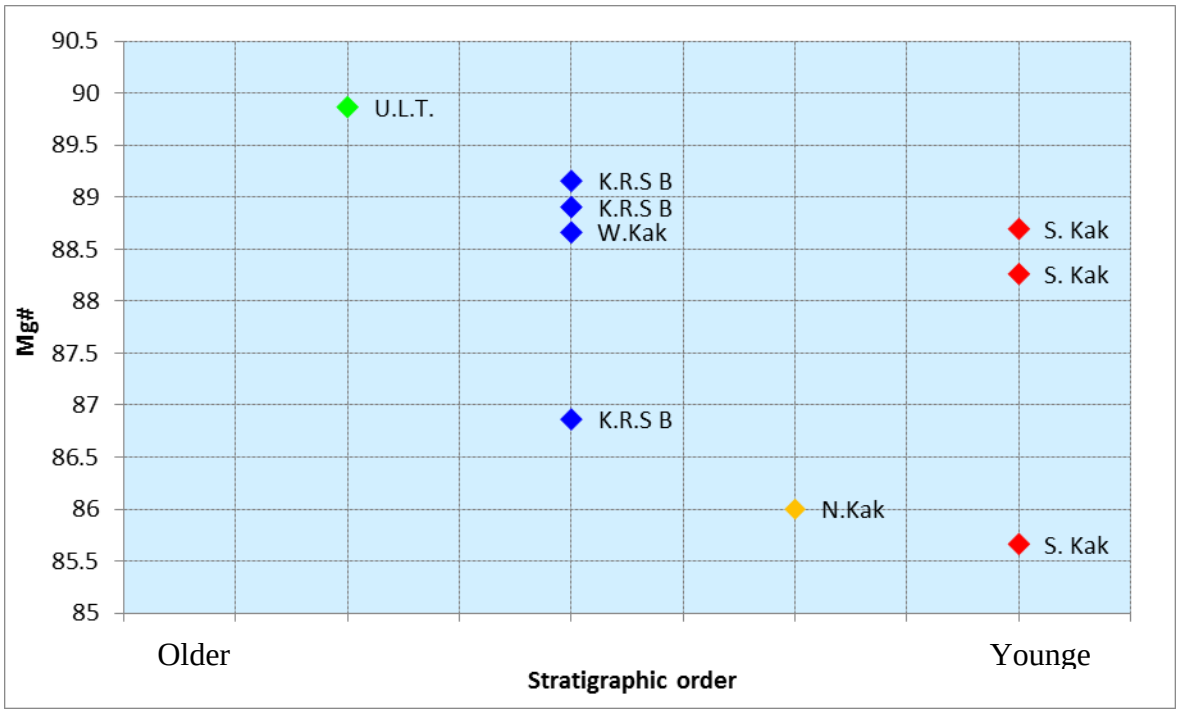

Figure 3.31: Mg# of chrome diopside crystals from various sites around Kakanui. Values decrease as deposits are inferred to be younger. North Kakanui is inferred to be younger than South Kakanui on the basis of geochemistry in chapter 3.4.

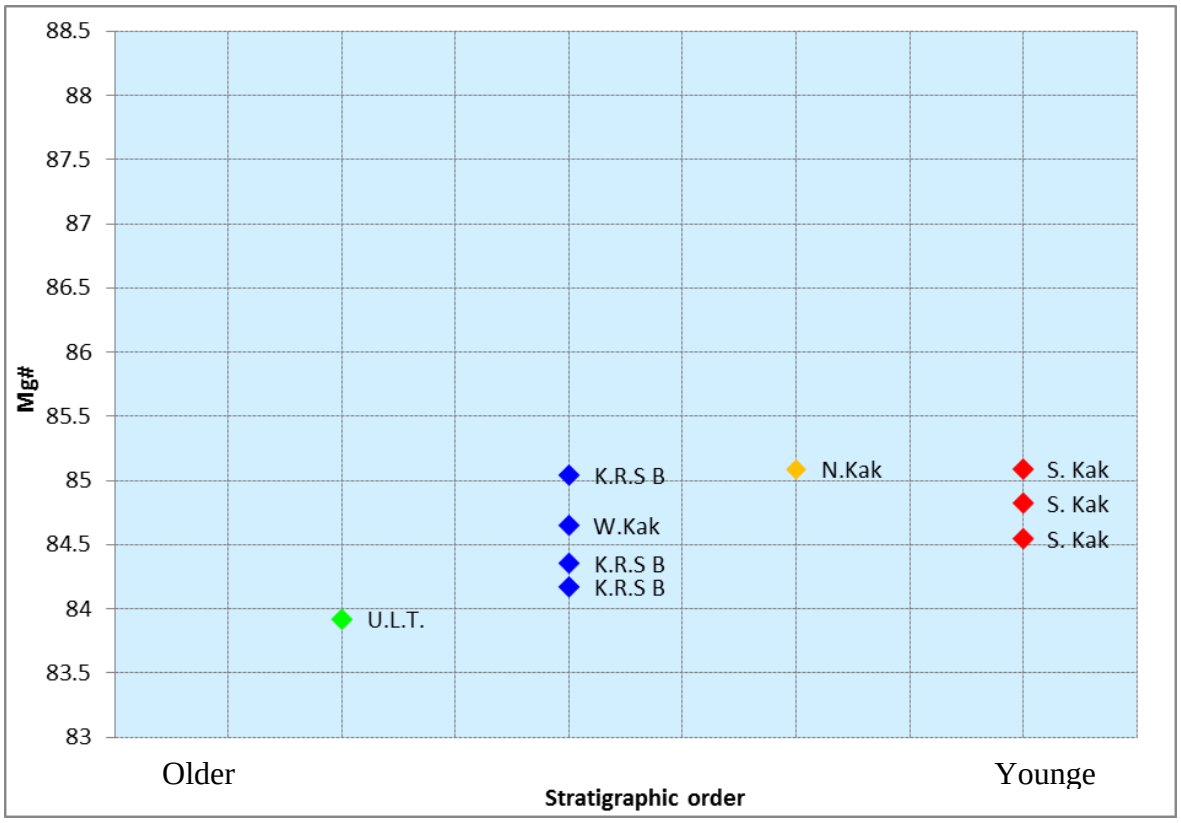

Figure 3.32: Mg# of olivine crystals from various sites around Kakanui. Values slightly increase as deposits are inferred to be younger.

3.4 Source area geochemistry

The XRF analysis provided good data, which was used to geochemically fingerprint Waiareka-Deborah volcanoes, as well as to aid in the understanding of the magmatic development of the volcanic field. Samples from the same locations tended to cluster together (Kakanui River Section Tuff B, South Kakanui Head, and to some extent the Upriver Lapilli Tuffs), even when taken from different forms of basalt (dikes, lapilli or bombs). These groupings support the use of this data for geochemically distinguishing different sites.

There are some limitations to the XRF data, and caution is needed before relying on it to draw conclusions. Previous authors (e.g. Coombs et al., 1986) have noted the tendency for Waiareka-Deborah deposits to be cemented, weathered, and altered, which can alter their geochemistry. Although care was taken to select and process samples to limit this, some level of contamination was unavoidable.

Loss on ignition (LOI) was generally low for whole basalt samples from bombs or dikes, but exceeded 5 % for some lapilli, and veined samples. This is likely due to the presence of clays or

cements which were lost during the analysis. Two samples with >10 % LOI were removed, and those with >5 % were used with caution.

High CaO percentages correlated with high LOI; varying from 5 % in the cleanest samples, to over 16 % in the removed samples. This can be attributed to the presence of calcite cements, which occur within fractures and pore spaces. However, the geochemical trends observed in the data remained unchanged when values were normalised to 5 % CaO. Therefore, it is believed that while cement traces may have slightly altered the results, they did not corrupt it.

Figure 3.33 shows the locations that were sampled for XRF. These locations are mostly around Kakanui, but include some samples from volcanics in other parts of the Waiarekah Deborah volcanic field.

Figure 3.33: Locations of basalt samples used for XRF. Colours correspond to the symbols used for the XRF graphs below.

The volcanics sampled showed a range of compositions, but plotted along continuous lines, confirming that they were genetically related. There was a strong positive correlation between MgO % and FeO%, and a negative correlation between MgO % and both SiO_2 and Al_2O_3 % (Figure 3.34). Interestingly, the oldest deposits (Aorere Point, Boatmans Harbour) have the most felsic compositions, while eruptions that occurred near the end of Waiareka-Deborah volcanism (Kakanui River Section Tuffs A and B, Gees Point, the Kakanui Headlands) are more mafic.

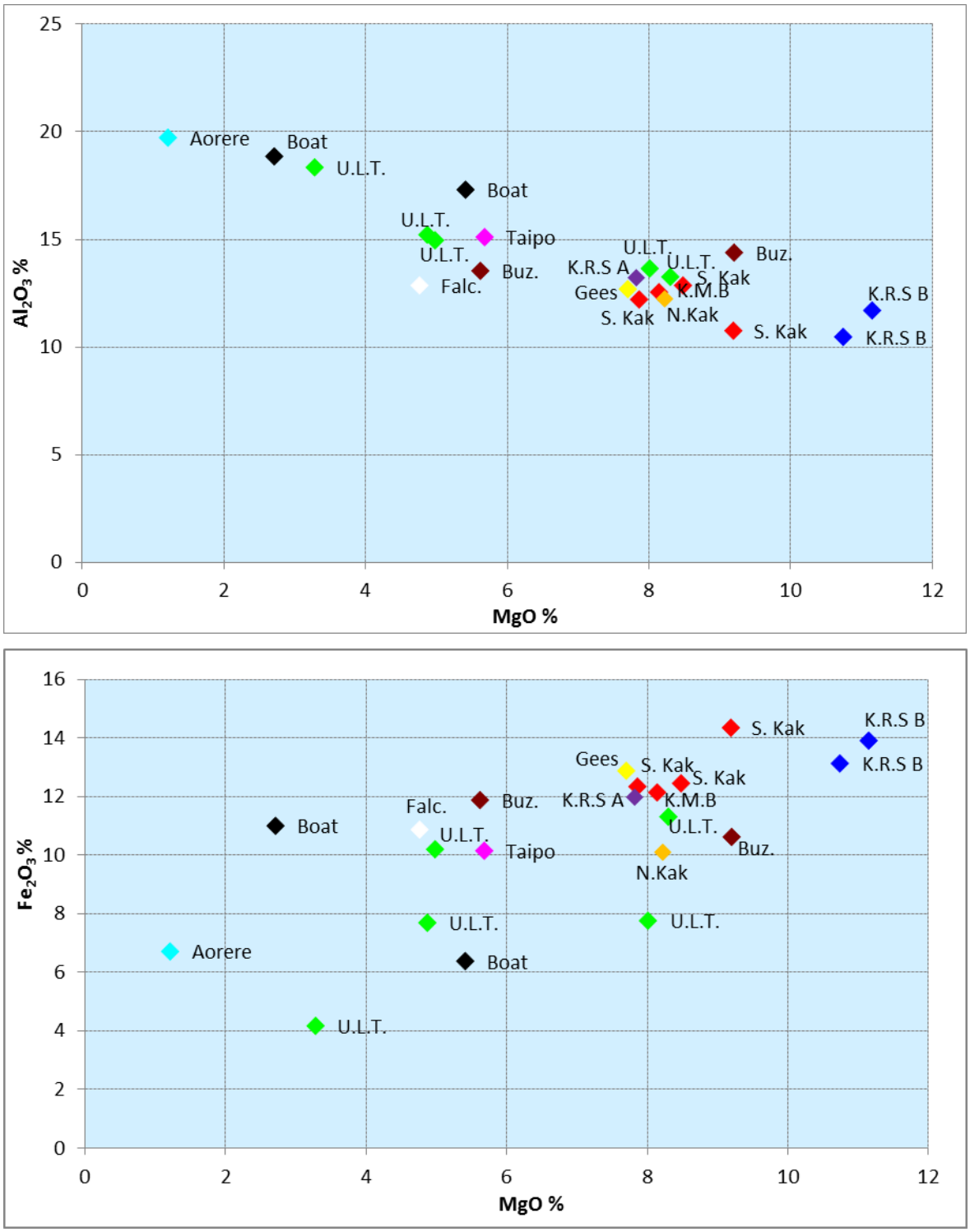

Figure 3.34: Major element concentrations of basalt samples from around Kakanui. **Top**: Al_2O_3 % decreases with increasing MgO %. **Bottom**: Fe_2O_3 % increases with increasing MgO % S. Kak. = South Kakanui Head; K.M.B. = Kakanui Mineral Breccia; K.R.S A = Kakanui River Section Tuff A; K.R.S B = Kakanui River Section Tuff B; U.L.T. = Upriver Lapilli Tuffs; Falc = Falconers Road; Boat = Boatmans Harbour; Buz. = Buzan Road; Aorere = Aorere Point.

The trends observed for mafic and felsic elements are also seen on trace element graphs, with the oldest edifices plotting on one extreme, and the youngest edifices plotting on the other. The overall pattern is an increase in enrichment through time. However, there are several interesting patterns that emerge. The younger, more mafic melts tend to have much higher incompatible/compatible (e.g. Nb/Y) and fluid immobile/fluid mobile (e.g. Nb/Zr) element ratios (Figure 3.35; Figure 3.36). The Kakanui South Head and Kakanui River Section Tuffs are particularly enriched in LREEs (e.g. Th, Ce) (Figure 3.37). However, Kakanui River Section Tuff B has surprisingly low concentrations of the Large Ion Lithiphile Elements Sr and Rb (Figure 3.38).

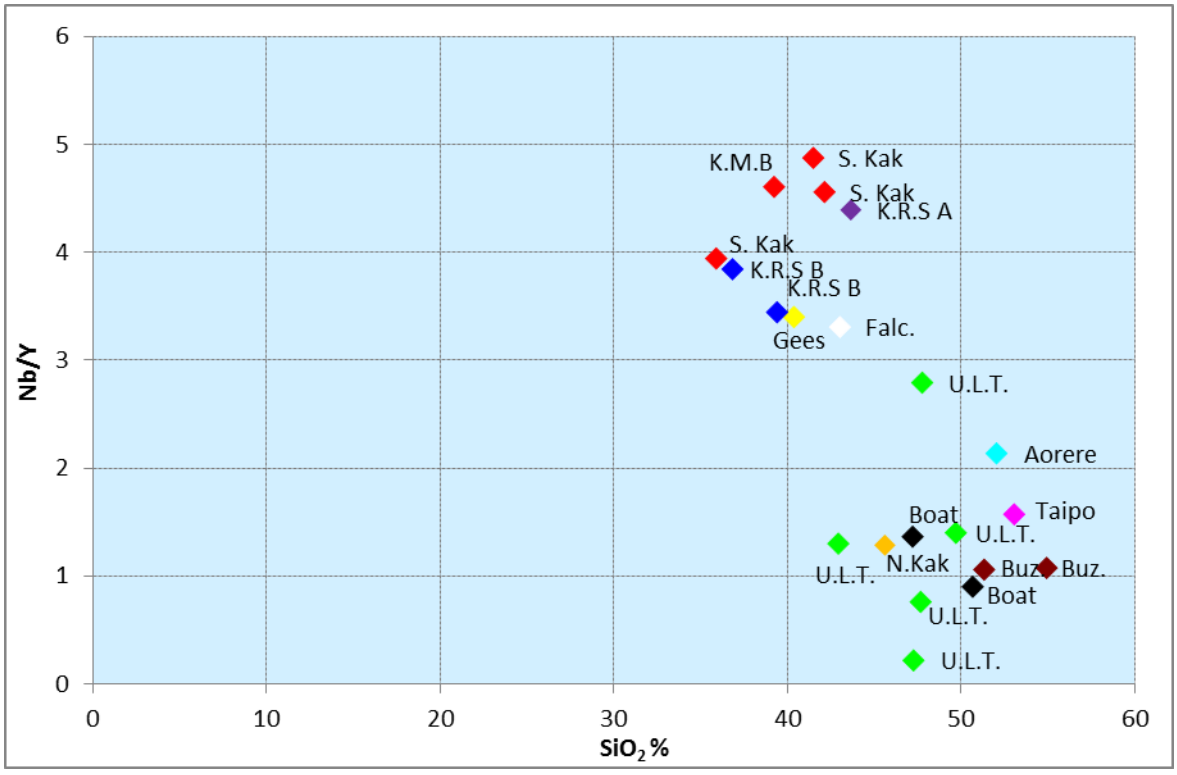

Figure 3.35: Nb/Y ratio vs SiO_2. Nb is more incompatible, while Y is less incompatible. S. Kak. = South Kakanui Head; K.M.B. = Kakanui Mineral Breccia; Riv. = Kakanui River Section; U.L.T. = Upriver Lapilli Tuffs; Falc = Falconers Road; Round = Round Hill, Boat = Boatmans Harbour; Buzan = Buzan Road; Bridge = Bridge Point; Aorere = Aorere Point.

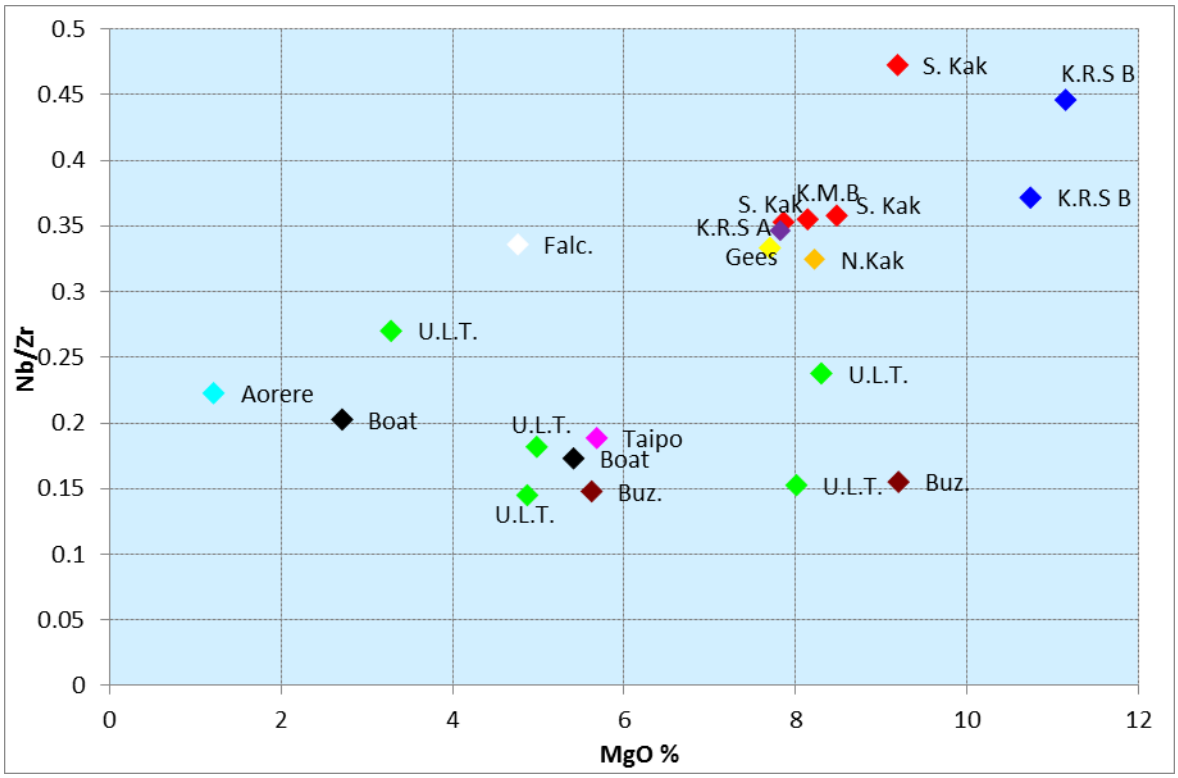

Figure 3.36: Trace elements from Waitaki basalt samples. Nb is fluid immobile, while Zr is fluid mobile.

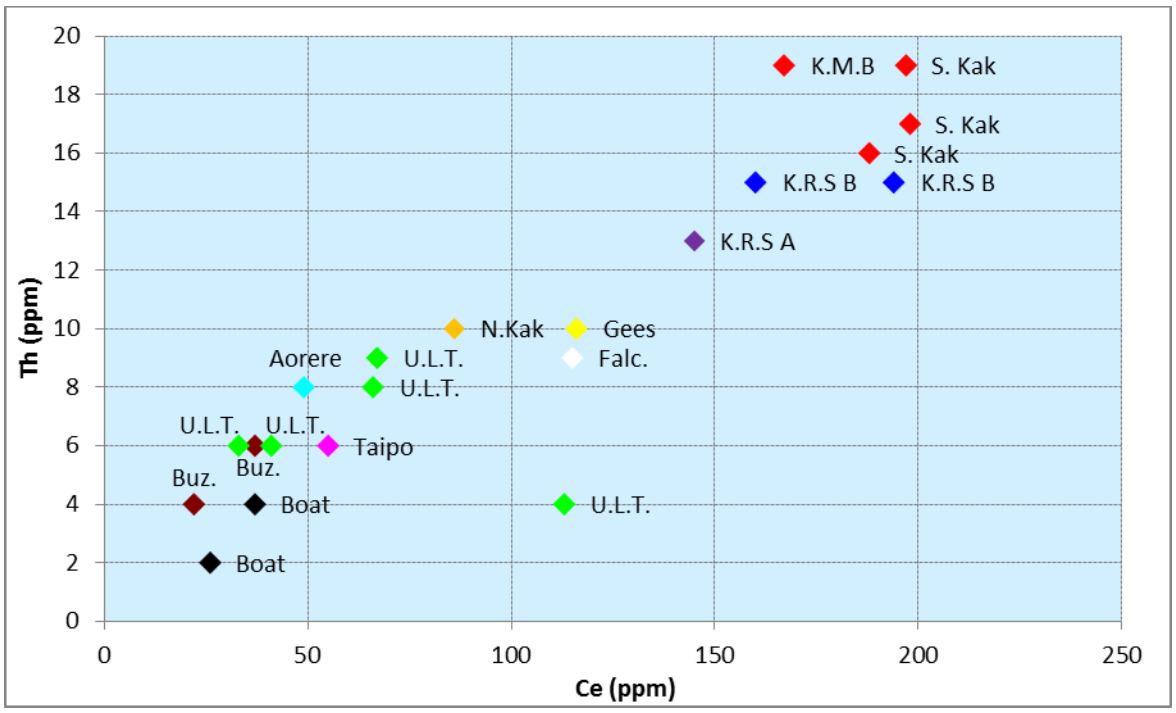

Figure 3.37: Trace elements from Waitaki basalt samples. Th and Ce are both LREEs. S. Kak. = South Kakanui Head; K.M.B. = Kakanui Mineral Breccia; Riv. = Kakanui River Section; U.L.T. = Upriver Lapilli Tuffs; Falc = Falconers Road; Round = Round Hill, Boat = Boatmans Harbour; Buzan = Buzan Road; Bridge = Bridge Point; Aorere = Aorere Point.

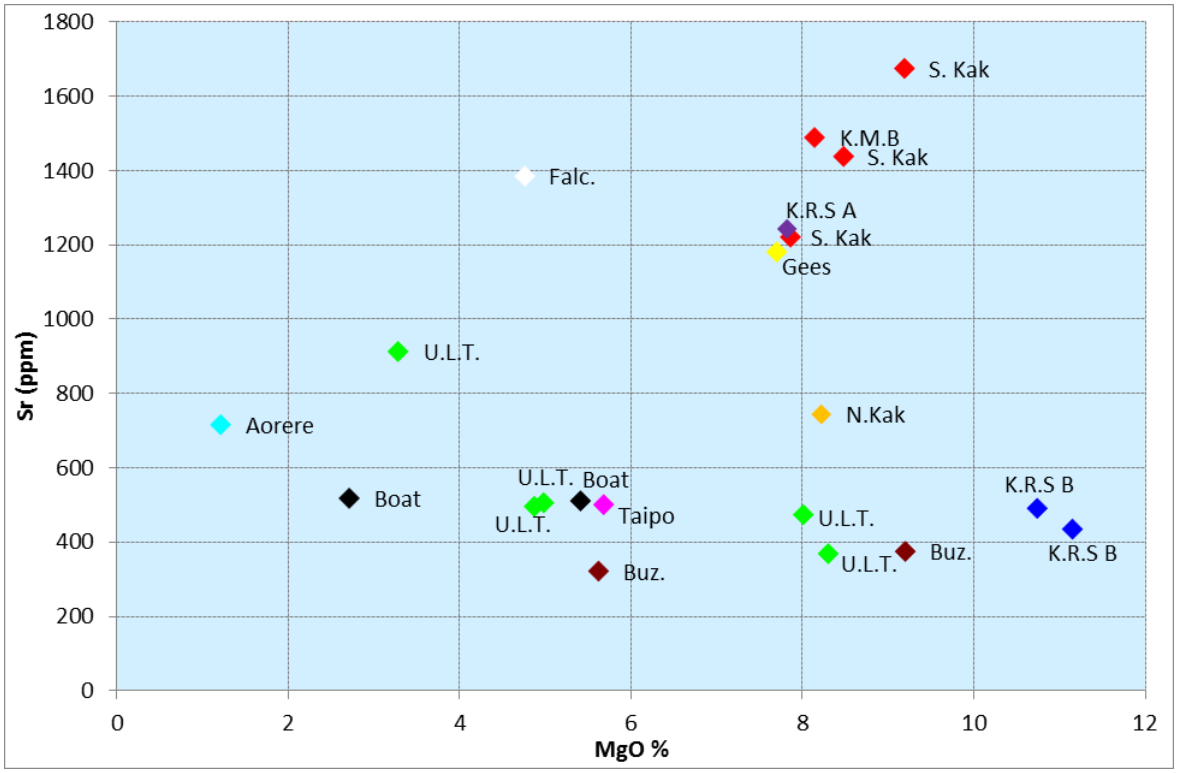

Figure 3.38: Trace elements from Waitaki basalt samples. Sr is a Large Ion Lithophile Element. S. Kak. = South Kakanui Head; K.M.B. = Kakanui Mineral Breccia; Riv. = Kakanui River Section; U.L.T. = Upriver Lapilli Tuffs; Falc = Falconers Road; Round = Round Hill, Boat = Boatmans Harbour; Buzan = Buzan Road; Bridge = Bridge Point; Aorere = Aorere Point.

The trends observed in the XRF data suggest that individual eruptions can have a distinct geochemistry. Furthermore, element concentrations seem to correlate with stratigraphic order, with eruptions becoming increasingly mafic, and enriched in incompatible and fluid immobile elements, and LREEs. This trend will be explored more in Chapter 4.2.

Discussion

4.1 Kakanui River Section Palaeoenvironmental Reconstruction

Detailed investigation of the limestones and volcanic deposits in the Kakanui River Section revealed that this area experienced a number of significant changes to palaeodepth, sediment transport mechanisms and sediment sources, which are discussed in this chapter.

The lowest unit of the Kakanui River Section is a massive bryozoan-rich packstone/grainstone, which outcrops from the base to around 2 m up the section. This unit has sub-angular to sub-rounded fine to coarse sand-sized grains and moderate sorting. These qualities, and the presence of volcanic material implies grainflow from a vent which was fairly close. The foraminiferal assemblage is rich in *Cibicides*, which has its greatest relative abundance in the inner to mid shelf (Hayward et al., 2010). It contains ~14 % planktic foraminifera, which indicates mid shelf on the planktic percentage depth diagram, and lacks large benthic foraminifera, which would indicate the photic zone. This environment was probably in the mid shelf on a volcanic high, which provided a solid, shallow base for bryozoans, echinoderms, benthic foraminifera and other marine organisms. It was reworked and deposited in the Kakanui River Section area, although it is unclear what the transport direction was, as there are no palaeoflow indicators in the deposit. However, the presence of terrestrial quartz sediments suggest that currents could have been moving away from the palaeoshoreline, and that the source was located closer to it; to the south or east of the Kakanui River Section.

Overlying the bryozoan-rich packstone/grainstone is Section 2: Kakanui River Section Tuff A. This is a unit of calcareous volcaniclastic sandstone, which grades to fossiliferous in some beds. This contains similar bioclastic components to the underlying bryozoan-rich packstone/grainstone, and is also interpreted as having come from a volcanic high. However, quartz content is higher in the calcareous volcaniclastic sandstone, indicating that it was sourced from a location closer to the palaeoshoreline, and suggesting that it does not share a source with the bryozoan-rich packstone/grainstone.

Section 3 contains the grey wackestone facies, which formed in a low energy, relatively deep mid shelf environment. Silt-sized clasts were deposited by suspension sedimentation, and occasional high-energy storm events which deposited thin beds of coarser clasts. Palaeodepth

can be determined by the 13 – 21 % planktic foraminiferal ratio, which is higher than other sections, and the abundance of sponge spicules and *Globocassidulina subglobosa*, which are rare in shallower waters. Because the energy levels were so low, bioclasts are considered in-situ, and diagnostic of the depositional environment.

The grey wackestone facies was appears to be a mud-rich lateral equivalent of the diatomite unit which outcrops beneath the volcaniclastics ~400 m along strike to the south-southwest. Waitaki diatom-rich rocks are estimated to have formed at depths of 75 – 150 m, and are associated with increased dissolved silica supplied by local volcanism (Edwards, 1991).

Although the grey wackestone section is only around 9 m thick, it probably represents a very significant time period. This can be deduced from several factors:

- The boundary between the Runangan and the Whaingaroan (34.6 Ma) occurs within this section (Clowes & Morgans, 1984). It is unlikely for a unit which formed quickly to cross the boundary between stages which cover millions of years.
- The formation of glauconite requires prolonged periods with low sedimentation rates
- Long-term accumulation rates for carbonate mudstone are likely to be ~5-10 mm/kyr (Saddler, 1999), meaning this section represents at least 70 – 140 thousand years.
- Heavy bioturbation implies a slow rate of deposition.

This makes it unlikely that the volcanic deposits which occur above and below this unit belong to the same source. Monogenetic volcanoes are unlikely to remain active over such a long period, nor to have eruptions separated by such lengthy hiatuses (Németh, 2010).

The transition from the turbidity currents of the calcareous volcaniclastic sandstone unit to the suspension sedimentation of the grey wackestone unit could have a number of causes. It is possible that the vent which supplied the sediment for the turbidity currents degraded too much, to generate them anymore. It is also possible that the palaeocurrent direction shifted, depositing turbidites elsewhere. It is also possible that sea level rise moved the source into a lower energy environment. The grey wackestone section does contain the deepest-water fossil assemblage, but it is difficult to tell if it is any deeper than the underlying turbidite beds, as the fossils within them were derived from a shallower source. The grey wackestone facies continues after the overlying volcaniclastic slump, indicating that this material was not thick enough to change the depositional environment.

Section 4: Kakanui River Section Tuff B overlies the grey wackestone unit. This contains a cross-bedded and laminated volcaniclastic unit and an even-bedded volcaniclastic unit. These probably represent the same fairly proximal source, since they have similar compositions, are both fairly thick, and show no evidence of a significant time gap between their depositions. However, they probably do not share a source with the calcareous volcaniclastic sandstone from section 2, which is a much thinner deposit, with a generally finer grainsize, and much more shelly material. Additionally, a monogenetic volcano is unlikely to have remained active during deposition of the ~9 m of wackestone which separates the two sections.

The Kakanui River Section Tuff B source vent erupted subaqueously, causing glass to alter to palagonite, but was shallow enough that the water's confining pressure did not prevent moderate lapilli vesicularity from developing (McBirney 1963; Fisher and Schmincke 1984). The eruptions included a gas column that mostly excluded water, allowing some accretionary lapilli to form (White, 2000). The material deposited in the river section is entirely reworked, as evidenced by the carbonate content, fossils, entrained and wackestone, and the sedimentary structures, such as high-angle cross-beds.

The westward-dipping orientations of Kakanui River Section Tuff B cross-beds indicate that their source was to the east-southeast. This material built up, became unstable, and was remobilised in a semi-cohesive slump. Deformed flame structures indicate that the slump also came from a slope east-southeast of the Kakanui River Section. This slope probably represents the volcaniclastic pile built up around the source edifice.

Following slumping, more volcanic material was deposited in the upper plane bed regime. This even-bedded volcaniclastic unit is fine- to medium sand-sized; slightly finer than the underlying cross-bedded and laminated volcaniclastic unit. The bedform change and grainsize reduction is probably because the underlying unit was a more proximal deposit, but slumping has shifted it out of its original depositional environment. The even-bedded volcaniclastic unit is a more distal, in situ deposit formed by turbidity currents.

After the volcaniclastics, the Kakanui River Section depositional environment returned to low energy suspension sedimentation, causing the grey wackestone facies to deposit again. This upper grey wackestone unit contains small crystals of kaersutite, indicating that some volcaniclastics remained exposed. Planktic foraminiferal percentages are slightly lower, and

Cibicides percentages slightly higher than the top of the lower grey wackestone unit, indicating a slight shallowing of the depositional environment, which is probably explained by the deposition of 19 m of volcaniclastics.

The uppermost grey wackestone unit is overlain by an unconformity which is associated with *Thalassinoides* burrows, and overlain by a glauconite-rich unit. *Thalassinoides* burrows are significant, as they are unlined, and can't form in soft sediment (Myrow, 1995). They indicate a depositional hiatus and the development of firm ground. This unconformity probably represents sea level fall, similar to firm ground deposits recorded in other Eocene-Oligocene Waitaki deposits (Thompson, 2012; Thompson et al., 2014). During these periods of lowered sea level, the palaeocoastline was closer, and more terrestrial clays were supplied for glauconite production. It is possible that this sea level fall corresponds to the EPi-2 oxygen isotope maxima event (Abreu & Anderson, 1998).

After the depositional hiatus, the glauconitic packstone/wackestone began to accumulate. This deposit is rich in bright green immature glauconite, particularly along the base, which probably formed nearby during the depositional hiatus. Lined *Ophiomorpha* burrows indicate that the sediment remained unconsolidated during deposition. The foraminiferal assemblage is diverse, and relatively poor in planktic varieties (10 %), indicating low stress conditions in an inner – mid-shelf environment. Energy conditions were probably moderate, with significant mud content, but also fragmented bioclasts and a larger average grainsize that the grey wackestone facies.

The glauconitic packstone/wackestone transitions gradationally to beds of bryozoan-rich packstone/grainstone. This shift is accompanied by an increased grainsize, a reduction in mud content, and the appearance of large body fossils concentrated along particular horizons. Foraminifera include the shallow, attaching *Cibicides pseudoconvexus*, and rare specimens of *Amphistegina* which have photosynthesising symbionts, and are restricted to the photic zone. While the glauconitic packstone represents reasonably in situ accumulation, this bryozoan-rich packstone/grainstone unit contains sediments transported from shallow environments; as evidenced by the well sorted well rounded clasts and photic zone organisms such as *Amphistegina*. Energy levels were high, leading to the removal of fines.

The deposits in the Kakanui River Section show the multiple processes which affected this area, and provide a window into the changing environment of mid-Cenozoic Waitaki. The evolution of the Kakanui River Section depositional environment is illustrated on Figure 4.1.

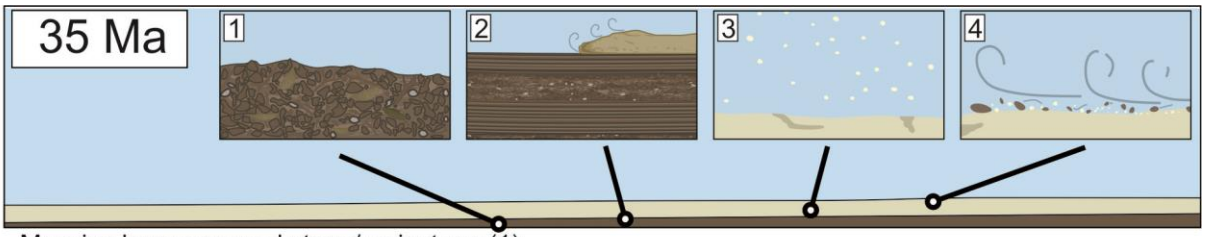

- Massive bryozoan packstone/grainstone (1)
- Turbidite deposits of calcareous volcaniclastic sandstone from colonised volcanic edifice (2)
- Turbidity currents stop reaching this area, and are replaced by suspension sedimentation (3), broken by occasional storm beds (4)

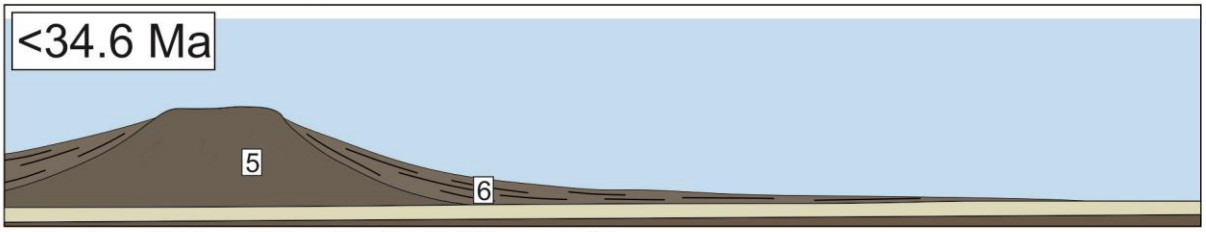

- Eruption of Kakanui River Section Tuff B source (5)
- Volcanic material reworked by marine processes (cross-bedded and laminated lapilli tuff facies) (6).

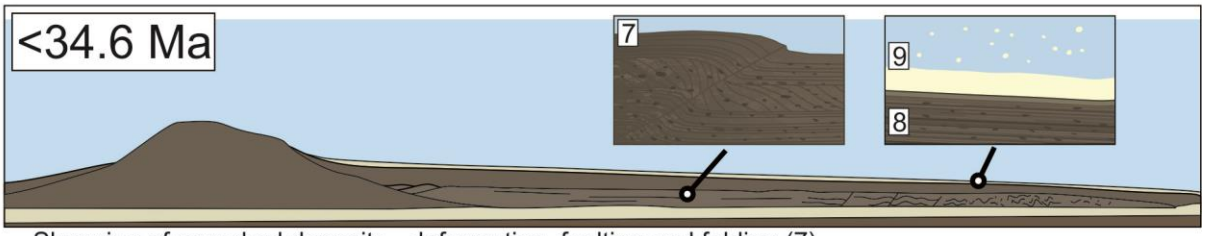

- Slumping of reworked deposits - deformation, faulting and folding (7)
- Turbidity currents deposit even-bedded volcaniclastics (8). Suspension sedimentation resumes (9)

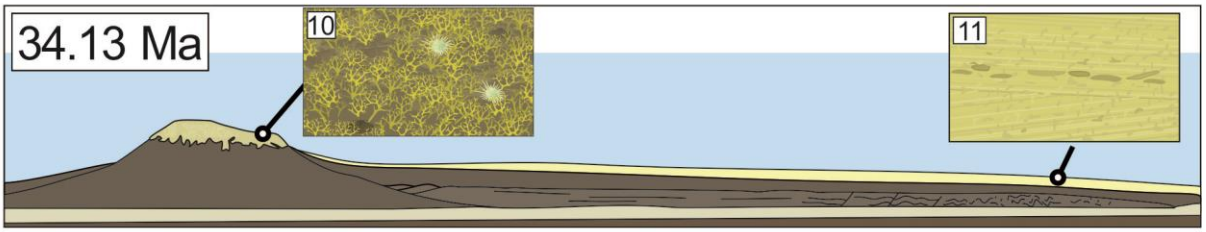

- Lowered sea level and unconformity development, followed by deposition of glauconitic packstone
- Colonisation of volcanic high (10) and deposition of bioclast material (11)

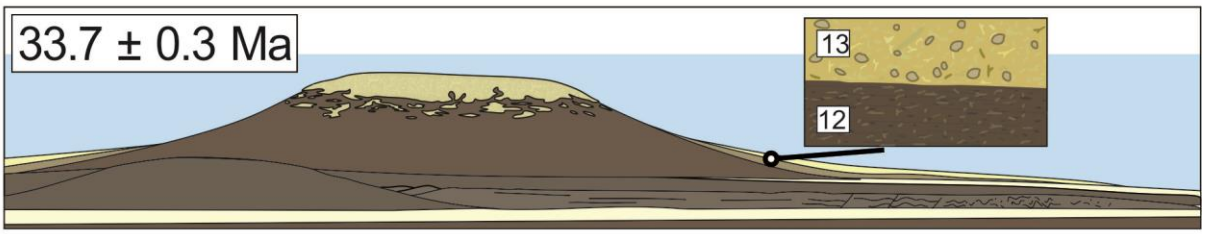

- Eruption of Kakanui South Head, which was eventually colonised by marine organisms.
- Deposition of calcareous volcaniclastics (12), and impure bryozoan-rich packstone/grainstone (13)

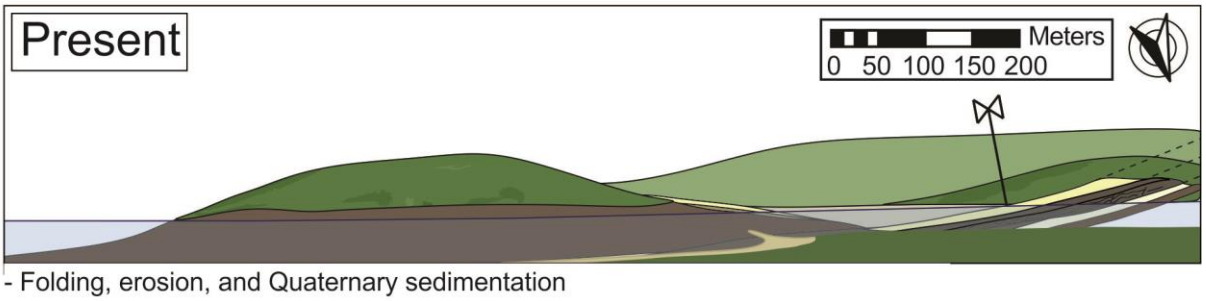

- Folding, erosion, and Quaternary sedimentation

Figure 4.1: Development of the volcanic and carbonate deposits around Kakanui.

4.2 Magmatic Development and Geochemical Fingerprinting

The geochemical and stratigraphic information collected for this thesis have been used to determine the relationship between Waiareka-Deborah edifices. Samples were collected from around Waitaki, with estimated ages ranging from ~38 Ma to <34 Ma, determined by 40Ar/39Ar dating (Hoernle et al., 2006) and stratigraphy (Cas et al., 1989; Hicks, 2014; Moorhouse 2015). This represents a significant portion of the Waiareka-Deborah volcanic field's 40 – 32 Ma period of activity (Cooper 2004; Coombs et al. 2008).

Mg# calculated for chrome diopside and olivine crystals from sites around Kakanui gives some clues to the geochemical changes occurring in the Waiareka-Deborah volcanic field. Values were almost all lower than that of primitive mantle (~89) (von Seckendorff & O'Neill, 1993), indicating that these minerals formed in a melt which was enriched in Fe. This agrees with the findings of Moorhouse (2015) at Boatmans Harbour. However, while chrome diopside showed a decrease in Mg# in stratigraphically higher units, olivine Mg# showed a subtle increase. The overall lower Mg# of olivine makes sense, as the Fe/Mg distribution coefficient (K_d) is greater than 1 for clinopyroxene in equilibrium with olivine in mantle phases (Perkins & Vielzeuf, 1992, Pearson et al., 2003).

Because of the opposite trends of the olivine and chrome diopside Mg# plots, the Fe/Mg K_d shows a notable decrease over time. Perkins and Vielzeuf (1992) note that olivine-clinopyroxene Fe-Mg exchange is fairly insensitive to pressure or temperature, but is a good indicator of magma mixing, since olivine solutions are less ideal than clinopyroxene solutions. Therefore, it is possible that the decreasing K_d is a result of changing magma geochemistry, related to the introduction of an Fe-enriched melt. This gives an interesting insight into the evolution of the Waiareka-Deborah volcanic field. However, because of the relatively small amount of variation between sites, combined with the reasonably significant variation within minerals from the same site, this method seems inappropriate for geochemically fingerprinting individual eruptions

Figure 4.2: Changing Fe/Mg distribution coefficient (K_d) for chrome diopside/olivine over time.

The megacrysts entrained in Waiareka-Deborah deposits formed in the mantle, at depths of 75 – 85 km, and temperatures of 1200° - 1350°C (Clark et al., 1969; McCallister et al., 1976; Moorhouse, 2015). Microprobe analysis of sampled megacrysts showed an average Mg# of 84.6 for olivines, and 88.0 for chrome diopside. This difference. Pristine mantle has an Mg# of ~89 so the lower values indicate

While olivine Mg# was relatively consistent in the sites sampled, chrome diopside Mg# was highest in older samples, and showed a decrease over time. This seems to indicate that chrome diopside precipitated within an evolving, increasingly Fe-rich magma. The first Waiareka-Deborah melts to erupt contained the older, more Mg-rich crystals, while later eruptions contained younger, Fe-rich crystals.

Chrome diopside Mg# showed a significant amount of variation between sites,. less However, as discussed in Section 3.4, the volcanics of the Kakanui River Section, and Kakanui North and South Head are compositionally similar.

XRF analysis shows that the volcanic samples have a range of compositions, from basaltic andesites to basanites and foidites. There is a linear distribution between endmembers, indicating that the sampled volcanoes are magmatically related, as expected. Interestingly, there is a trend of increasing Mg and Fe, and decreasing Al and Si through time. This is the opposite of a normal fractional crystallisation trend (#), and indicates that the evolution of the Waiareka-Deborah volcanic field was driven by some other factor. One possibility is increasing degrees of partial melting. The initial melts were enriched in fluid-mobile, As the degree of partial melting increases, different minerals control the melt composition, which can result in decreased concentrations of incompatible elements (Colson, 1998). This could have resulted in the shift from relatively compatible-poor melts, to compatible-rich melts.

Some Kakanui volcanoes, including the Headland volcanics, and Kakanui River Section Tuff A and Tuff B have different chemistries from other localities. These sites show higher compatible to incompatible element ratios (e.g. Nb/Y), higher fluid immobile to fluid mobile element ratios (e.g. Nb/Zr), and an enrichment in LREEs (e.g. Ce, Th). When plotting these ratios, the LREE-enriched samples cluster separately from other samples. The gap between them implies that the enrichment was relatively sudden, and not a gradual evolution of the magma source. It has been speculated that the xenoliths and xenocrysts of the Kakanui Mineral Breccia were derived from a stagnant magma body within the mantle (e.g. Dickey, 1968; Merrill & Wyllie, 1975; Garden, 2001). It is possible that multiple Kakanui melts intersected this same magma body, gaining a similar geochemical signature to the Kakanui Mineral Breccia, but not undergoing whatever magmatic process eventually resulted in the eruption of xenoliths and xenocrysts. If so, this enrichment adds another layer to the geochemical evolution of the area (Figure 4.3).

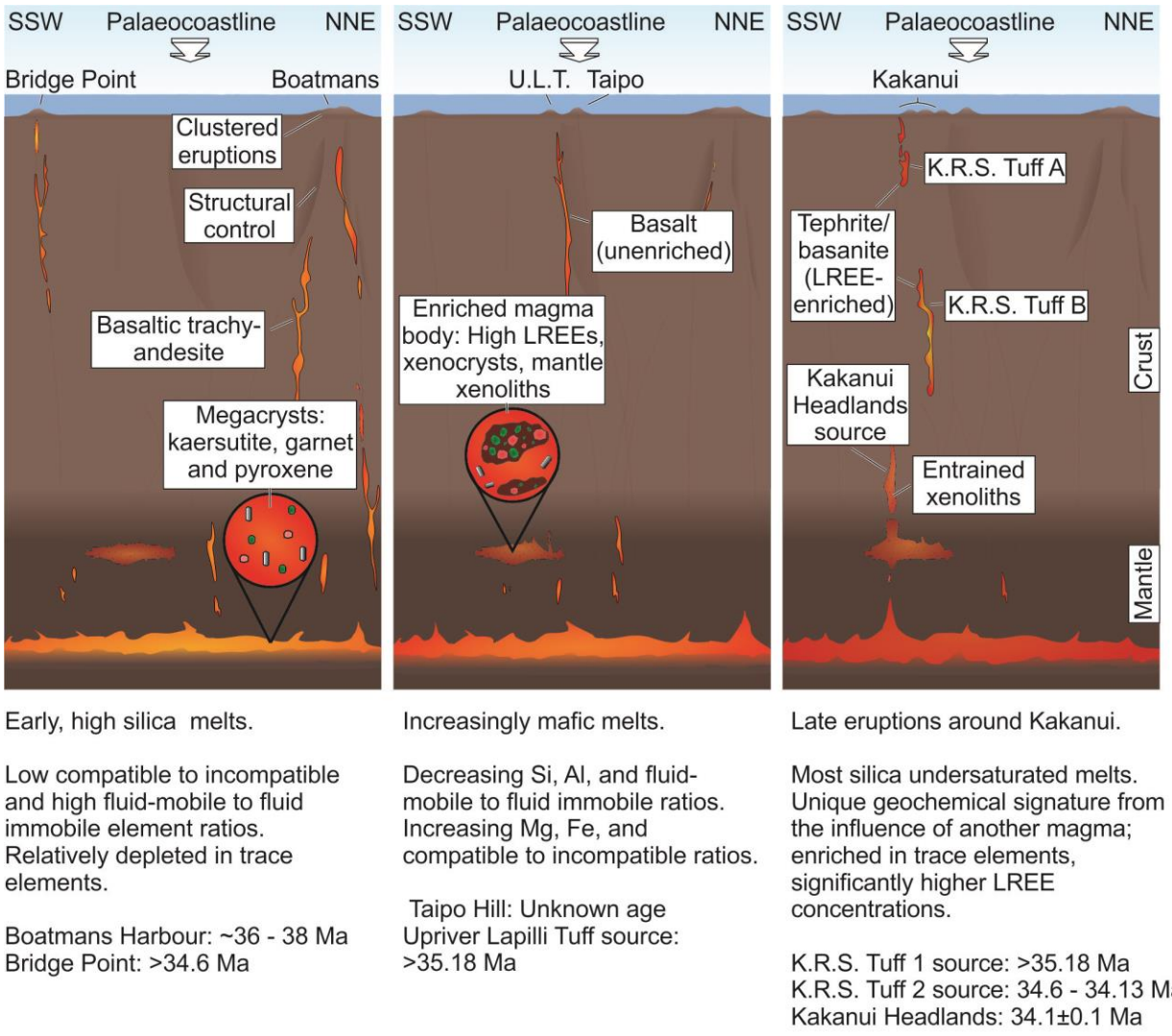

Figure 4.3: Magma development of the Waiareka-Deborah volcanics.

While Kakanui River Section Tuff 2 clusters with the other compatible-rich, LREE enriched volcanics around Kakanui, it has anomalously low Rb, Sr, and K concentrations. These elements would have been mostly incorporated into feldspars, which have relatively low density, and could have been segregated from other minerals in either the Kakanui River Section magma (Hargraves, 2014) or from the volcaniclastic sediment as it was transported post-eruption. It is also possible that the sampling process did not collect large enough lapilli to include many feldspars, while the bombs from Kakanui South Head and Falconers Road did contain feldspars. It is also possible that this deposit was weathered, and certain elements were leached out.

Despite alteration, cementation, and some anomalous values, the geochemical results of this study suggest that it is indeed possible to geochemically fingerprint different eruption sources. Because of the steady shift of magma composition to more compatible-enriched and mafic, and

the influence of the LREE-enriched magma body on some deposits, magmas have a distinct geochemistry. Because of this, adjacent deposits, such as Kakanui River Section Tuff 1, and the Upriver Lapilli Tuffs were linked to different source cones. However, deposits which were far apart sometimes had very similar geochemistries, and could be confused for the same eruption. Therefore, while geochemical fingerprinting is a useful technique, it may need to be used with other tools to achieve the most accurate results.

4.3 Relationship between Kakanui South Head and Kakanui River Section

The Kakanui River Section deposits occur very close to the Kakanui South Head edifice. However, these two outcrops are not in contact, and the beds of each section dip towards each other. Because of the ambiguity of this relationship, previous authors have disagreed about stratigraphy.

Early models (e.g. Park, 1904, Dickey, 1966) inferred the presence of a syncline deforming Kakanui South Head and the Kakanui River Section. They also claimed that the Kakanui River Section volcaniclastics and overlying limestones were extensions of units outcropping at Kakanui South Head. However, this investigation found that while the volcanic deposits from each area probably formed from related batches of magma, they were geochemically distinct. Furthermore, the limestones which occur at the top of each location also appear to be different units. The Kakanui South Head volcanics are immediately overlain by calcareous volcaniclastics, followed by impure packstones with high volcanic content. By contrast, the Kakanui River Section volcanics are followed by units of grey wackestone, representing slow accumulation in a deep environment, followed by an unconformity, and units of glauconitic packstone/wackestone, finally followed by bryozoan-rich packstone/grainstone. The Kakanui River Section upper limestones have very little volcanic content, and contain much larger unbroken body fossils than Kakanui South Head. Because of the different depositional histories and compositions of Kakanui South Head and Kakanui River Section limestones, these sections are interpreted as unrelatd deposits.

Corcoran and Moore (2008) claim that the Kakanui River Section dip is a combination of the 10° regional deformation, and the original slope that the sediments were deposited on. There are some reasons to believe such a slope could have existed, such as the slumping, which was

probably triggered by over-steepening; and the abundance of volcaniclastic deposits, which could indicate a cone nearby. Unfortunately, while this hypothesis offers a simple explanation, several factors argue against it.

There is evidence that the sources of the Kakanui River Section volcanics were located to the east, rather than up-dip to the west. Firstly, the cross-beds in the slumped cross-bedded volcaniclastics dip towards the west, indicating westward sediment transport. Secondly, flame structure tips in the slumped unit are bent towards the west, making it likely that the slump slid in this direction and deformed them. Both of these factors make it unlikely that the Kakanui River Section rocks were deposited on an eastward-dipping slope.

There are several geopetal indicators which suggest that the Kakanui River Section rocks were originally deposited across a reasonably flat area. Vertical burrows in the glauconitic packstone, and the thin bedded ash facies tend to be perpendicular to the bedding surface, as would be expected if that surface had been tilted. Some shells are infilled with material which seems to have settled parallel to the dip of the bed. Additionally, there are no known modern examples of shelf limestones accumulate on slopes of 10°. Even the presence of the slump doesn't require this section to be on a slope: the compressional structures indicate that this deposit is at the toe end, which may have been running out across a flat surface.

If the Kakanui River Section was originally horizontal, then this area must have experienced around 20° of tilting to the ENE. However, this creates problems at South Kakanui Head, where the dipping beds appear to be almost entirely due to the original cone shape. If a 20° correction were applied, some of the eastward slopes would become nearly horizontal, the breccia layers in the interior of the cone would have dips of almost 60°, and the westward slopes which have accumulated limestone would dip over 35°. The most likely explanation is that the gap between outcrops hides a subtle structural change, and that Kakanui South Head has been tilted by up to 10 – 15° less than the Kakanui River Section.

4.4 Volcanic edifice position

Despite the fact that Waiareka-Deborah deposits comprise of tens of cubic kilometres of volcanic material (Coombs et al., 1986), only a fraction of the edifices required to produce that material have been preserved and exposed in the present. Surtseyan edifices made of loose volcaniclastic material are often reworked shortly after they erupt (e.g. Hoffmeister, 1929, Sohn

& Chough, 1992, Okubo, 2014), unless they are protected by capping lava, as occurred at Surtsey (Thorarinson, 1967). Even preserved edifices are small enough to be easily buried by more recent sedimentation, e.g. Boring Volcanic Field (Blakey et al., 1995). Because of this, modern outcropping Waiareka-Deborah edifices tend to either be those that produced significant lava flows and so were more competent and resistant (e.g. Taipo Hill, Boatmans Harbour), or those that occur along the coast, and have been uncovered by coastal erosion (Gees Point, Kakanui Headlands, Lookout Bluff, etc.). This limited edifice preservation complicates attempts to characterise and understand the evolution of the Waiareka-Deborah volcanic field.

This investigation has inferred the location of a number of cones which are no longer preserved. These include an edifice near Falconer's Road sample, The Kakanui River Section Tuff B source, and the Upriver Lapilli Tuff edifice. The locations of these edifices were determined based on several factors:

(1) The occurrence of volcanic deposits with chemical signatures distinct from any known local cone.

(2) Positive topographic features which could represent a buried cone, or sediments accumulated from a reworked cone.

(3) Sedimentary structures such as cross-bedding and slump structures, which indicate the direction of the source.

(4) Dip of bedding, originating from cone morphology.

(5) Evidence of proximal or distal volcanic facies, such as grain size or bomb sags.

Although edifices are more likely to be exposed along the coast, the high concentration of vents at some sites still seems unusually high. Boatmans Harbour, for example, consists of six overlapping edifices, formed intermittently over two million years (Moorhouse, 2015). The deposits at Lookout Bluff represent three separate eruptions, two of which were simultaneous, and one of which occurred after a significant time gap (Maicher, 2003). With this in mind, the high number of edifices around Kakanui may not be simply due to chance or coastal erosion, but instead due to some factor controlling eruption locations.

In their study of the spatial distribution of vents in monogenetic volcanic fields, Le Corvec et al., (2013) concluded that clustering was a common phenomenon, and clusters often show the same alignment as the dominant tectonic features. This may be the case in Waitaki, where groups of edifices have a NNE-SSW orientation, which matches both the long axis of the volcanic field, and the likely alignment of normal faults formed during crustal extension. It is possible that the

high numbers of volcanoes along the Kakanui coastline occur due to zone of long-term structural weakness.

4.5 Development of the Kakanui Area through Time

The study area of Kakanui underwent a complex development throughout the mid-Cenozoic. Waiareka-Deborah volcanism began around 40 Ma (Cooper 2004; Coombs et al. 2008), and the large influx of material built up a palaeohigh offshore. Scattered deposits of this early volcanism occur around Kakanui (Fordyce 2001), but this investigation did not find enough information to determine the timing or location of any of these eruptions. Shallow marine organisms began to colonise areas of this volcanic high, leading to the development of limestone deposits (Thompson, 2013).

Taipo Hill is probably the oldest Kakanui deposit investigated in this thesis. It appears to stratigraphically underlie the Upriver Lapilli Tuffs, and has a similar geochemistry to Boatmans Harbour (38 – 36 Ma). This edifice produced some volcaniclastics, but it is most notable for the lava flows which have capped and preserved the edifice. These contain hyaloclastite, confirming that sea level was still fairly high, and volcanism was subaqueous.

The Upriver Lapilli Tuff edifice erupted sometime after Taipo Hill, as the magmatic field was becoming more mafic. The volcaniclastic sediment flows were syn-volcanic, and occurred alongside eruption of ballistic bombs, and dike formation. Because of this concurrent activity, it seems likely that the sediment flows were pyroclastically generated. Sedimentary structures indicate that deposition was in an eastward direction, and it is possible that this reflects the palaeoflow at the time.

Overlying the Upriver Lapilli Tuff deposits are the first units of the Kakanui River Section, deposited in the Runangan. The Basal Limestone and Kakanui River Section Tuff A units probably both represent nearby volcanic cones, although the higher quartz content, and better sorting and rounding of the Tuff A deposit indicates a different source. These deposits represent the typical life-cycle of a Waiareka-Deborah cone: eruption and growth, followed by colonisation, and finally, failure and reworking.

The eruption of Kakanui River Section Tuff A was followed by a prolonged period of low energy sedimentation, finally broken by the eruption of the Whaingaroan Kakanui River Section

Tuff B. The two River Section volcanic units are geochemically related, and represent the end stages of the evolution of the Waiareka-Deborah volcanic field. These deposits show enrichment in LREES, compatible, and fluid immobile elements, and possibly reflect the influence of a new magma.

Volcaniclastic accumulation and sea level fall dictated the last deposits of the Kakanui River Section. Shallow water bioclasts were able to accumulate locally; possibly on the remains of the Kakanui River Section Tuff B edifice. This resulted in thick beds of limestone, which probably kept depositing until at least 34.13 Ma (Nelson et al., 2004)

The Kakanui South Head edifice overlies the Kakanui River Section. This deposit is characterised by outer beds of reasonably typical volcaniclastics, followed by the eruption of the Kakanui Mineral Breccia. Sea level was still fairly low, and marine organisms were able to colonise this edifice, resulting in the deposition of bioclast-rich volcanics, and volcanic-rich limestones on the flanks of the volcano. Further sea level fall subaerially exposed these limestones, resulting in the development of a karst surface. The overall evolution of mid-Cenozoic Kakanui is illustrated in Figure 4.4.

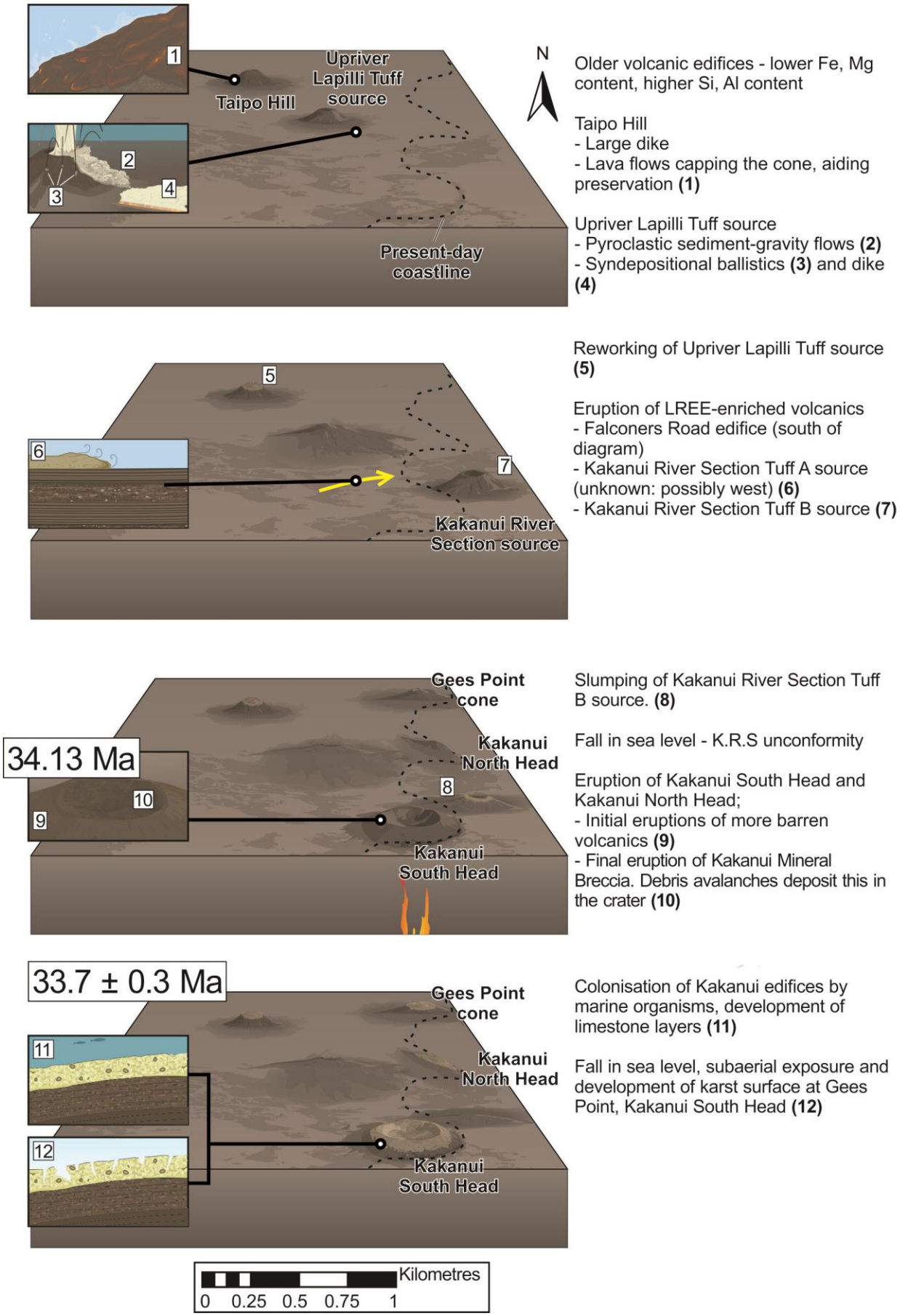

Figure 4.4: Volcanic development of the Waiareka-Deborah volcanics around Kakanui.

4.6 Conclusion

The area around Kakanui contains a number of different facies, representing a range of palaeoenvironmental conditions. These facies were influenced by multiple interrelated factors, including:

- The introduction or depletion of different sediment sources, such as new volcanic edifices, and new areas colonised by marine organisms.
- Different sediment transport mechanisms, such as turbidity currents, suspension sedimentation, slumping.
- Sea level changes, which influence accumulation and erosion rates, but also control where marine organisms can colonise, and where authogenic minerals such as glauconite can form.

This investigation used a multidisciplinary approach to characterise this complex depositional environment. The combination of sedimentary, palaeontological, and geochemical investigations helped to build a more complete picture than could have been achieved using only one of those techniques.

4.7 Recommendations

This thesis touched on a number of subjects which could be expanded on by future work. Palaeontological investigation of the Kakanui River Section could yield more information if a greater number of foraminifera were sampled, and these were identified to the species level. This would be especially useful if it could be combined with foraminiferal abundance investigations of other Waitaki limestones, in order to draw more connections between sources and deposits.

We recommend more volcanic sampling and XRF analysis, to confirm the geochemical trends and possible groups we propose here. This could be combined with relative or absolute dating, in order to gain insight into the evolution of the volcanic field over time. Microprobe analysis of minerals from older deposits than the Upriver Lapilli Tuffs could help to determine the nature, magnitude, and cause of the changing Fe/Mg K_d for chrome diopside/olivine.

The multidisciplinary approach of this investigation was able to obtain complementary information, which helped to build a deeper understanding of the depositional environment around Kakanui. A similar approach could be helpful for investigating palaeoenvironment at other carbonate and volcanic locations around Waitaki.

References

Abreu, V. S., & Anderson, J. B. (1998). Glacial eustasy during the Cenozoic: sequence stratigraphic implications. *AAPG bulletin*, *82*(7), 1385-1400.

Ayress, M. A. (1993). Ostracod biostratigraphy and palaeoecology of the Kokoamu Greensand and Otekaike Limestone (Late Oligocene to Early Miocene), North Otago and South Canterbury, New Zealand. *Alcheringa*, *17*(2), 125-151.

Basu, A. R., & Murthy, V. R. (1977). Kaersutites, suboceanic low-velocity zone, and the origin of mid-oceanic ridge basalts. *Geology*, *5*(6), 365-368.

Batt, G. E. (1993). Aspects of an Early Miocene Unconformity in North Otago and South Canterbury. University of Otago.

Benson, W. N. (1942). The basic igneous rocks of eastern Otago and their tectonic environment. Roy. Soc. New Zealand, Trans, 72, 160-85.

Blakely, R. J., Wells, R. E., Yelin, T. S., Madin, I. P., & Beeson, M. H. (1995). Tectonic setting of the Portland-Vancouver area, Oregon and Washington: Constraints from low-altitude aeromagnetic data. *Geological Society of America Bulletin*, *107*(9), 1051-1062.

Bosellini, A. (1984). Progradation geometries of carbonate platforms: examples from the Triassic of the Dolomites, northern Italy. *Sedimentology*, 31(1), 1-24.

Brenna, M., Cronin, S. J., Smith, I. E., Sohn, Y. K., & Németh, K. (2010). Mechanisms driving polymagmatic activity at a monogenetic volcano, Udo, Jeju Island, South Korea. *Contributions to Mineralogy and Petrology*, *160*(6), 931-950.

Budd, D. A. (1992). Dissolution of high-Mg calcite fossils and the formation of biomolds during mineralogical stabilization. *Carbonates and Evaporites*, 7(1), 74-81.

Burchette, T. P., & Wright, V. P. (1992). Carbonate ramp depositional systems. *Sedimentary Geology*, 79(1-4), 3-57.

Cas, R. A. F., Landis, C. A., & Fordyce, R. E. (1989). A monogenetic, Surtla-type, Surtseyan volcano from the Eocene-Oligocene Waiareka-Deborah volcanics, Otago, New Zealand: a model. *Bulletin of Volcanology*, *51*(4), 281-298.

Clark, J. R., Appleman, D. E., & Papike, J. J. (1969). Crystal-chemical characterization of clinopyroxenes based on eight new structure refinements. *Mineralogical Society of America Special Paper*, 2, 31-50.

Clowes, C. D. (2009). Dinoflagellate taxonomy and biostratigraphy of the Mid-to Late Eocene and Early Oligocene of New Zealand.

Clowes, C. D., & Morgans, H. E. (1984). Micropaleontology of the Runangan-Whaingaroan (Eocene-Oligocene) Totara Limestone, Kakanui River, New Zealand. *New Zealand Geological Survey record*, *3*(3), 0-40.

Colson, R. O. (1998). Unexpected results of some simple exercises in equilibrium melting based on experimentally determined partition coefficients. *International geology review*, *40*(10), 936-943.

Coombs, D. S., Cas, R. A., Kawachi, Y., Landis, C. A., McDonough, W. F., & Reay, A. (1986). Cenozoic volcanism in north, east and central Otago. *Royal Society of New Zealand Bulletin*, 23, 278-312.

Cooper, R. A., & Agterberg, F. P. (2004). *The New Zealand geological timescale* (Vol. 22). Institute of Geological & Nuclear Sciences Limited.

Corcoran, P. L., & Moore, L. N. (2008). Subaqueous eruption and shallow-water reworking of a small-volume Surtseyan edifice at Kakanui, New Zealand. *Canadian Journal of Earth Sciences*, *45*(12), 1469-1485.

Corliss, B. H. (1985). Microhabitats of benthic foraminifera within deep-sea sediments.

Cox, S. C., & Sutherland, R. (2007). Regional geological framework of South Island, New Zealand, and its significance for understanding the active plate boundary. *A Continental Plate Boundary: Tectonics at South Island, New Zealand*, 19-46.

Dasch, E. J., Evans, A. L., & Essene, E. (1970). Radiometric and petrologic data from eclogites and megacrysts of the Kakanui Mineral Breccia, New Zealand. In *Geological Society of America Abstracts with Programme* (Vol. 7, pp. 532-533).

Davy, B., & Wood, R. (1994). Gravity and magnetic modelling of the Hikurangi Plateau. *Marine geology*, *118*(1-2), 139-151.

Davy, B., Hoernle, K., & Werner, R. (2008). Hikurangi Plateau: Crustal structure, rifted formation, and Gondwana subduction history. *Geochemistry, Geophysics, Geosystems*, *9*(7).

Dawson, J. B., & Smith, J. V. (1982). Upper-mantle amphiboles: a review. *Mineralogical Magazine*, *45*(337), 35-46.

Dickey, J. S. (1966). *A study of the mineral breccia member of the Deborah Volcanic Formation at Kakanui, New Zealand*. University of Otago.

Dickey, J. S. (1968a). Eclogitic and other inclusions in mineral breccia member of Deborah Volcanic Formation at Kakanui New Zealand. *American mineralogist*, *53*(7-8), 1304.

Dickey Jr, J. S. (1968b). Observations on the Deborah Volcanic Formation near Kakanui, New Zealand. *New Zealand Journal of Geology and Geophysics*, *11*(5), 1159-1162.

Díez, M., Connor, C. B., Kruse, S. E., Connor, L., & Savov, I. P. (2009). Evidence of small-volume igneous diapirism in the shallow crust of the Colorado Plateau, San Rafael Desert, Utah. *Lithosphere*, *1*(6), 328-336.

Edwards, A.R. (1991). The Oamaru Diatomite. *New Zealand Geological Survey Paleontological Bulletin* 64: 1-260.

Exon, N. F., Kennett, J. P., & Malone, M. J. (2004). Leg 189 synthesis: Cretaceous–Holocene history of the Tasmanian gateway. In *Proceedings of the ocean drilling program, scientific results* (Vol. 189, No. 1, pp. 1-37).

Finlay, H. J. (1939a). New Zealand foraminifera: key species in stratigraphy. No. 1. In *Transactions of the Royal Society of New Zealand* (Vol. 68, pp. 504-543).

Finlay, H. J. (1939b). New Zealand foraminifera: key species in stratigraphy, No. 2. In *Transactions of the Royal Society of New Zealand* (Vol. 69, No. 1, pp. 89-128).

Finlay, H. J. (1939c). New Zealand foraminifera: key species in stratigraphy, No. 3. In *Transactions of the Royal Society of New Zealand* (Vol. 69, No. 3, pp. 309-329).

Finlay, H. J. (1940). New Zealand foraminifera: key species in stratigraphy, No. 4. In *Transactions of the Royal Society of New Zealand* (Vol. 69, No. 4, pp. 448-472).

Fisher, R. V., & Schmincke, H. U. (1984). Pyroclastic rocks, 472 pp. *Springer, Berlin, doi*, *10*, 978-3.

Fisher, R. V., & Waters, A. C. (1970). Base surge bed forms in maar volcanoes. *American Journal of Science*, *268*(2), 157-180.

Forsyth, P. J. (2001). *Geology of the Waitaki Area: Scale 1: 250 000*. Institute of Geological & Nuclear Sciences.

Gage, M. (1957). *The geology of Waitaki subdivision* (No. 55). New Zealand Department of Scientific and Industrial Research.

Gair, H. S. (1967). Sheet 20 Mt Cook Geological Map of New Zealand 1: 250,000. Department of Scientific and Industrial Research, Wellington, New Zealand.

Goldstein, S. T. (1999). Foraminifera: a biological overview. In *Modern foraminifera* (pp. 37-55). Springer Netherlands.

Garden, B. P. (2001). *The Kakanui Mineral Breccia: Experimental and Mineral Geochemistry*. University of Otago.

Hargraves, R. B. (2014). *Physics of magmatic processes*. Princeton University Press.

Hassold, N. J., Rea, D. K., van der Pluijm, B. A., & Parés, J. M. (2009). A physical record of the Antarctic Circumpolar Current: Late Miocene to recent slowing of abyssal circulation. *Palaeogeography, Palaeoclimatology, Palaeoecology*, *275*(1), 28-36.

Haynes, J. R. (1981). *Foraminifera.* John Wiley & Sons, Ltd.

Hayward, B. W. (2010). *Recent New Zealand deep-water benthic foraminifera: Taxonomy, ecologic distribution, biogeography and use in paleoenvironmental assessment*. GNS Science.

Hayward, B. W., & Triggs, C. M. (2016). Using Multi-Foraminiferal-Proxies to Resolve the Paleogeographic History of a Lower Miocene, Subduction-Related, Sedimentary Basin (Waitemata Basin, New Zealand). *The Journal of Foraminiferal Research*, *46*(3), 285-313.

Hector, J. (1865). On the Geology of Otago, New Zealand. *Quarterly Journal of the Geological Society*, *21*(1-2), 123-128.

Hector, J. (1884). Progress report, 1883. *Reports of geological explorations*, *16:*ix-xxxviii

Hicks, S. B. (2014). *Paleoecology and sedimentology of the volcanically active Late Eocene continental shelf, Northeast Otago, New Zealand*(Doctoral dissertation, University of Otago).

Hoernle, K., White, J. V., van den Bogaard, P., Hauff, F., Coombs, D. S., Werner, R., ... & Cooper, A. F. (2006). Cenozoic intraplate volcanism on New Zealand: Upwelling induced by lithospheric removal. *Earth and Planetary Science Letters*, *248*(1), 350-367.

Hoffmeister, J. E., Ladd, H. S., & Alling, H. L. (1929). Falcon Island. *American Journal of Science*, (108), 461-471.

Hornibrook, N. D. B. (1961). *Tertiary Foraminifera from Oamaru District (NZ)* (Vol. 34). RE Owen, Govt. printer.

Hornibrook, N. D. B. (1971). *A revision of the Oligocene and Miocene Foraminifera from New Zealand described by Karrer and Stache in the reports of the Novara Expedition (1864)* (Vol. 43). Dept. of Scientific and Industrial Research.

Hutton, F. W. (1886). On the geology of the country between Oamaru and Moeraki. In *Transactions of the New Zealand Institute* (Vol. 19, pp. 415-480).

Irving, A. J., & Frey, F. A. (1984). Trace element abundances in megacrysts and their host basalts: constraints on partition coefficients and megacryst genesis. *Geochimica et Cosmochimica Acta*, *48*(6), 1201-1221.

Jakobsson, S. P. (1968). The geology and petrography of the Vestmann Islands: A preliminary report. *Surtsey Res. Prog. Rep*, *4*, 113-129.

Keating, G. N., Valentine, G. A., Krier, D. J., & Perry, F. V. (2008). Shallow plumbing systems for small-volume basaltic volcanoes. *Bulletin of Volcanology*, *70*(5), 563-582.

Kennett, J. P., & Vonderborch, C. C. (1986). Southwest Pacific Cenozoic paleoceanography. *Initial Reports of the Deep Sea Drilling Project*, *90*, 1493-1517.

King, P. R. (2000, March). New Zealand's changing configuration in the last 100 million years: plate tectonics, basin development, and depositional setting. In *2000 New Zealand Petroleum Conference Proceedings* (Vol. 15). Crown Minerals, Ministry of Commerce Wellington, New Zealand.

Klügel, A., Hoernle, K. A., Schmincke, H. U., & White, J. D. (2000). The chemically zoned 1949 eruption on La Palma (Canary Islands): Petrologic evolution and magma supply dynamics of a rift zone eruption. *Journal of Geophysical Research: Solid Earth*, *105*(B3), 5997-6016.

Kokelaar, B. P. (1983). The mechanism of Surtseyan volcanism. *Journal of the Geological Society*, 140(6), 939-944.

Laird, M. G., & Bradshaw, J. D. (2004). The break-up of a long-term relationship: the Cretaceous separation of New Zealand from Gondwana. *Gondwana Research*, *7*(1), 273-286.

Landis, C. A., Campbell, H. J., Begg, J. G., Mildenhall, D. C., Paterson, A. M., & Trewick, S. A. (2008). The Waipounamu Erosion Surface: questioning the antiquity of the New Zealand land surface and terrestrial fauna and flora. *Geological Magazine*, *145*(02), 173-197.

Lawver, L. A., & Gahagan, L. M. (2003). Evolution of Cenozoic seaways in the circum-Antarctic region. *Palaeogeography, Palaeoclimatology, Palaeoecology*, *198*(1), 11-37.

Lawver, L. A., Gahagan, L. M., & Coffin, M. F. (1992). The development of paleoseaways around Antarctica. *The Antarctic Paleoenvironment: A Perspective on Global Change: Part One*, 7-30.

Le Corvec, N., Spörli, K. B., Rowland, J., & Lindsay, J. (2013). Spatial distribution and alignments of volcanic centers: clues to the formation of monogenetic volcanic fields. *Earth-Science Reviews*, *124*, 96-114.

Lewis, K. B. (1971). Slumping on a continental slope inclined at 1–4. *Sedimentology*, *16*(1-2), 97-110.

Lever, H. (2007). Review of unconformities in the late Eocene to early Miocene successions of the South Island, New Zealand: ages, correlations, and causes. *New Zealand Journal of Geology and Geophysics*, *50*(3), 245-261.

Lyle, M., Gibbs, S., Moore, T. C., & Rea, D. K. (2007). Late Oligocene initiation of the Antarctic circumpolar current: evidence from the South Pacific. *Geology*, *35*(8), 691-694.

Maicher, D. (2000). Architecture and development of a shallow marine tuff cone at Lookout Bluff, New Zealand. In *International Maar Conference* (pp. 309-317).

Maicher, D. (2003). A cluster of Surtseyan volcanoes at Lookout Bluff, North Otago, New Zealand: Aspects of edifice spacing and time. *Explosive Subaqueous Volcanism*, 167-178.

Mantell, G. A. (1850). Notice of the Remains of the Dinornis and other Birds, and of Fossils and Rock-specimens, recently collected by Mr. Walter Mantell in the Middle Island of New Zealand; with Additional Notes on the Northern Island With Note on Fossiliferous Deposits in the Middle Island of New Zealand. By Prof. E. Forbes, FRS &c. *Quarterly Journal of the Geological Society*, *6*(1-2), 319-342.

Mason, B., & Allen, R. O. (1973). Minor and Trace Elements in Augite, Hornblende, and Pyrope Megacrysts from Kakanui, New Zeland. *New Zealand Journal of Geology and Geophysics*, *16*(4), 935-947.

Mason, B. (1968). Eclogitic xenoliths from volcanic breccia at Kakanui, New Zealand. *Contributions to Mineralogy and Petrology*, *19*(4), 316-327.

McBirney, A. R. (1963). Factors governing the nature of submarine volcanism. *Bulletin of Volcanology*, *26*(1), 455-469.

McCallister, R. H., Finger, L. W., & Ohashi, Y. (1976). Intracrystalline Fe (super 2+)-Mg equilibria in three natural Ca-rich clinopyroxenes. *American Mineralogist*, *61*(7-8), 671-676.

McGee, L. E., & Smith, I. E. (2016). Interpreting chemical compositions of small scale basaltic systems: A review. *Journal of Volcanology and Geothermal Research*, *325*, 45-60.

McKay, A. (1876). Oamaru and Waitaki districts. *NZ Geological Survey report of geological explorations*, *77*(10), 41-66.

McMillan, S. G. (1999). *Geology of Northeast Otago: Hampden (J42) and Palmerston (J43)*. Institute of Geological & Nuclear Sciences.

McRae, S. G. (1972). Glauconite. *Earth-Science Reviews*, *8*(4), 397-440.

Mellis, R. A. (2016). The Kakanui hydrothermal system.

Molloy, C., Shane, P., & Augustinus, P. (2009). Eruption recurrence rates in a basaltic volcanic field based on tephra layers in maar sediments: implications for hazards in the Auckland volcanic field. *Geological Society of America Bulletin*, 121(11-12), 1666-1677.

Moorhouse, B. L. (2015). *The emplacement of overlapping submarine deposits of monogenetic Surtseyan-style volcanoes onto a submerged continental shelf that built-up over millions of years in the Waiareka-Deborah Volcanic Field, New Zealand* (Doctoral dissertation, University of Otago).

Mortimer, N., Hoernle, K., Hauff, F., Palin, J. M., Dunlap, W. J., Werner, R., & Faure, K. (2006). New constraints on the age and evolution of the Wishbone Ridge, southwest Pacific Cretaceous microplates, and Zealandia–West Antarctica breakup. *Geology*, *34*(3), 185-188.

Murray, J. W. (2006). *Ecology and applications of benthic foraminifera*. Cambridge University Press.

Mutch, A. R. (1963). Sheet 23 Oamaru. Geological map of New Zealand 1: 250 000. Department of Scientific and Industrial Research, Wellington.

Myrow, P. M. (1995). Thalassinoides and the enigma of Early Paleozoic open-framework burrow systems. *Palaios*, 58-74.

Nelson, C. S., Lee, D., Maxwell, P., Maas, R., Kamp, P. J., & Cooke, S. (2004). Strontium isotope dating of the New Zealand Oligocene. *New Zealand Journal of Geology and Geophysics*, *47*(4), 719-730.

Németh, K. (2010). Monogenetic volcanic fields: origin, sedimentary record, and relationship with polygenetic volcanism. *Geological Society of America Special Papers*, *470*, 43-66.

Németh, K., Stewart, R. B., & Pécskay, Z. (2013, April). Episodically rejuvenating Cenozoic subaqueous mafic monogenetic volcanism in the Chatham Island (SW-Pacific). In *Basalt 2013 Cenozoic Magmatism in Central Europe Conference*.

Németh, K., White, J. D., Reay, A., & Martin, U. (2003). Compositional variation during monogenetic volcano growth and its implications for magma supply to continental volcanic fields. *Journal of the Geological Society*, *160*(4), 523-530.

Norris, R. J., Carter, R. M., & Turnbull, I. M. (1978). Cainozoic sedimentation in basins adjacent to a major continental transform boundary in southern New Zealand. *Journal of the Geological Society*, *135*(2), 191-205.

Odin, G. S., & Matter, A. (1981). Origin of glauconites. *Sedimentology*, *28*(5), 611-641.

Odin, G. S., & Fullagar, P. D. (1988). Geological significance of the glaucony facies. In: Green Marine Clays (GS Odin, editor). *Developments in Sedimentology*, *45*, 295-332.

Okubo, C. H. (2014). Brittle deformation and slope failure at the North Menan butte tuff cone, eastern Snake River plain, Idaho. *Journal of Volcanology and Geothermal Research*, *278*, 86-95.

Park, J. (1905). On the marine Tertiaries of Otago and Canterbury, with special reference to the relations existing between the Pareora and Oamaru Series. In *Trans. NZ Inst* (Vol. 37, pp. 489-551).

Park, J. (1918). *The geology of the Oamaru district, North Otago (eastern Otago division)* (No. 20). Government Printer.

Pearson, D. G., Canil, D., & Shirey, S. B. (2003). Mantle samples included in volcanic rocks: xenoliths and diamonds. *Treatise on geochemistry*, *2*, 568.

Pekar, S. F., & Christie-Blick, N. (2008). Resolving apparent conflicts between oceanographic and Antarctic climate records and evidence for a decrease in pCO_2 during the Oligocene through early Miocene (34–16 Ma). *Palaeogeography, Palaeoclimatology, Palaeoecology*, *260*(1), 41-49.

Pekar, S. F., Christie-Blick, N., Kominz, M. A., & Miller, K. G. (2002). Calibration between eustatic estimates from backstripping and oxygen isotopic records for the Oligocene. *Geology*, *30*(10), 903-906.

Perkins, D., & Vielzeuf, D. (1992). Experimental investigation of Fe-Mg distribution between olivine and clinopyroxene: Implications for mixing properties of Fe-Mg in clinopyroxene and garnet-clinopyroxene thermometry Dnxrnn PnnrrNs. *American Mineralogist*, *77*, 774-783.

Pfuhl, H. A., & McCave, I. N. (2005). Evidence for late Oligocene establishment of the Antarctic Circumpolar Current. *Earth and Planetary Science Letters*, *235*(3), 715-728.

Reay, A., Chappell, D., & Garden, B. (2002). A new garnet-bearing mineral breccia from North Otago, New Zealand. *New Zealand Journal of Geology and Geophysics*, *45*(4), 461-466.

Reay, A., Johnstone, R. D., & Kawachi, Y. (1993). Anorthoclase, a second microprobe standard from Kakanui, New Zealand. *Geostandards Newsletter*, 17(1), 135-136.

Sadler, P. M. (1999, June). The influence of hiatuses on sediment accumulation rates. In *GeoResearch Forum* (Vol. 5, No. 1).

Shane, P., Gehrels, M., Zawalna-Geer, A., Augustinus, P., Lindsay, J., & Chaillou, I. (2013). Longevity of a small shield volcano revealed by crypto-tephra studies (Rangitoto volcano, New Zealand): change in eruptive behavior of a basaltic field. *Journal of Volcanology and Geothermal Research*, *257*, 174-183.

Smith, A. M., & Nelson, C. S. (2003). Effects of early sea-floor processes on the taphonomy of temperate shelf skeletal carbonate deposits. *Earth-Science Reviews*, 63(1), 1-31.

Sohn, Y. K., & Chough, S. K. (1992). The Ilchulbong tuff cone, Cheju Island, South Korea. *Sedimentology*, *39*(4), 523-544.

Stickley, C. E., Brinkhuis, H., Schellenberg, S. A., Sluijs, A., Röhl, U., Fuller, M., ... & Williams, G. L. (2004). Timing and nature of the deepening of the Tasmanian Gateway. *Paleoceanography*, *19*(4).

Storey, B. C. (1995). The role of mantle plumes in continental breakup: case histories from Gondwanaland. *Nature*, *377*(6547), 301-308.

Storey, B. C., Leat, P. T., Weaver, S. D., Pankhurst, R. J., Bradshaw, J. D., & Kelley, S. (1999). Mantle plumes and Antarctica-New Zealand rifting: evidence from mid-Cretaceous mafic dykes. *Journal of the Geological Society*, *156*(4), 659-671.

Thompson, N. K. (2013). Cool-water Carbonate Sedimentology and Sequence Stratigraphy of the Waitaki Region, South Island, New Zealand.

Thompson, N. K., Bassett, K. N., & Reid, C. M. (2014). The effect of volcanism on cool-water carbonate facies during maximum inundation of Zealandia in the Waitaki–Oamaru region. *New Zealand Journal of Geology and Geophysics*, *57*(2), 149-169.

Thomson, J. A. (1906). The gem gravels of Kakanui, with remarks on the geology of the district. In *Transactions of the New Zealand Institute* (Vol. 38, pp. 81-494).

Thorarinsson, S. (1967). *Surtsey: the new island in the North Atlantic*. Viking Press.

Timm, C., Hoernle, K., Werner, R., Hauff, F., van den Bogaard, P., White, J., ... & Garbe-Schönberg, D. (2010). Temporal and geochemical evolution of the Cenozoic intraplate volcanism of Zealandia. *Earth-Science Reviews*, *98*(1), 38-64.

Toggweiler, J. R., & Key, R. M. (2003). Thermohaline circulation. *Encyclopedia of Ocean Sciences*.

Udgata, D. (2007). *Glauconite as an indicator of sequence stratigraphic packages in a lower Paleocene passive-margin shelf succession, Central Alabama* (Doctoral dissertation).

Uttley, G. H. (1916). The Geology of the Neighbourhood of Kakanui. In *Trans. NZ Inst* (Vol. 48, pp. 19-27).

Uttley, G. H. (1918). The volcanic rocks of Oamaru, whith special reference to their position in the stratigraphial series. *NZ Inst Trans Proc*, *50*, 106-117.

Valentine, G. A., & Hirano, N. (2010). Mechanisms of low-flux intraplate volcanic fields—Basin and Range (North America) and northwest Pacific Ocean. *Geology*, *38*(1), 55-58.

von Seckendorff, V., & O'Neill, H. S. C. (1993). An experimental study of Fe-Mg partitioning between olivine and orthopyroxene at 1173, 1273 and 1423 K and 1.6 GPa. *Contributions to Mineralogy and Petrology*, *113*(2), 196-207.

Waight, T. E., Weaver, S. D., Maas, R., & Eby, G. N. (1998a). French Creek Granite and Hohonu Dyke Swarm, South Island, New Zealand: Late Cretaceous alkaline magmatism and the opening of the Tasman Sea*. *Australian Journal of Earth Sciences*, *45*(6), 823-835.

Waight, T. E., Weaver, S. D., & Muir, R. J. (1998b). Mid-Cretaceous granitic magmatism during the transition from subduction to extension in southern New Zealand: a chemical and tectonic synthesis. *Lithos*, *45*(1), 469-482.

Walker, G. P. (1973). Explosive volcanic eruptions—a new classification scheme. *Geologische Rundschau*, 62(2), 431-446.

Weaver, S. D., Storey, B. C., Pankhurst, R. J., Mukasa, S. B., DiVenere, V. J., & Bradshaw, J. D. (1994). Antarctica-New Zealand rifting and Marie Byrd Land lithospheric magmatism linked to ridge subduction and mantle plume activity. *Geology*, *22*(9), 811-814.

White, A. J. R., Chappell, B. W., & Jakeš, P. (1972). Coexisting clinopyroxene, garnet and amphibole from an “eclogite”, Kakanui, New Zealand. *Contributions to Mineralogy and Petrology*, *34*(3), 185-191.

White, J. D. (2000). Subaqueous eruption-fed density currents and their deposits. *Precambrian Research*, *101*(2), 87-109.

White, J. D., & Schmincke, H. U. (1999). Phreatomagmatic eruptive and depositional processes during the 1949 eruption on La Palma (Canary Islands). *Journal of Volcanology and Geothermal Research, 94*(1), 283-304.

Zachos, J. C., Breza, J. R., & Wise, S. W. (1992). Early Oligocene ice-sheet expansion on Antarctica: Stable isotope and sedimentological evidence from Kerguelen Plateau, southern Indian Ocean. *Geology*, *20*(6), 569-573.

Appendix

Table 5.1: Lithofacies present in the Kakanui River Section.

Lithofacies	Description	Typical components
F1: Bryozoan-rich packstone/ grainstone	Contains fine – coarse sand-sized bioclasts deposited by grain-flow processes. Dominantly branching bryozoans, shell fragments and unidentified fossils. Body fossils of pectens, brachiopods and calcareous worm-tube clusters occur in some sections.	Bryozoans (50 – 80 %) Echinoderms (1 – 5 %) Foraminifera (1 – 3 %) Pecten (0 – 3 %) Unidentified bioclasts (10 – 30 %) Volcanic clasts (1 – 20 %)
F2: Calcareous volcaniclastic sandstone	Contains a mixture of volcanic grains and fossil fragments. Fossils concentrations vary, dominating some beds (>70 %) and being rare in others (<5 %). In places, this facies is in gradational contact with F1: bryozoan-rich packstone/grainstone	Bryozoans (up to 75 %) Echinoderms (1 – 5 %) Foraminifera (1 – 3 %) Brachiopods (0 – 1 %) Pecten (0 – 3 %) Kaersutite (1 – 2 %) Olivine (<1 %) Chrome diopside (<1 %) Quartz grains (1 – 3 %) Calcareous cement (1 – 15 %)
F3: Grey wackestone	Bioturbated fine sand-silt sized carbonate rocks. Contains *Rhizocorallium*, *Planolites*, *Zoophychos*, and *Chondrites*. Small patches of orange staining occur occasionally, from altered pyrite nodules. Glauconite is present as rounded, very fine sand-sized grains and as glauconitisation of bioclasts .	Carbonate mud matrix (~ 80 %), Planktic foraminifera (1 – 3 %) Benthic foraminifera (2 – 5 %) Sponge spicules (1 – 5 %) Glauconite (1 – 6 %) Quartz grains (<1 - 2 %) Kaersutite (0 – 3 %)

	Where this facies occurs above the even-bedded lapilli tuffs (F6) it contains rare kaersutite crystals.	
F4: Thin bedded ash	This facies consists of grey beds of ash which occur as thin layers within other units.	Fine – medium ash. Other components not identified.
F5: Even-bedded volcaniclastics	This facies contains mm- to cm- thick planar beds of lapilli tuff, with occasional finer tuff layers, and coarser, fine pebble-rich layers. Beds are parallel and laterally continuous, although there is minor tapering and swelling. Some coarser beds also contain rip-up clasts of wackestone. This facies is dominated with rare and Calcite cement concentration can vary between different beds, with cement-poor layers and well cemented layers	Juvenile volcanic clasts (50 – 70 %) Accretionary lapilli (1 – 2 %), Palagonatised ash (10 - 20 %). Kaersutite (3 – 5 %) Chrome diopside (1 %) Olivine (1 %) Feldspar (<1 %), and b Biotite (<1 %). Calcite cement (1 – 15%)
F6: Glauconitic packstone/ wackestone	Contains greenish-grey massive bioturbated packstone, with sections of wackestone. It is characterised by high concentrations of glauconite at the base. Bioturbation, particularly *Ophiomorpha* traces, is pervasive, and conceals any original bedding Foraminifera are dominantly benthic.	Detrital glauconite (15 – 40%) Bryozoans (20 – 40 %) Unidentified bioclasts (20 – 60 %) Quartz grains (1 – 5 %). Brachiopods (0 – 2 %) Pecten (0 – 3 %) Echinoderms (0 – 3 %) Calcareous worm-tube clusters (0 – 2 %)

Table 5.2: Picked foraminifera samples from the Kakanui River Section and, the limestones overlying Kakanui South Head, at Kakanui River mouth.

	MB8-02	MB17-01	MB17-02	MB16-04	MB16-05	MB16-06	MB16-07	MB16-08
	Kakanui River Section						Kakanui South Head	
	Bryozoan-rich packstone/ grainstone	Grey wackestone (lower unit)	Grey wackestone (lower unit)	Grey wackestone (upper unit)	Glauconitic packstone/ wackestone	Bryozoan-rich packstone/ grainstone	Bryozoan-rich packstone/ grainstone	Hydrothermally influenced calcareous volcaniclastics
Amphistegina	0	0	0	0	0	2	22	1
Anomalinoides	5	0	5	1	0	0	0	0
Arenodosaria	0	0	0	0	1	0	0	0
Bolivina	0	1	1	2	0	1	0	0
Bolivinosis	0	0	1	0	1	0	1	0
Bulimina	0	0	0	0	0	1	0	0
Cassidulina	0	0	0	0	0	60	5	0
Cibicides	36	11	38	20	10	20	9	17
Fissurina	0	2	0	0	0	0	0	0
Globigerina	7	17	14	10	7	10	12	5
Globocassidulina	7	20	10	21	14	0	0	14
Globorotalia	0	0	1	0	0	0	0	0
Guttulina	0	3	0	0	1	0	0	0
Gyroidinoides	0	2	2	0	2	2	6	1
Hanzawaia	0	2	0	0	1	1	0	0
Lagena	0	2	0	1	1	1	0	0
Lenticulina	0	0	0	0	0	2	0	0
Melonis	1	1	1	1	0	9	8	0
Nodosaria	0	1	1	2	0	0	0	0

Notorotalia	1	0	0	0	5	0	0	0
Nuttallides	0	0	0	0	0	0	2	0
Oridorsalis	0	0	1	0	2	0	0	0
Planulina	0	4	0	1	1	0	0	0
Pullenia	0	2	0	0	0	0	0	0
Rectuvigerina	0	0	0	0	0	2	0	0
Stilostomella	0	3	1	0	2	2	0	1
Trifarina	0	0	0	0	0	0	0	1
Unidentified benthic	3	10	42	18	25	15	31	10
Unidentified planktic	2	0	0	3	0	0	0	2
Total	62	81	120	80	73	128	98	52

Table 5.3: Trace element concentrations in volcanic samples from around Kakanui, and the larger Waitaki area, determined by x-ray fluorescence (XRF). Boat = Boatmans Harbour; Falc = Falconer's Road; Taipo = Taipo Hill; K.S.H = Kakanui South Head; K.N.H = Kakanui North Head

	Sample	V (ppm)	Cr (ppm)	Ni (ppm)	Zn (ppm)	Zr (ppm)	Nb (ppm)	Ba (ppm)	La (ppm)	Ce (ppm)	Nd (ppm)	Ga (ppm)	Pb (ppm)	Rb (ppm)	Sr (ppm)	Th (ppm)	Y (ppm)
Boat	36541	111	224	330	117	156	27	110	12	37	33	26	1	4	511	4	30
Boat	36542	109	166	125	117	148	30	60	5	26	32	20	3	18	518	2	22
Falc.	36543	161	380	400	144	256	86	592	50	115	66	20	1	50	1385	9	26
Taipo	36545	140	178	119	113	175	33	236	14	55	27	22	5	23	501	6	21
K.S.H	36546	135	125	198	183	442	156	335	91	188	91	26	1	51	1221	16	32
K.S.H	36624	159	141	152	191	433	155	447	57	197	87	26	1	48	1438	19	34
K.S.H	36625	170	111	137	170	292	138	266	59	198	79	19	2	35	1675	17	35
K.M.B	36626	140	123	141	171	428	152	565	50	167	65	22	4	37	1489	19	33
K.N.H		157	379	208	170	194	63	234	13	86	50	17	<1	15	744	10	49
Aorere	36548	106	208	30	106	211	47	176	15	49	28	23	3	24	716	8	22
Buz.	36549	95	175	238	102	116	18	213	5	22	18	20	3	12	375	4	17
Buz.	36550	179	38	12	103	196	29	159	5	37	20	23	4	20	322	6	27
Gees		161	268	296	161	255	85	445	14	116	56	23	<1	15	1181	10	25
U.L.T	36551	127	216	153	171	131	20	136	60	113	61	24	4	12	474	4	92
U.L.T	36627	162	314	453	71	131	19	83	5	33	16	26	2	3	496	6	25
U.L.T	36628	149	275	207	145	248	67	393	5	66	33	24	1	11	913	8	24
U.L.T	36552	262	260	92	88	154	28	213	11	41	33	23	2	12	506	6	20
U.L.T	36621	202	302	207	214	164	39	120	5	67	26	26	2	21	369	9	30
K.R.S B	36622	189	234	330	167	331	123	234	38	160	63	17	6	12	491	15	32
K.R.S B	36623	224	174	147	260	278	124	197	60	194	80	20	4	7	435	15	36
K.R.S A		163	171	323	166	355	123	723	30	145	51	25	2	50	1243	13	28

	Sample	SiO_2 (%)	TiO_2 (%)	Al_2O_3 (%)	Fe_2O_3 (%)	MnO (%)	MgO (%)	CaO (%)	Na_2O (%)	K_2O (%)	P_2O_5 (%)	LOI (%)	Total (%)
Boat	36541A	50.68	2.04	17.31	6.38	0.09	5.41	8.99	4.67	0.98	0.89	2.02	99.46
Boat	36542A	47.22	2.24	18.86	11	0.1	2.71	6.81	4.73	1.56	0.49	3.58	99.31
Falc.	36543A	43.03	2.26	12.86	10.87	0.17	4.76	12.73	2.6	2.6	1.13	6.28	99.28
Taipo	36545A	53.07	1.67	15.11	10.15	0.13	5.68	7.89	4.1	0.98	0.3	0.87	99.95
K.S.H	36546A	41.5	1.64	12.21	12.34	0.16	7.86	10.71	4.14	2.24	1.49	5.04	99.32
K.S.H	36624A	42.14	1.73	12.86	12.45	0.24	8.48	9.98	3.76	2.01	1.55	4.74	99.94
K.S.H	36625A	35.9	2.45	10.76	14.35	0.25	9.19	14.25	2.97	1.23	1.8	6.75	99.9
K.M.B	36626A	39.24	1.62	12.55	12.14	0.19	8.14	12.45	4.59	1.57	1.49	5.95	99.92
K.N.H	36632A	45.62	2.27	12.24	10.1	0.11	8.22	10.02	2.76	1.14	1.39	6.09	99.94
Aorere	36548A	52.05	2.2	19.73	6.71	0.03	1.21	7.94	5.44	1.47	1.29	1.42	99.49
Buz.	36549A	51.34	1.37	14.39	10.62	0.12	9.2	7.39	3.02	0.51	0.19	1.77	99.92
Buz.	36550A	54.94	2.14	13.54	11.88	0.08	5.62	5.65	3.52	0.87	0.32	1.34	99.91
Gees	36631A	40.38	2.03	12.69	12.88	0.17	7.7	12.17	3.06	1.06	1.33	6.45	99.92
U.L.T	36551A	47.27	1.43	13.65	7.76	0.04	8.01	9.35	2.61	1.25	2.91	5.37	99.63
U.L.T	36552A	47.68	1.71	15.22	7.69	0.1	4.87	10.59	3.43	1.59	0.56	6.47	99.92
U.L.T	36627A	47.77	1.76	18.35	4.17	0.09	3.28	13.45	3.98	0.52	0.49	5.65	99.51
U.L.T	36628A	49.71	2.15	14.96	10.2	0.16	4.98	9.99	4.04	0.98	0.66	1.79	99.61
U.L.T	36621A	42.94	1.81	13.26	11.31	0.11	8.3	9.48	1.7	1.28	1.07	8.71	99.97
K.R.S	36622A	36.84	2.54	10.47	13.13	0.19	10.74	13.58	1.67	0.64	1.83	8.33	99.97
K.R.S	36623A	39.41	3.05	11.7	13.91	0.13	11.15	8.63	2.31	0.69	1.9	7.01	99.89
K.R.S Base	36633A	43.66	2.39	13.22	11.98	0.18	7.82	9.85	2.15	2.3	1.24	5.16	99.97

Table 5.4: Chrome Diopside microprobe analysis

Kakanui River Section samples = K.R.S 1, K.R.S 3, K.R.S 4; Campbells bay = Camp; Upriver Lapilli Tuffs = U.L.T; Kakanui South Head = K.S.H; Kakanui North Head = K.N.H; Kakanui Western Slope = K.W.S; STANDARD = Microprobe standards

Location	Sample	CaO	TiO2	Na2O	MgO	SiO2	Al2O3	NiO	Cr2O3	FeO	MnO	Total
STANDARD	Px1-01	24.074	0.09	0.058	17.018	54.24	0.413	0.036	0.249	2.935	0.067	99.18
STANDARD	Px2-02	24.684	0.093	0.081	17.047	53.807	0.462	0.005	0.15	2.917	0.074	99.32
STANDARD	Hypersthene-01	1.16	0.04	0	26.491	54.142	0.686	0	0.618	15.694	0.443	99.274
STANDARD	Hypersthene-02	1.19	0.029	0	26.787	53.782	0.676	0.009	0.57	15.877	0.464	99.384
STANDARD	Springwater-01	0.01	0	0	43.83	39.203	0	0.018	0	17.028	0.296	100.385
STANDARD	Springwater-02	0	0	0.025	43.661	39.264	0	0	0.068	17.108	0.338	100.464
K.R.S. 1	Riv-1_A1	20.513	0.255	0.483	14.645	51.749	8.321	0.013	0.795	1.878	0.051	98.703
K.R.S. 1	Riv-1_A2	20.013	0.269	0.519	14.548	51.703	8.766	0.013	0.809	2.55	0.089	99.279
K.R.S. 1	Riv-1_A3	20.39	0.26	0.504	14.338	51.698	8.795	0.072	0.746	2.626	0.092	99.521
K.R.S. 1	Riv-1_B1	20.094	0.186	0.455	14.764	52.053	8.587	0.07	0.798	1.881	0.065	98.953
K.R.S. 1	Riv-1_B2	19.824	0.199	0.448	14.944	52.084	8.432	0.075	0.823	2.507	0.102	99.438
K.R.S. 1	Riv-1_B3	19.803	0.184	0.479	14.92	51.892	8.67	0.04	0.787	2.507	0.072	99.354
K.R.S. 1	Riv-1_C1	18.192	0.117	0.599	15.245	52.662	7.887	0.043	1.048	2.938	0.082	98.813
K.R.S. 1	Riv-1_C2	18.447	0.078	0.64	15.427	53.24	7.44	0.07	1.076	2.869	0.084	99.371
K.R.S. 1	Riv-1_C3	18.138	0.114	0.557	15.417	52.65	7.925	0	0.908	2.924	0.09	98.723
K.R.S. 1	Riv-1_D1	20.142	0.244	0.467	14.497	51.758	9.247	0.101	0.857	1.99	0.077	99.38
K.R.S. 1	Riv-1_D2	20.38	0.297	0.478	14.616	51.707	8.983	0	0.773	1.947	0.104	99.285
K.R.S. 1	Riv-1_D3	20.315	0.257	0.451	14.672	51.808	8.742	0	0.703	2.603	0.07	99.621
K.R.S. 1	Riv-1_E1	21.376	0.07	0.358	15.703	52.753	6.248	0.075	0.876	1.566	0.083	99.108
K.R.S. 1	Riv-1_E2	21.148	0.103	0.334	15.522	52.599	6.664	0.005	0.957	1.637	0.093	99.062
K.R.S. 1	Riv-1_E3	21.278	0.081	0.346	15.494	52.606	6.693	0	1.052	1.564	0.047	99.161
Camp	16-01_A1	20.238	0.297	0.489	14.158	51.142	9.807	0.032	0.737	2.641	0.073	99.614

Camp	16-01_A2	20.466	0.281	0.479	13.881	51.266	10.047	0.018	0.646	1.954	0.102	99.14
Camp	16-01_A3	20.681	0.327	0.422	14.066	51.285	9.486	0.045	0.631	2.47	0.081	99.494
Camp	16-01_B1	20.393	0.221	0.42	14.874	51.781	8.955	0	0.663	2.608	0.103	100.018
Camp	16-01_B2	19.759	0.205	0.444	14.654	51.342	9.176	0.039	0.648	2.066	0.092	98.425
Camp	16-01_B3	19.976	0.236	0.482	14.792	51.481	9.332	0.048	0.719	2.833	0.111	100.01
Camp	16-01_C1	20.511	0.248	0.464	14.857	51.637	8.587	0	0.886	2.377	0.085	99.652
STANDARD	Px1-01	24.496	0.106	0.057	17.082	53.857	0.442	0.021	0.233	2.821	0.062	99.177
STANDARD	Px1-02	24.5	0.102	0.03	17.157	53.912	0.441	0.043	0.182	2.845	0.072	99.284
STANDARD	Hypersthene-01	1.261	0.022	0.015	26.966	54.318	0.566	0.061	0.493	15.715	0.515	99.932
STANDARD	Hypersthene-02	1.083	0.015	0.004	27.039	54.511	0.519	0	0.448	15.734	0.456	99.809
STANDARD	Springwater-01	0	0	0	43.526	39.362	0	0.014	0.051	17.131	0.293	100.377
STANDARD	Springwater-02	0	0	0.005	43.592	39.47	0	0.004	0.067	17.314	0.329	100.781
U.L.T.	13-10_A1	19.538	0.077	0.458	14.796	52.216	7.828	0	0.918	1.703	0.093	97.627
U.L.T.	13-10_A2	21.113	0.089	0.444	15.203	52.625	7.382	0	0.862	1.585	0.075	99.378
U.L.T.	13-10_A3	20.846	0.084	0.44	14.986	52.062	7.835	0.107	0.996	1.713	0.06	99.129
U.L.T.	13-10_B1	22.64	0.082	0.127	16.272	51.813	5.733	0	0.982	1.835	0.051	99.535
U.L.T.	13-10_B2	21.052	0.104	0.405	15.423	52.741	6.971	0.018	0.763	1.577	0.077	99.131
U.L.T.	13-10_B3	22.086	0.127	0.194	16.4	52.524	5.409	0.073	0.955	1.749	0.068	99.585
U.L.T.	13-10_C1	20.823	0.115	0.454	14.917	52.6	7.894	0.082	0.876	1.643	0.075	99.479
U.L.T.	13-10_C2	20.982	0.118	0.476	14.859	52.433	7.709	0.005	0.95	1.645	0.039	99.216
U.L.T.	13-10_C3	20.91	0.11	0.471	15.006	52.569	7.77	0.05	0.902	1.764	0.072	99.624
U.L.T.	13-10_D1	20.597	0.093	0.449	15.064	52.514	8.039	0	0.855	1.743	0.08	99.434
U.L.T.	13-10_D2	20.965	0.123	0.427	14.786	52.311	7.78	0.066	0.947	1.647	0.07	99.122
U.L.T.	13-10_D3	21.181	0.105	0.443	14.876	52.246	7.721	0.005	0.941	1.553	0.083	99.154
U.L.T.	13-10_E1	20.849	0.107	0.518	15.114	52.388	7.835	0.013	0.964	2.172	0.094	100.054
U.L.T.	13-10_E2	21.104	0.093	0.41	15.117	52.568	7.248	0.073	0.81	1.615	0.093	99.131
U.L.T.	13-10_E3	20.975	0.109	0.45	15.008	52.258	7.75	0.048	0.89	1.743	0.077	99.308
U.L.T.	13-10_F1	20.549	0.076	0.449	14.934	52.434	7.997	0.075	1.001	1.7	0.096	99.311

U.L.T.	13-10_F2	20.693	0.076	0.449	15.255	52.871	7.182	0.059	0.843	1.609	0.032	99.069
U.L.T.	13-10_F3	20.831	0.08	0.426	15.022	52.657	7.522	0.034	0.843	1.673	0.087	99.175
U.L.T.	13-10_G1	20.791	0.083	0.458	14.876	52.598	7.782	0	0.849	1.647	0.075	99.159
U.L.T.	13-10_G2	21.148	0.087	0.392	15.112	52.418	7.606	0.038	0.968	1.632	0.087	99.488
U.L.T.	13-10_G3	20.724	0.102	0.429	14.812	52.466	7.455	0.057	0.83	2.244	0.093	99.212
K.R.S. 4	Riv-4-A1	19.982	0.174	0.547	14.731	52.458	7.643	0	1.21	1.589	0.095	98.429
K.R.S. 4	Riv-4-A2	20.183	0.217	0.56	14.558	52.054	7.567	0.02	1.285	1.562	0.076	98.082
K.R.S. 4	Riv-4-A3	20.014	0.182	0.53	14.723	52.101	7.636	0.052	1.212	1.444	0.048	97.942
K.R.S. 4	Riv-4-B1	19.928	0.205	0.555	14.272	52.037	8.588	0.034	1.113	1.596	0.061	98.389
K.R.S. 4	Riv-4-B2	19.896	0.203	0.57	14.291	52.142	8.327	0.054	1.137	1.55	0.068	98.238
K.R.S. 4	Riv-4-B3	19.806	0.24	0.566	14.435	51.935	8.315	0.02	1.148	1.56	0.116	98.141
K.R.S. 4	Riv-4-C1	21.559	0.056	0.3	15.551	52.51	5.995	0.03	0.893	1.496	0.05	98.44
K.R.S. 4	Riv-4-C2	21.562	0.069	0.311	15.371	52.185	6.116	0.07	1.033	1.491	0.046	98.254
K.R.S. 4	Riv-4-C3	21.52	0.067	0.343	15.758	52.424	5.954	0.023	1.006	1.544	0.097	98.736
K.R.S. 4	Riv-4-D1	19.146	0.091	0.512	15.134	52.468	7.312	0.041	0.903	1.827	0.053	97.487
K.R.S. 4	Riv-4-D2	19.188	0.109	0.544	15.271	52.56	7.259	0.007	0.979	2.574	0.097	98.588
K.R.S. 4	Riv-4-D3	19.222	0.104	0.547	15.096	52.344	7.289	0.086	0.897	1.883	0.103	97.571
K.R.S. 4	Riv-4-E1	20.87	0.004	0.459	15.681	54.176	2.961	0.05	0.971	1.893	0.098	97.163
K.R.S. 4	Riv-4-E2	20.91	0.037	0.421	15.864	54	2.844	0.048	0.862	2.407	0.099	97.492
K.R.S. 4	Riv-4-E3	20.593	0.009	0.479	15.85	54.44	2.834	0.043	0.954	2.518	0.097	97.817
K.R.S. 4	Riv-4-F1	18.538	0.224	0.517	14.928	51.431	8.031	0.036	1.08	2.522	0.086	97.393
K.R.S. 4	Riv-4-F2	18.667	0.261	0.516	14.783	51.544	8.068	0.004	1.196	2.631	0.086	97.756
K.R.S. 4	Riv-4-G1	20.142	0.15	0.453	14.795	51.7	8.272	0.084	0.716	1.809	0.065	98.186
K.R.S. 4	Riv-4-G2	20.423	0.14	0.479	14.572	52.082	8.21	0.13	0.787	1.783	0.06	98.666
K.R.S. 4	Riv-4-G3	20.314	0.137	0.411	14.699	51.986	7.996	0.032	0.797	1.803	0.095	98.27
K.R.S. 3	11-09_A1	21.749	0.04	0.314	15.588	52.4	5.453	0	1.261	1.477	0.059	98.341
K.R.S. 3	11-09_A2	21.883	0.03	0.255	16.009	52.691	4.777	0.041	0.947	1.376	0.076	98.085
K.R.S. 3	11-09_A3	21.73	0.022	0.329	15.724	52.589	5.597	0.082	1.218	1.606	0.065	98.962

K.R.S. 3	11-09_B1	19.644	0.305	0.524	14.498	51.499	8.891	0.014	0.736	1.91	0.1	98.121
K.R.S. 3	11-09_B2	19.528	0.311	0.516	14.685	51.502	8.824	0.077	0.77	2.611	0.101	98.925
K.R.S. 3	11-09_B3	19.435	0.282	0.537	14.65	51.882	8.622	0.055	0.714	2.672	0.085	98.934
K.R.S. 3	11-09_C1	19.44	0.342	0.552	14.897	51.524	8.108	0.05	1.148	2.427	0.054	98.542
K.R.S. 3	11-09_C2	19.558	0.355	0.527	14.725	51.047	8.27	0.004	1.234	1.74	0.065	97.525
K.R.S. 3	11-09_C3	19.53	0.371	0.538	14.883	51.756	8.17	0.063	1.147	1.756	0.073	98.287
K.R.S. 3	11-09_D1	21.53	0.022	0.282	15.545	52.492	5.909	0.05	0.857	1.539	0.111	98.337
K.R.S. 3	11-09_D2	21.687	0.011	0.273	16.058	52.547	5.714	0.013	0.737	2.057	0.068	99.165
K.R.S. 3	11-09_D3	21.692	0	0.275	15.935	52.688	5.591	0.046	0.762	1.563	0.094	98.646
K.R.S. 3	11-09_E1	19.533	0.327	0.596	14.612	51.76	8.226	0.038	1.027	2.571	0.071	98.761
K.R.S. 3	11-09_E2	19.489	0.363	0.556	14.393	51.488	8.711	0	1.084	2.495	0.082	98.661
K.R.S. 3	11-09_E3	19.48	0.361	0.559	14.39	51.396	8.851	0.034	1.062	1.871	0.084	98.088
K.R.S. 3	11-09_F1	21.112	0.05	0.284	16.037	52.549	5.787	0.046	0.961	1.645	0.068	98.539
K.R.S. 3	11-09_F2	21.066	0.023	0.28	15.951	52.288	5.914	0.116	0.904	1.67	0.109	98.321
K.R.S. 3	11-09_F3	21.033	0.035	0.277	16.087	52.608	5.696	0.03	0.809	1.653	0.084	98.312
K.R.S. 3	11-09_G1	21.496	0.12	0.404	14.843	52.566	6.033	0	1.423	1.35	0.076	98.311
K.R.S. 3	11-09_G2	21.585	0.115	0.39	15.129	52.432	5.693	0.091	1.338	1.403	0.069	98.245
K.R.S. 3	11-09_G3	21.368	0.129	0.399	15.025	52.506	5.93	0.016	1.251	1.482	0.066	98.172
K.N.H	4-14_A1	20.717	0.103	0.489	14.394	53.092	3.916	0.091	0.557	4.26	0.141	97.76
K.N.H	4-14_A2	19.502	0.269	0.5	14.252	51.276	9.124	0.007	0.821	2.743	0.103	98.597
K.N.H	4-14_A3	20.049	0.293	0.489	14.17	51.454	9.017	0.111	0.652	1.945	0.092	98.272
STANDARD	Px1-01	24.437	0.088	0.062	16.932	53.837	0.467	0	0.281	2.643	0.044	98.791
STANDARD	Px1-02	24.448	0.125	0.056	17.058	54.278	0.422	0.023	0.218	2.883	0.065	99.576
STANDARD	Hypersthene-01	1.21	0.045	0	26.756	53.9	0.795	0.011	0.553	15.797	0.513	99.58
STANDARD	Hypersthene-02	1.189	0.025	0	26.781	54.138	0.734	0.02	0.494	15.687	0.488	99.556
STANDARD	Springwater-01	0	0	0	43.846	39.447	0	0.028	0.025	17.412	0.288	101.046
STANDARD	Springwater-02	0	0	0.009	43.454	39.382	0.002	0	0.036	17.146	0.313	100.342
K.N.H	4-14_B1	19.773	0.277	0.434	14.149	51.102	8.9	0	0.672	2.66	0.097	98.064

K.N.H	4-14_B2	19.468	0.272	0.517	14.607	51.659	9.117	0.029	0.573	2.817	0.078	99.137
K.N.H	4-14_B3	19.419	0.22	0.504	14.63	51.627	8.645	0.016	0.497	2.175	0.099	97.832
K.N.H	4-14_C1	19.625	0.247	0.49	14.701	51.646	8.522	0.057	0.669	2.405	0.089	98.451
K.N.H	4-14_C2	19.882	0.252	0.509	14.822	51.762	8.537	0.061	0.696	2.546	0.063	99.13
K.N.H	4-14_C3	19.802	0.227	0.528	14.881	51.706	8.492	0.034	0.807	1.808	0.078	98.363
K.N.H	4-14_D1	20.135	0.145	0.519	14.619	52.008	8.194	0.025	0.795	1.846	0.072	98.358
K.N.H	4-14_D3	19.936	0.152	0.446	14.699	51.695	8.231	0	0.778	2.549	0.057	98.543
K.N.H	4-14_E1	19.324	0.33	0.501	14.422	50.974	9.4	0.025	0.642	2.193	0.067	97.878
K.N.H	4-14_E2	19.222	0.308	0.519	14.806	51.262	9.006	0.077	0.638	3.049	0.118	99.005
K.N.H	4-14_E3	19.293	0.313	0.531	14.482	51.208	9.101	0.03	0.608	2.956	0.053	98.575
K.N.H	4-14_F1	20.279	0.056	0.412	15.695	52.353	6.948	0.073	0.831	1.836	0.076	98.559
K.N.H	4-14_F2	20.352	0.062	0.321	15.694	52.332	6.906	0.036	1	1.868	0.059	98.63
K.N.H	4-14_F3	20.33	0.068	0.371	15.669	52.274	6.884	0.057	0.747	1.805	0.077	98.282
K.N.H	4-14_G1	18.645	0.16	0.543	14.843	52.206	8.312	0.075	0.88	2.007	0.096	97.767
K.N.H	4-14_G2	18.735	0.136	0.581	14.696	52.167	8.447	0	0.808	2.575	0.049	98.194
K.N.H	4-14_G3	18.766	0.136	0.568	14.882	52.064	8.447	0.064	1.017	1.997	0.061	98.002
K.W.S	13-02-A1	19.665	0.12	0.477	14.863	51.754	8.395	0.066	0.939	2.46	0.069	98.808
K.W.S	13-02-A2	19.704	0.098	0.49	14.836	51.702	8.349	0.055	0.997	1.847	0.081	98.159
K.W.S	13-02-A3	19.725	0.132	0.496	14.828	51.818	8.428	0.02	1	1.877	0.078	98.402
K.W.S	13-02-B1	19.497	0.026	0.538	16.139	53.126	5.501	0.05	0.938	1.821	0.061	97.697
K.W.S	13-02-B3	19.281	0.059	0.508	15.778	53.032	5.935	0	1.024	1.848	0.099	97.564
K.W.S	13-02-C1	20.808	0.047	0.356	16.085	52.623	5.901	0	1.007	1.831	0.08	98.738
K.W.S	13-02-C2	20.439	0.012	0.366	15.991	52.547	6.088	0.084	0.909	1.842	0.094	98.372
K.W.S	13-02-C3	20.379	0.021	0.368	15.922	52.679	6.116	0.002	0.911	2.386	0.071	98.855
Camp	16-01-A2	21.595	0.011	0.25	16.073	52.482	4.519	0.02	1.01	1.685	0.097	97.742
Camp	16-01-A3	21.848	0.028	0.233	15.972	52.749	4.352	0	1.002	1.653	0.075	97.912
STANDARD	Px1-01	24.435	0.087	0.024	17.061	53.918	0.472	0	0.188	2.879	0.063	99.127
STANDARD	Px1-02	24.565	0.068	0.055	17.247	54.091	0.47	0.02	0.17	2.949	0.049	99.684

STANDARD	Hypersthene-01	1.111	0.032	0.021	26.877	54.404	0.69	0	0.64	15.851	0.535	100.161
STANDARD	Hypersthene-02	1.159	0.016	0	26.569	53.919	0.689	0	0.53	15.707	0.491	99.08
STANDARD	Springwater-01	0	0	0	43.734	39.45	0.016	0	0	17.048	0.313	100.561
STANDARD	Springwater-02	0.006	0	0.011	43.886	39.23	0	0.018	0	17.146	0.345	100.642
Camp	16-01_B1	19.736	0.327	0.518	14.619	51.609	8.976	0.055	0.595	1.931	0.09	98.456
Camp	16-01_B2	19.65	0.297	0.511	14.522	51.269	8.932	0.041	0.597	1.952	0.105	97.876
Camp	16-01_B3	19.804	0.346	0.506	14.598	51.535	8.915	0.023	0.531	2.58	0.087	98.925
Camp	16-01_C1	20.433	0.302	0.493	14.247	51.656	8.533	0.004	0.607	1.823	0.093	98.191
Camp	16-01_C2	20.457	0.305	0.466	14.339	51.459	8.49	0.073	0.695	2.41	0.107	98.801
Camp	16-01_C3	20.221	0.278	0.471	14.361	51.407	8.567	0.062	0.64	1.755	0.088	97.85
K.S.H	6-02_A1	9.647	0.07	0.175	24.7	52.851	5.885	0.021	0.52	4.552	0.115	98.536
K.S.H	6-02_A2	18.686	0.14	0.434	17.052	51.885	7.344	0.059	1.019	1.816	0.082	98.517
K.S.H	6-02_A3	20.215	0.169	0.513	14.622	51.11	8.838	0.078	0.976	1.567	0.074	98.162
K.S.H	6-02_B1	20.42	0.274	0.454	14.444	51.611	8.68	0.055	0.687	1.77	0.095	98.49
K.S.H	6-02_C1	22.182	0.016	0.205	15.977	52.793	4.844	0.02	1.064	1.628	0.09	98.819
K.S.H	6-02_C2	22.337	0.024	0.184	16.155	52.713	4.745	0.066	0.836	2.177	0.059	99.296
K.S.H	6-02_C3	22.056	0.018	0.206	16.018	52.563	4.703	0.027	0.929	1.652	0.095	98.267
K.W.S	O_13-10_D	0.25	0.015	0.027	33.121	54.271	6.208	0.121	0.553	6.195	0.101	100.862
K.W.S	O_13-10_D2	0.362	0.012	0	32.542	54.43	5.756	0.098	0.454	6.068	0.097	99.819
K.W.S	O_13-10_D3	0.272	0.004	0.03	32.531	54.199	5.919	0.1	0.34	5.922	0.144	99.461
STANDARD	Px1-01	24.395	0.097	0.046	16.894	53.986	0.46	0.064	0.247	2.258	0.081	98.528
STANDARD	Px1-02	24.505	0.091	0.042	17.129	54.115	0.466	0.059	0.232	2.922	0.09	99.651
STANDARD	Hypersthene-01	1.24	0.028	0	26.822	54.378	0.604	0	0.575	15.517	0.505	99.669
STANDARD	Hypersthene-02	1.183	0.015	0.003	26.511	53.839	0.683	0.055	0.566	15.698	0.483	99.036
STANDARD	Springwater-01	0.002	0	0	43.849	39.416	0	0.062	0.059	16.975	0.289	100.652
STANDARD	Springwater-02	0	0	0.006	43.575	39.341	0	0	0.045	16.966	0.29	100.223

Table 5.4: Olivine microprobe analysis

Kakanui River Section samples = K.R.S 1, K.R.S 3, K.R.S 4; Campbells bay = Camp; Upriver Lapilli Tuffs = U.L.T; Kakanui South Head = K.S.H; Kakanui North Head = K.N.H; Kakanui Western Slope = K.W.S

Location	Sample	CaO	TiO2	Na2O	MgO	SiO2	Al2O3	NiO	Cr2O3	FeO	MnO	Total
K.W.S	O_13-10_D	0.25	0.015	0.027	33.121	54.271	6.208	0.121	0.553	6.195	0.101	100.862
K.W.S	O_13-10_D2	0.362	0.012	0	32.542	54.43	5.756	0.098	0.454	6.068	0.097	99.819
K.W.S	O_13-10_D3	0.272	0.004	0.03	32.531	54.199	5.919	0.1	0.34	5.922	0.144	99.461
STANDARD	Px1-01	24.395	0.097	0.046	16.894	53.986	0.46	0.064	0.247	2.258	0.081	98.528
STANDARD	Px1-02	24.505	0.091	0.042	17.129	54.115	0.466	0.059	0.232	2.922	0.09	99.651
STANDARD	Hypersthene-01	1.24	0.028	0	26.822	54.378	0.604	0	0.575	15.517	0.505	99.669
STANDARD	Hypersthene-02	1.183	0.015	0.003	26.511	53.839	0.683	0.055	0.566	15.698	0.483	99.036
STANDARD	Springwater-01	0.002	0	0	43.849	39.416	0	0.062	0.059	16.975	0.289	100.652
STANDARD	Springwater-02	0	0	0.006	43.575	39.341	0	0	0.045	16.966	0.29	100.223
K.W.S	O_13-10_A1	0.285	0.023	0.038	32.842	54.747	5.8	0.089	0.413	5.937	0.123	100.297
K.W.S	O_13-10_A2	0.28	0.01	0	32.806	54.599	5.75	0.064	0.372	6.163	0.164	100.208
K.W.S	O_13-10_A3	0.295	0	0.012	32.957	54.384	5.75	0.045	0.497	6.084	0.135	100.159
K.W.S	O_13-10_B1	0.338	0	0	33.974	55.606	3.836	0.066	0.486	5.554	0.133	99.993
K.W.S	O_13-10_B2	0.372	0	0.001	33.499	55.327	3.926	0.084	0.576	5.576	0.117	99.478
K.W.S	O_13-10_B3	0.397	0	0.005	33.345	55.211	4.229	0.102	0.646	5.493	0.124	99.552
K.W.S	O_13-10_C1	0.312	0.026	0.026	32.806	54.533	6.009	0.086	0.427	6.174	0.14	100.539
K.W.S	O_13-10_C2	1.301	0.013	0.051	32.271	54.29	5.991	0.1	0.483	6.018	0.109	100.627
K.W.S	O_13-10_C3	0.29	0.016	0.001	32.827	54.595	5.999	0.105	0.505	6.059	0.142	100.539
K.W.S	O_13-10_E1	2.37	0.004	0.082	31.193	54.591	5.908	0.073	0.425	5.561	0.154	100.361
K.W.S	O_13-10_E2	0.295	0.011	0.026	32.687	54.584	5.916	0.121	0.447	6.151	0.135	100.373
K.W.S	O_13-10_E3	0.398	0	0.04	32.392	54.75	5.799	0.061	0.424	5.838	0.171	99.873
K.W.S	O_13-10_F1	0.319	0.014	0.025	32.78	54.385	5.82	0.082	0.525	5.985	0.133	100.068
K.W.S	O_13-10_F2	0.293	0.004	0.013	32.841	54.767	5.844	0.109	0.427	5.959	0.138	100.395

K.W.S	O_13-10_F3	0.288	0.015	0.015	32.541	54.322	5.987	0.048	0.418	6.154	0.141	99.929
K.W.S	O_13-10_G1	0.205	0.008	0.009	33.062	54.998	5.161	0.037	0.441	6.104	0.153	100.178
K.W.S	O_13-10_G2	0.295	0.03	0	32.805	54.62	5.795	0.132	0.464	6.104	0.131	100.376
K.W.S	O_13-10_G3	0	0.002	0.023	32.844	54.762	5.914	0.093	0.368	6.149	0.141	100.296
N.K.H	O_4-14_A1	0.194	0.024	0	33.675	55.562	4.162	0.082	0.232	6.078	0.155	100.164
N.K.H	O_4-14_A2	0.218	0.022	0.027	33.364	55.686	4.238	0.089	0.334	5.723	0.128	99.829
N.K.H	O_4-14_B1	0.382	0.039	0.032	32.342	54.145	6.28	0.116	0.408	6.367	0.154	100.265
N.K.H	O_4-14_B2	0.352	0.029	0.04	32.295	54.443	6.004	0.077	0.394	6.18	0.11	99.924
N.K.H	O_4-14_B3	0.347	0.03	0.019	32.38	54.657	6.198	0.123	0.357	6.098	0.097	100.306
N.K.H	O_4-14_C1	0.334	0	0.019	32.842	54.663	5.419	0.116	0.4	5.889	0.12	99.802
N.K.H	O_4-14_C2	0.338	0	0	32.97	54.969	5.407	0.117	0.444	5.663	0.143	100.051
N.K.H	O_4-14_C3	0.32	0.003	0.02	33.028	55.1	5.365	0.05	0.394	5.878	0.126	100.284
N.K.H	O_4-14_D1	0.257	0.006	0.032	33.231	54.847	5.13	0.018	0.45	5.674	0.148	99.793
N.K.H	O_4-14_D2	0.297	0.018	0.03	32.862	54.704	5.45	0.098	0.449	6.084	0.116	100.108
N.K.H	O_4-14_D3	0.307	0.011	0.056	32.754	54.538	5.47	0.103	0.366	5.574	0.116	99.295
N.K.H	O_4-14_E1	0.334	0.004	0.028	32.782	54.821	5.241	0.085	0.438	5.767	0.13	99.63
N.K.H	O_4-14_E2	0.347	0.008	0.036	32.997	54.938	5.355	0.128	0.432	5.644	0.128	100.013
N.K.H	O_4-14_E3	0.346	0	0.036	32.867	55.026	5.307	0.064	0.458	5.744	0.13	99.978
Camp	O_16-01_A1	0.263	0	0.022	33.385	55.153	4.276	0.076	0.655	5.602	0.115	99.547
Camp	O_16-01_A2	0.253	0	0.004	33.468	54.701	4.243	0.078	0.646	5.651	0.132	99.176
Camp	O_16-01_A3	0.274	0	0	33.396	54.862	4.182	0.098	0.571	5.621	0.156	99.16
Camp	O_16-01_B1	0.28	0.03	0.029	32.729	54.632	5.38	0.039	0.353	6.236	0.123	99.831
Camp	O_16-01_B2	0.292	0.046	0.003	32.672	54.893	5.271	0.036	0.429	6.236	0.132	100.01
Camp	O_16-01_B3	0.252	0.028	0.01	32.927	54.963	4.994	0.053	0.336	6.071	0.152	99.786
Camp	O_16-01_C1	0.26	0	0.024	33.714	55.333	4.304	0.1	0.632	5.73	0.169	100.266
Camp	O_16-01_C2	0.269	0	0.023	33.442	55.26	4.261	0.108	0.644	5.684	0.133	99.824
Camp	O_16-01_C3	0.258	0	0.003	33.572	55.303	4.286	0.066	0.658	5.811	0.154	100.111
K.S.H	O_6-02_A1	0.302	0.048	0.018	31.623	54.186	6.114	0.112	0.271	7.238	0.15	100.062

K.S.H	O_6-02_A3	0.329	0.054	0.032	31.75	54.164	6.031	0.137	0.213	7.333	0.162	100.205
K.S.H	O_6-02_B1	0.005	0.003	0	48.874	40.55	0.014	0.408	0	9.806	0.122	99.782
K.S.H	O_6-02_B2	0.124	0.006	0.022	33.517	55.01	4.496	0.103	0.339	6.242	0.149	100.008
K.S.H	O_6-02_B3	0.204	0.019	0.019	32.976	54.597	5.35	0.059	0.422	6.459	0.134	100.239
K.S.H	O_6-02_C1	0.278	0.007	0.007	33.988	56.248	2.937	0.078	0.487	5.579	0.102	99.711
K.S.H	O_6-02_C2	0.118	0	0.016	34.415	56.116	2.532	0.071	0.403	5.731	0.168	99.57
K.S.H	O_6-02_C3	0.173	0	0	34.192	56.074	2.998	0.089	0.427	5.489	0.137	99.579
K.R.S 1	O_Riv-1_A1	0.304	0	0.019	33.467	55.087	4.013	0.057	0.571	5.828	0.133	99.479
K.R.S 1	O_Riv-1_A2	0.311	0.018	0.004	33.33	54.87	4.063	0.046	0.585	5.774	0.145	99.146
K.R.S 1	O_Riv-1_A3	0.305	0.006	0.01	33.431	55.116	4.005	0.119	0.651	5.795	0.113	99.551
K.R.S 1	O_Riv-1_B1	0.337	0	0.066	33.042	55.113	5.037	0.151	0.586	5.576	0.146	100.054
K.R.S 1	O_Riv-1_B2	0.314	0.008	0.025	33.077	54.799	5.008	0.121	0.429	5.623	0.147	99.551
K.R.S 1	O_Riv-1_B3	0.363	0	0.029	32.913	55.213	4.991	0.091	0.545	5.62	0.119	99.884
K.R.S 1	O_Riv-1_C1	0.296	0.038	0.011	32.774	54.903	4.834	0.114	0.408	5.946	0.163	99.487
K.R.S 1	O_Riv-1_C2	0.31	0.064	0.016	32.917	54.763	4.911	0.067	0.457	6.059	0.119	99.683
K.R.S 1	O_Riv-1_C3	0.284	0.047	0.01	32.751	54.906	4.97	0.078	0.393	6.044	0.14	99.623
K.R.S 1	O_Riv-1_D1	0.319	0.001	0	32.876	54.734	5.569	0.117	0.536	5.541	0.119	99.812
K.R.S 1	O_Riv-1_D2	0.328	0	0.022	32.776	54.831	5.558	0.096	0.499	5.674	0.119	99.903
K.R.S 1	O_Riv-1_D3	0.32	0	0.025	33.179	55.013	5.475	0.071	0.495	5.913	0.122	100.613
K.R.S 1	O_Riv-1_E1	0.312	0.001	0.025	32.534	54.607	5.512	0.126	0.376	6.07	0.163	99.726
K.R.S 1	O_Riv-1_E2	0.266	0	0.012	33.058	55.043	5.145	0.087	0.301	6.167	0.112	100.191
K.R.S 1	O_Riv-1_E3	0.335	0	0	32.925	54.813	5.54	0.119	0.408	6.04	0.163	100.343
K.R.S 1	O_Riv-1_F1	0.318	0	0.01	33.371	55.338	4.392	0.098	0.487	5.65	0.164	99.828
K.R.S 1	O_Riv-1_F2	0.348	0.008	0.038	33.213	55.147	4.447	0.048	0.449	5.451	0.145	99.294
K.R.S 1	O_Riv-1_F3	0.363	0	0.017	33.396	55.21	4.32	0.092	0.452	5.522	0.117	99.489
STANDARD	Px1-01	24.435	0.076	0.038	17.083	53.972	0.449	0	0.24	2.815	0.052	99.16
STANDARD	Px1-02	24.411	0.073	0.032	16.959	54.098	0.462	0	0.243	2.909	0.091	99.278
STANDARD	Hypersthene-01	1.172	0.042	0	26.608	54.244	0.718	0	0.616	15.934	0.517	99.851

STANDARD	Hypersthene-02	1.225	0.026	0.002	26.363	53.861	0.626	0.014	0.586	15.522	0.514	98.739
STANDARD	Springwater-01	0.011	0	0	43.775	39.408	0	0.014	0.067	16.888	0.323	100.486
STANDARD	Springwater-02	0.006	0	0	43.846	39.288	0	0.018	0.095	17.082	0.298	100.633
K.S.H	O_f_6-02_A1	0.233	0	0.032	33.302	55.182	5.448	0.128	0.387	6.159	0.161	101.032
K.S.H	O_f_6-02_A2	0.961	0.027	0.014	32.774	55.574	5.278	0.027	0.361	6.298	0.128	101.442
K.S.H	O_f_6-02_A3	0.895	0.016	0.012	32.827	55.295	5.555	0.043	0.587	6.156	0.173	101.559
K.S.H	O_f_6-02_B1	0.258	0.029	0.023	33.218	55.811	4.71	0.06	0.22	6.322	0.159	100.81
K.S.H	O_f_6-02_B2	0.242	0.017	0	33.492	55.625	4.786	0.057	0.188	6.427	0.186	101.02
K.S.H	O_f_6-02_B3	0.212	0.026	0.039	32.855	55.331	4.785	0.043	0.205	6.452	0.151	100.099
K.S.H	O_f_6-02_C1	0.298	0.034	0	32.921	55.216	5.682	0.085	0.352	6.318	0.142	101.048
K.S.H	O_f_6-02_C2	0.267	0.014	0.016	33.025	55.25	5.37	0.156	0.381	6.375	0.153	101.007
K.S.H	O_f_6-02_C3	0.247	0.034	0	33.199	55.404	4.845	0.085	0.225	6.305	0.137	100.481
K.S.H	O_f_6-02_D1	0.26	0.029	0.002	33.382	55.418	5.412	0.08	0.202	6.577	0.142	101.504
K.S.H	O_f_6-02_D2	0.259	0.025	0.02	32.933	55.279	5.709	0.16	0.283	6.277	0.133	101.078
K.S.H	O_f_6-02_D3	0.219	0.066	0.014	33.05	55.066	5.714	0.097	0.254	6.459	0.159	101.098
Camp	O_f_16-01_A1	0.298	0	0.016	33.908	55.963	3.845	0.069	0.567	5.54	0.115	100.321
Camp	O_f_16-01_A2	0.302	0	0	33.915	55.944	3.854	0.083	0.518	5.503	0.125	100.244
Camp	O_f_16-01_A3	0.32	0	0.025	34.181	56.218	3.862	0.126	0.622	5.657	0.156	101.167
STANDARD	Px1-01	24.566	0.081	0.048	16.975	54.208	0.483	0.065	0.313	2.893	0.085	99.717
STANDARD	Px1-02	24.352	0.108	0.059	17.102	54.41	0.476	0.028	0.248	2.903	0.055	99.741
STANDARD	Hypersthene-01	1.183	0.024	0.008	26.996	54.758	0.563	0.046	0.613	15.831	0.53	100.552
STANDARD	Hypersthene-02	1.141	0.042	0	26.543	53.913	0.718	0.011	0.571	15.628	0.53	99.097
STANDARD	Springwater-01	0.014	0.003	0	43.64	39.398	0	0	0	17.321	0.31	100.686
STANDARD	Springwater-02	0	0	0.01	43.664	39.356	0	0.005	0.042	16.93	0.3	100.307
Camp	O_f_16-01_B1	0.271	0.05	0.02	32.581	55.01	5.025	0.108	0.314	6.64	0.155	100.174
Camp	O_f_16-01_B2	0.262	0.032	0.001	33.046	55.583	4.896	0.073	0.323	6.599	0.158	100.973
Camp	O_f_16-01_B3	0.289	0.04	0.011	32.874	55.097	5.229	0.057	0.366	6.794	0.158	100.915
Camp	O_f_16-01_C1	0.318	0.055	0.042	32.284	54.879	6.155	0.071	0.276	6.831	0.129	101.04

Camp	O_f_16-01_C2	0.315	0.044	0.033	31.985	54.603	6.508	0.129	0.369	6.77	0.165	100.921
Camp	O_f_16-01_C3	0.337	0.041	0.019	32.185	54.6	6.24	0.097	0.331	6.903	0.129	100.882
Camp	O_f_16-01_D1	0.292	0	0.01	33.812	56.22	3.963	0.085	0.584	5.662	0.134	100.762
Camp	O_f_16-01_D2	0.294	0	0	34.035	55.938	3.742	0.025	0.44	5.506	0.15	100.13
Camp	O_f_16-01_D3	0.285	0	0.024	33.685	55.971	3.882	0.14	0.575	5.498	0.087	100.147
K.W.S	O_f_13-02_A1	18.759	0.264	0.544	14.865	51.996	9.343	0.092	0.706	2.948	0.097	99.614
K.W.S	O_f_13-02_A2	18.782	0.267	0.552	15.025	51.862	9.447	0.065	0.646	3.041	0.089	99.776
K.W.S	O_f_13-02_A3	18.616	0.278	0.605	15.065	52.159	9.638	0.113	0.602	2.959	0.11	100.145
K.W.S	O_f_13-02_B1	0.371	0	0	34.113	56.516	3.223	0.103	0.575	5.383	0.118	100.402
K.W.S	O_f_13-02_B2	0.396	0.002	0.031	34.25	56.439	3.118	0.106	0.532	5.309	0.117	100.3
K.W.S	O_f_13-02_B3	0.381	0.004	0.012	34.122	56.278	3.194	0.09	0.572	5.456	0.134	100.243
K.W.S	O_f_13-02_C1	0.304	0.049	0.029	32.826	55.265	5.686	0.108	0.308	6.249	0.123	100.947
K.W.S	O_f_13-02_C2	0.288	0.047	0.053	32.688	55.1	5.819	0.124	0.346	6.391	0.161	101.017
K.W.S	O_f_13-02_C3	0.291	0.052	0.047	32.649	54.785	5.792	0.055	0.23	6.373	0.137	100.411
K.R.S 3	O_f_11-09_A1	0.294	0.029	0.011	33.142	55.72	5.173	0.058	0.424	6.119	0.139	101.109
K.R.S 3	O_f_11-09_A2	0.303	0.054	0.005	33.3	55.525	5.024	0.088	0.358	6.04	0.132	100.829
K.R.S 3	O_f_11-09_A3	0.302	0.026	0.011	32.884	55.211	5.114	0.115	0.372	5.999	0.137	100.171
K.R.S 3	O_f_11-09_B1	20	0.059	0.464	13.501	50.712	13.071	0.034	0.162	3.432	0.127	101.562
K.R.S 3	O_f_11-09_B2	20.097	0.068	0.43	13.506	50.876	12.994	0	0.144	3.44	0.137	101.692
K.R.S 3	O_f_11-09_B3	19.956	0.083	0.44	13.445	50.663	13.131	0	0.217	3.474	0.128	101.537
K.R.S 3	O_f_11-09_C1	0.177	0.034	0.007	32.931	54.826	6.15	0.087	0.501	6.309	0.123	101.145
K.R.S 3	O_f_11-09_C2	0.214	0.026	0.005	32.565	54.755	6.113	0.092	0.434	6.685	0.16	101.049
K.R.S 3	O_f_11-09_C3	0.226	0.04	0.008	32.656	54.698	6.046	0.065	0.452	6.444	0.143	100.778
K.R.S 3	O_f_11-09_D1	0.25	0.024	0.026	34.137	56.059	4.389	0.014	0.456	5.486	0.157	100.998
K.R.S 3	O_f_11-09_D2	0.21	0.017	0.052	33.822	56.124	4.498	0.032	0.459	5.381	0.113	100.708
K.R.S 3	O_f_11-09_D3	0.269	0.024	0.068	33.825	56.175	4.599	0.055	0.488	5.236	0.12	100.859
K.R.S 3	O_f_11-09_E1	0.281	0.042	0.021	32.784	55.124	5.598	0.092	0.279	6.604	0.152	100.977
K.R.S 3	O_f_11-09_E2	0.293	0.032	0.033	32.528	55.184	5.806	0.051	0.353	6.515	0.14	100.935

K.R.S 3	O_f_11-09_E3	0.266	0.049	0.024	32.717	55.117	5.62	0.019	0.287	6.616	0.179	100.894
K.R.S 3	O_f_11-09_F1	0.271	0	0.012	33.495	55.802	4.48	0.111	0.43	5.515	0.125	100.241
K.R.S 3	O_f_11-09_F2	0.292	0	0	33.69	55.806	4.854	0.113	0.481	5.882	0.168	101.286
K.R.S 3	O_f_11-09_F3	0.298	0.019	0.037	33.289	55.721	4.828	0.097	0.473	5.587	0.106	100.455
K.R.S 3	O_f_11-09_G1	2.365	0.033	0.039	31.911	55.445	5.098	0.069	0.453	5.977	0.114	101.504
K.R.S 3	O_f_11-09_G2	0.303	0.016	0	32.858	55.08	5.438	0.118	0.478	6.277	0.143	100.711
K.R.S 3	O_f_11-09_G3	0.957	0	0	33.084	55.338	5.544	0.081	0.432	6.189	0.139	101.764
STANDARD	Px1-01	24.392	0.098	0.07	17.001	53.974	0.449	0.018	0.286	2.879	0.046	99.213
STANDARD	Px1-02	24.222	0.08	0.049	17.045	54.273	0.477	0.053	0.298	2.848	0.079	99.424
STANDARD	Hypersthene-01	1.238	0.026	0.003	27.019	54.561	0.681	0.049	0.642	16.009	0.494	100.722
STANDARD	Hypersthene-02	1.202	0.036	0	26.794	54.249	0.675	0	0.575	15.819	0.493	99.843
STANDARD	Springwater-01	0.007	0	0.021	43.612	39.431	0	0	0	17.146	0.366	100.583
STANDARD	Springwater-02	0.003	0	0	43.263	39.231	0	0.03	0.017	16.953	0.318	99.815
K.R.S 4	O_f_Riv-4_A2	16.264	0.964	0.414	14.628	49.51	11.721	0	0	6.569	0.124	100.194
K.R.S 4	O_f_Riv-4_A3	16.232	1	0.412	14.698	49.506	11.923	0.012	0.02	7.071	0.13	101.004
K.R.S 4	O_f_Riv-4_B1	0.392	0	0.032	32.942	55.668	5.614	0.083	0.443	6.267	0.129	101.57
K.R.S 4	O_f_Riv-4_B2	0.228	0.017	0.015	33.139	55.368	5.606	0.062	0.348	6.13	0.137	101.05
K.R.S 4	O_f_Riv-4_B3	0.251	0.014	0	33.088	55.049	5.345	0.06	0.423	6.098	0.139	100.467
K.R.S 4	O_f_Riv-4_C1	0.339	0	0.028	32.851	55.371	4.76	0.072	0.576	6.101	0.139	100.237
K.R.S 4	O_f_Riv-4_C2	0.371	0	0.039	33.077	55.419	4.77	0.102	0.642	5.906	0.144	100.47
K.R.S 4	O_f_Riv-4_C3	0.382	0.013	0.042	33.198	55.592	4.712	0.102	0.559	6.077	0.132	100.809
K.R.S 4	O_f_Riv-4_D1	0.252	0.037	0.012	32.431	54.958	6.71	0.111	0.4	6.441	0.171	101.523
K.R.S 4	O_f_Riv-4_D2	0.222	0.067	0	33.261	55.137	5.237	0.106	0.547	6.317	0.149	101.043
K.R.S 4	O_f_Riv-4_D3	0.21	0.059	0	33.42	55.444	5.075	0.115	0.538	6.261	0.13	101.252
K.R.S 4	O_f_Riv-4_E1	0.864	0.005	0	32.963	55.666	4.527	0.078	0.553	6.104	0.135	100.895
K.R.S 4	O_f_Riv-4_E2	0.197	0	0.008	33.458	55.359	4.774	0.092	0.423	6.475	0.153	100.939
K.R.S 4	O_f_Riv-4_E3	0.22	0	0	33.326	55.862	4.681	0.037	0.382	6.51	0.146	101.164
K.R.S 4	O_f_Riv-4_F3	19.682	0.231	0.503	14.687	51.922	9.584	0.048	0.475	2.874	0.091	100.097

STANDARD	Px1-01	24.457	0.071	0.062	17.07	54.343	0.513	0	0.165	2.917	0.066	99.664
STANDARD	Px1-02	24.374	0.087	0.051	16.962	54.255	0.503	0	0.25	2.874	0.071	99.427
STANDARD	Hypersthene-01	1.15	0.035	0	26.835	54.061	0.687	0	0.48	15.651	0.5	99.399
STANDARD	Hypersthene-02	1.098	0.033	0.015	26.694	54.111	0.669	0.023	0.527	15.608	0.476	99.254
STANDARD	Springwater-01	0.002	0	0	43.675	39.253	0	0	0.014	17.291	0.295	100.53
STANDARD	Springwater-02	0	0	0.016	43.712	39.453	0	0.018	0.006	16.953	0.305	100.463

Table 5.4: Kaersutite microprobe analysis.

Kakanui River Section samples = K.R.S 1, K.R.S 3, K.R.S 4; Campbells bay = Camp; Upriver Lapilli Tuffs = U.L.T; Kakanui South Head = S.K.H; Kakanui North Head = K.N.H; Kakanui Western Slope = K.W.S

Note: The microprobe spectrometer stopped working properly due to earthquake damage. K2O returned as zero, and these results are considered unreliable.

Location	Sample	CaO	TiO2	Na2O	MgO	SiO2	Al2O3	K2O	Cr2O3	FeO	MnO	Total
STANDARD	Hornblende-01	10.849	2.654	1.936	1.142	39.415	9.764	0	0	25.945	0.433	92.138
STANDARD	Hornblende-02	10.811	2.848	1.911	1.173	39.259	9.788	0	0.025	26.217	0.397	92.429
Taipo Hill	PTH_A3	8.024	1.586	0.645	6.476	52.854	14.85	0	0.029	10.345	0.147	94.956
Taipo Hill	PTH_B1	8.171	1.602	3.146	6.412	51.688	14.568	0	0.064	10.259	0.137	96.047
Taipo Hill	PTH_B2	8.177	1.594	3.213	6.384	51.72	14.518	0	0	10.247	0.146	95.999
Taipo Hill	PTH_B3	8.154	1.584	3.122	6.349	51.594	14.72	0	0.02	10.326	0.106	95.975
Taipo Hill	PTH_C1	8.115	1.591	3.164	6.226	52.365	14.723	0	0.032	10.228	0.117	96.561
Taipo Hill	PTH_C2	8.166	1.511	3.028	6.24	52.062	14.651	0	0.078	10.241	0.123	96.1
Taipo Hill	PTH_C3	8.104	1.545	3.072	6.251	51.738	14.438	0	0	10.052	0.155	95.355
Taipo Hill	PTH_D1	8.496	1.614	0.597	6.074	53.491	14.934	0	0.046	10.378	0.137	95.767
Taipo Hill	PTH_D2	8.528	1.6	0.719	6.121	53.689	14.963	0	0	10.429	0.127	96.176
Taipo Hill	PTH_E1	8.157	1.474	2.977	6.359	52.184	14.69	0	0.023	10.555	0.118	96.537
Taipo Hill	PTH_E2	8.082	1.503	3.049	6.439	51.926	14.547	0	0.012	10.296	0.142	95.996
Taipo Hill	PTH_E3	8.206	1.576	3.216	6.374	52.17	14.613	0	0	10.435	0.118	96.708
Taipo Hill	PTH_F1	8.471	1.648	0.451	6.109	53.068	14.935	0	0.026	10.559	0.125	95.392
Taipo Hill	PTH_F2	10.451	1.793	0.418	6.523	48.565	14.32	0	0.029	10.481	0.086	92.666
Taipo Hill	PTH_F3	8.61	1.606	0.447	5.988	53.54	14.937	0	0.032	10.272	0.138	95.57
U.L.T	13-10_A1	9.684	3.901	2.806	10.699	40.2	13.007	0	0.012	12.271	0.065	92.645
U.L.T	13-10_A3	9.597	3.948	2.794	10.837	40.204	13.141	0	0	13.404	0.111	94.036
U.L.T	13-10_B1	9.924	4.216	2.478	13.01	40.578	14.201	0	0	9.85	0.066	94.323
U.L.T	13-10_B2	9.876	4.166	2.47	12.966	40.444	14.179	0	0.012	9.972	0.061	94.146

U.L.T	13-10_B3	9.98	4.124	2.524	12.903	40.603	14.041	0	0.035	9.876	0.055	94.141
U.L.T	13-10_C1	9.753	4.061	2.711	11.71	40.51	13.49	0	0	11.711	0.094	94.04
U.L.T	13-10_C2	9.921	4.041	2.657	11.742	40.333	13.511	0	0	11.508	0.05	93.763
U.L.T	13-10_C3	9.798	4.067	2.578	11.777	40.094	13.611	0	0	11.808	0.078	93.811
U.L.T	13-10_D1	9.952	4.247	2.729	11.775	40.316	13.585	0	0	11.469	0.044	94.117
U.L.T	13-10_D2	9.784	4.208	2.682	11.617	40.544	13.415	0	0	11.491	0.068	93.809
U.L.T	13-10_D3	9.978	4.211	2.541	11.928	40.407	13.62	0	0	10.851	0.098	93.634
U.L.T	13-10_E1	9.877	4.11	2.705	11.811	40.458	13.501	0	0.038	11.542	0.085	94.127
U.L.T	13-10_E2	9.938	4.141	2.572	11.909	40.416	13.535	0	0.02	11.435	0.108	94.074
U.L.T	13-10_E3	9.85	4.147	2.677	11.765	40.473	13.656	0	0.023	11.31	0.094	93.995
U.L.T	13-10_F1	9.735	4.006	2.853	11.039	40.139	13.335	0	0	12.961	0.066	94.134
U.L.T	13-10_F2	9.659	4.039	2.652	11.066	40.23	13.311	0	0.04	13.038	0.098	94.133
U.L.T	13-10_F3	9.741	3.931	2.798	11.118	40.422	13.328	0	0.006	12.806	0.085	94.235
U.L.T	13-10_G1	9.72	3.947	2.895	10.896	40.546	13.18	0	0	13.696	0.093	94.973
U.L.T	13-10_G2	9.769	3.911	2.746	10.612	40.191	13.048	0	0	13.647	0.14	94.064
U.L.T	13-10_G3	9.748	3.943	2.879	10.756	40.225	13.177	0	0.023	13.58	0.114	94.445
STANDARD	Hornblende-01	10.817	2.556	1.913	4.426	39.841	9.971	0	0.03	26.223	0.367	96.144
STANDARD	Hornblende-02	10.834	2.873	1.911	4.218	39.808	9.82	0	0	26.023	0.34	95.827
K.S.H	6-02_A1	10.315	4.162	2.523	11.779	40.076	13.229	0	0.038	11.67	0.119	93.911
K.S.H	6-02_A2	9.952	3.939	2.79	11.411	40.449	13.32	0	0	12.361	0.076	94.298
K.S.H	6-02_A3	10.328	3.943	2.487	12.345	40.2	13.313	0	0	11.136	0.041	93.793
K.S.H	6-02_B1	9.524	3.954	2.891	10.692	40.164	12.991	0	0.011	13.426	0.111	93.764
K.S.H	6-02_B2	9.59	3.982	2.844	10.614	40.089	13.087	0	0.009	13.696	0.066	93.977
K.S.H	6-02_B3	9.506	3.92	2.997	10.632	40.2	13.073	0	0	13.775	0.116	94.219
K.S.H	6-02_C1	9.597	3.932	2.848	10.405	40.201	13.028	0	0.009	13.368	0.094	93.482
K.S.H	6-02_C2	9.658	3.959	2.952	10.807	40.051	13.002	0	0.017	13.833	0.097	94.376
K.S.H	6-02_C3	9.578	3.927	2.927	10.729	40.21	13.095	0	0	13.778	0.111	94.355
K.S.H	6-02_D1	9.715	3.969	2.801	10.748	40.288	13.037	0	0	13.014	0.092	93.664

K.S.H	6-02_D2	9.748	3.909	2.811	10.771	40.251	12.961	0	0	13.289	0.096	93.836
K.S.H	6-02_E1	9.626	3.921	2.731	10.821	40.053	13.083	0	0.092	13.478	0.096	93.901
K.S.H	6-02_E2	9.588	4.044	2.85	10.731	40.186	13.136	0	0.058	13.357	0.06	94.01
K.S.H	6-02_E3	9.661	3.984	2.806	10.598	40.117	12.989	0	0.023	13.218	0.111	93.507
K.S.H	6-02_F1	9.62	4.083	2.668	11.252	40.094	13.487	0	0.012	12.038	0.121	93.375
K.S.H	6-02_F2	9.476	4.038	2.758	11.186	40.43	13.4	0	0	12.291	0.054	93.633
K.S.H	6-02_F3	9.69	3.992	2.642	11.436	39.896	13.228	0	0	12.351	0.069	93.304
K.W.S	13-02_A1	22.49	1.843	0.466	12.956	47.786	5.46	0	0.163	7.143	0.105	98.412
K.W.S	13-02_A2	4.217	0	9.247	0	62.829	22.781	0	0	0.158	0	99.232
K.W.S	13-02_A3	21.803	3.509	0.567	10.318	43.077	8.724	0	0	9.035	0.133	97.166
K.W.S	13-02_B1	9.709	2.471	1.238	4.014	45.719	16.358	0	0.02	11.442	0.192	91.163
K.W.S	13-02_B2	13.331	0.022	3.496	0.023	51.132	29.251	0	0	0.472	0.001	97.728
K.W.S	13-02_B3	22.61	2.142	0.431	13.033	48.166	5.074	0	0.047	7.288	0.099	98.89
STANDARD	Hornblende-01	10.705	2.719	1.964	4.265	39.698	9.845	0	0.017	26.273	0.404	95.89
STANDARD	Hornblende-02	10.684	2.799	1.899	4.245	39.695	10.05	0	0.033	26.422	0.354	96.181
K.W.S	13-02_C3	0.767	0.016	0.132	31.794	54.772	4.341	0	0.379	6.946	0.101	99.248
K.W.S	13-02_C1	22.343	3.068	0.419	11.842	45.397	6.961	0	0.032	7.905	0.108	98.075
K.W.S	13-02_C2	0.061	1.74	0	15.343	0.026	52.777	0	0.048	26.369	0.078	96.442
K.W.S	13-02_D1	20.664	0.399	0.503	14.369	49.006	5.754	0	0.118	6.326	0.114	97.253
K.W.S	13-02_D2	16.436	0.375	1.924	13.405	49.777	8.242	0	0.068	7.54	0.088	97.855
K.W.S	13-02_D3	16.398	0.363	1.865	13.532	49.9	8.271	0	0.056	7.535	0.118	98.038
K.W.S	13-02_E1	21.798	1.975	0.369	12.966	47.792	5.136	0	0.133	7.802	0.093	98.064
K.W.S	13-02_E2	22.119	2.606	0.523	11.801	45.45	7.565	0	0.327	7.467	0.092	97.95
K.W.S	13-02_E_Darker	2.362	0.048	0	0	81.2	10.797	0	0	5.523	0.021	99.951
K.W.S	13-02_F1	22.149	2.785	0.484	12.107	45.766	7.347	0	0.189	7.037	0.113	97.977
K.W.S	13-02_F2	11.657	0.079	4.382	0.034	52.977	27.947	0	0.057	0.466	0.002	97.601
K.W.S	13-02_F3	12.57	0.023	3.73	0.015	51.757	28.693	0	0	0.412	0	97.2
K.W.S	13-02_G1	20.337	0.346	0.468	15.273	49.971	5.836	0	0.059	5.719	0.13	98.139

K.W.S	13-02_G2	15.768	0.362	1.442	14.464	49.255	9.282	0	0.079	7.408	0.158	98.218
K.W.S	13-02_G3	16.435	0.351	1.419	14.506	49.755	8.247	0	0.024	7.298	0.157	98.192
K.R.S 3	11-09_A1	9.841	4.091	2.711	11.253	39.706	13.148	0	0.014	12.123	0.118	93.005
K.R.S 3	11-09_A2	9.742	4.037	2.555	11.374	39.686	13.226	0	0.006	12.054	0.07	92.75
K.R.S 3	11-09_A3	9.761	4.101	2.633	11.331	39.658	13.24	0	0	12.021	0.077	92.822
K.R.S 3	11-09_B1	9.835	4.058	2.525	11.598	39.757	13.19	0	0	11.534	0.091	92.588
K.R.S 3	11-09_B2	9.825	4.023	2.536	11.83	39.807	13.239	0	0.032	11.588	0.129	93.009
K.R.S 3	11-09_B3	9.901	4.032	2.516	11.755	39.881	13.367	0	0.026	11.505	0.094	93.077
K.R.S 3	11-09_C1	9.744	4.005	2.56	10.723	39.715	12.977	0	0	12.744	0.102	92.57
K.R.S 3	11-09_C2	9.811	3.97	2.537	11.082	39.756	12.988	0	0	12.871	0.103	93.118
K.R.S 3	11-09_C3	9.608	4.013	2.662	10.889	39.686	12.974	0	0	12.926	0.051	92.809
K.R.S 4	Riv4_A1	9.508	4.029	2.853	9.598	39.514	12.613	0	0.031	14.904	0.1	93.15
K.R.S 4	Riv4_A2	9.431	3.967	2.751	9.41	39.36	12.584	0	0.043	13.191	0.134	90.871
K.R.S 4	Riv4_A3	9.58	4.072	2.737	9.423	39.285	12.61	0	0.04	14.544	0.1	92.391
K.R.S 4	Riv4_B1	9.722	4.084	2.537	11.382	39.695	13.192	0	0.029	11.471	0.084	92.196
K.R.S 4	Riv4_B2	9.814	4.069	2.679	11.365	39.736	13.278	0	0	11.859	0.063	92.863
K.R.S 4	Riv4_B3	9.709	4.106	2.673	11.575	39.506	13.17	0	0.04	11.861	0.056	92.696
K.R.S 4	Riv4_C1	9.662	3.858	2.883	10.267	37.575	11.952	0	0.02	13.921	0.135	90.273
K.R.S 4	Riv4_C2	9.653	3.919	2.813	10.375	39.864	12.614	0	0.017	13.913	0.078	93.246
K.R.S 4	Riv4_C3	9.651	3.835	2.744	10.271	39.691	12.76	0	0.006	13.72	0.127	92.805
K.R.S 4	Riv4_D1	9.572	3.847	2.945	10.032	39.591	12.719	0	0.037	14.412	0.127	93.282
K.R.S 4	Riv4_D2	9.62	3.86	2.888	10.121	39.424	12.65	0	0	14.158	0.104	92.825
K.R.S 4	Riv4_D3	9.44	3.865	2.811	10.147	39.387	12.653	0	0.014	14.109	0.114	92.54
K.R.S 4	Riv4_E1	9.607	4.019	2.645	10.639	39.497	13.069	0	0.009	13.079	0.124	92.688
K.R.S 4	Riv4_E2	9.582	3.98	2.67	10.68	39.318	12.887	0	0	13.131	0.119	92.367
K.R.S 4	Riv4_E3	9.758	4.028	2.741	10.641	39.341	12.997	0	0.003	13.026	0.085	92.62
STANDARD	Hornblende-01	10.767	2.885	2.006	4.212	39.398	9.862	0	0	25.595	0.405	95.13
STANDARD	Hornblende-02	10.765	2.941	1.912	4.15	39.468	9.934	0	0	25.914	0.397	95.481

K.R.S 4	Riv_4_F1	9.498	3.87	2.782	10.242	39.705	12.585	0	0	13.693	0.104	92.479
K.R.S 4	Riv_4_F2	9.566	3.897	2.887	10.433	39.423	12.548	0	0	13.823	0.117	92.694
K.R.S 4	Riv_4_F3	9.53	3.896	2.873	10.24	39.409	12.651	0	0	13.867	0.086	92.552
K.N.H	4-14_A1	9.592	3.911	2.853	10.444	39.596	12.868	0	0	13.472	0.099	92.835
K.N.H	4-14_A2	9.65	3.951	2.781	10.467	39.762	12.96	0	0	13.359	0.129	93.059
K.N.H	4-14_A3	9.579	3.878	2.76	10.396	39.559	12.85	0	0.009	13.474	0.087	92.592
K.N.H	4-14_B1	9.405	3.81	2.824	9.53	39.94	12.197	0	0	15.401	0.131	93.238
K.N.H	4-14_B2	9.53	4.33	2.607	9.833	38.057	11.879	0	0	16.667	0.14	93.043
K.N.H	4-14_B3	9.263	3.735	2.881	9.232	39.643	12.223	0	0.006	15.943	0.133	93.059
K.N.H	4-14_C1	9.352	3.727	2.704	9.038	39.406	12.258	0	0	15.837	0.118	92.44
K.N.H	4-14_C2	9.366	3.674	2.993	9.14	39.648	12.306	0	0	16.289	0.108	93.524
K.N.H	4-14_C3	9.465	3.727	3.003	9.015	39.497	12.169	0	0	16.032	0.076	92.984
K.N.H	4-14_D1	9.445	3.729	3.059	9.231	39.496	12.214	0	0.02	15.937	0.146	93.277
K.N.H	4-14_D2	9.619	3.798	2.778	9.635	39.542	11.917	0	0.023	15.478	0.09	92.88
K.N.H	4-14_D3	9.484	3.806	2.828	9.422	39.653	12.247	0	0.009	15.688	0.113	93.25
K.N.H	4-14_E1	9.413	3.788	2.95	9.748	39.726	12.557	0	0	14.98	0.122	93.284
K.N.H	4-14_F1	9.425	3.551	2.916	9.253	39.827	12.26	0	0	15.642	0.119	92.993
K.N.H	4-14_F2	9.541	3.765	2.892	9.423	39.932	12.146	0	0	15.617	0.147	93.463
K.N.H	4-14_F3	9.322	3.668	2.725	9.365	40.078	12.421	0	0	14.831	0.12	92.53
STANDARD	Hornblende-01	10.801	2.704	2.058	4.224	39.313	10.064	0	0.008	26.391	0.406	95.969
STANDARD	Hornblende-02	10.671	2.63	1.989	4.18	39.666	9.957	0	0.022	26.047	0.401	95.563
K.R.S 1	Riv1_A1	9.615	4.899	2.804	12.203	39.689	13.588	0	0.02	9.121	0.108	92.047
K.R.S 1	Riv1_A2	9.679	4.932	2.846	12.425	39.712	13.6	0	0	9.514	0.087	92.795
K.R.S 1	Riv1_A3	9.631	4.929	2.762	12.333	39.476	13.453	0	0.009	9.268	0.099	91.96
K.R.S 1	Riv1_B1	9.599	3.865	2.721	10.505	39.461	12.756	0	0.023	13.585	0.098	92.613
K.R.S 1	Riv1_B2	9.594	3.896	2.751	10.46	39.452	12.751	0	0.034	13.634	0.097	92.669
K.R.S 1	Riv1_B3	9.547	3.857	2.723	10.556	39.602	12.728	0	0.063	13.608	0.095	92.779
K.R.S 1	Riv1_C1	9.32	3.654	2.375	8.567	39.56	11.917	0	0	17.533	0.116	93.042

K.R.S 1	Riv1_C3	9.194	3.623	3.201	8.907	39.97	12.175	0	0.02	16.124	0.14	93.354
K.R.S 1	Riv1_D1	16.293	0.309	1.402	14.656	49.177	8.076	0	0.094	6.732	0.099	96.838
K.R.S 1	Riv1_D2	16.33	0.326	1.395	14.481	48.943	8.27	0	0.077	6.605	0.126	96.553
K.R.S 1	Riv1_D3	16.327	0.307	1.318	14.704	48.907	8.145	0	0.021	6.602	0.125	96.456
K.R.S 1	Riv1_E1	9.717	3.958	2.713	11.038	39.45	12.968	0	0.032	12.619	0.102	92.597
K.R.S 1	Riv1_E2	9.725	4.007	2.657	10.998	39.543	12.879	0	0	12.638	0.119	92.566
K.R.S 1	Riv1_E3	9.622	4.038	2.651	10.977	39.49	12.838	0	0.037	12.859	0.114	92.626
Camp	16-01_A1	9.353	3.83	2.774	9.81	39.596	12.534	0	0.026	14.793	0.119	92.835
Camp	16-01_A2	9.374	3.79	2.871	9.799	39.768	12.462	0	0.003	14.796	0.089	92.952
Camp	16-01_C1	9.364	3.843	2.916	9.848	39.592	12.499	0	0.031	14.704	0.15	92.947
Camp	16-01_C2	9.404	3.804	2.865	9.778	39.479	12.529	0	0	14.611	0.102	92.572
Camp	16-01_C3	9.504	3.87	2.864	9.789	39.537	12.43	0	0.029	14.352	0.081	92.456
Camp	16-01_D1	9.543	3.971	2.777	10.579	39.561	12.776	0	0	13.454	0.075	92.736
Camp	16-01_D2	9.508	3.964	2.823	10.422	39.579	12.77	0	0	13.462	0.111	92.639
Camp	16-01_D3	9.522	3.91	2.627	10.458	39.374	12.751	0	0.026	13.479	0.099	92.246
STANDARD	Hornblende-01	10.74	2.896	2.045	4.097	39.7	10.002	0	0	26.449	0.401	96.33
STANDARD	Hornblende-02	10.714	2.159	1.945	4.383	39.959	10.257	0	0.08	26.363	0.402	96.262
Camp	16-01_E1	9.358	3.803	2.819	9.773	39.649	12.425	0	0.02	14.672	0.073	92.592
Camp	16-01_E2	9.55	3.796	2.757	9.93	39.438	12.435	0	0.037	14.667	0.097	92.707
Camp	16-01_E3	9.327	3.834	2.874	9.882	39.561	12.429	0	0	14.713	0.123	92.743
Camp	16-01_G1	9.35	3.829	2.965	9.837	39.678	12.467	0	0	14.786	0.116	93.028
Camp	16-01_G2	9.435	3.868	2.817	9.902	39.548	12.469	0	0	14.372	0.092	92.503
Camp	16-01_G3	9.404	3.765	2.911	9.861	39.781	12.382	0	0.034	14.88	0.103	93.121
STANDARD	Hornblende-01	10.727	2.899	1.919	4.249	39.319	9.933	0	0	26.308	0.366	95.72
STANDARD	Hornblende-02	10.699	2.735	1.956	1.124	39.411	9.874	0	0	26.174	0.417	92.39